GEOLOGICA ULTRAIECTINA

Mededelingen van de
Faculteit Aardwetenschappen der
Rijksuniversiteit te Utrecht

no. 65

SILICATES WITH INCORPORATION OF NH_4^+, Rb^+, OR Cs^+

J. H. L. VONCKEN

SILICATES WITH INCORPORATION OF

NH_4^+, Rb^+, OR Cs^+

SILIKATEN MET INBOUW VAN
NH_4^+, Rb^+ OF Cs^+

(MET EEN SAMENVATTING IN HET NEDERLANDS)

TER VERKRIJGING VAN DE GRAAD VAN DOCTOR AAN DE
RIJKSUNIVERSITEIT TE UTRECHT, OP GEZAG VAN DE
RECTOR MAGNIFICUS, PROF. DR. J.A. VAN GINKEL,
INGEVOLGE HET BESLUIT VAN HET COLLEGE VAN DEKANEN
IN HET OPENBAAR TE VERDEDIGEN
OP 20 MAART 1990 DES NAMIDDAGS TE 14.30 UUR

DOOR

JAKOBUS HUBERTUS LAMBERTUS VONCKEN

GEBOREN OP 17 APRIL 1959 TE HEERLEN

PROMOTOR : PROF. DR. R.D. SCHUILING
CO-PROMOTOR : DR. J.B.H. JANSEN

CIP-GEGEVENS KONINKLIJKE BIBLIOTHEEK, DEN HAAG

Voncken, Jakobus Hubertus Lambertus

Silicates with incorporation of $NH4^+$, Rb^+, or Cs^+ / Jakobus Hubertus Lambertus Voncken. – [Utrecht : Instituut voor Aardwetenschappen der Rijksuniversiteit Utrecht]. – (Geologica Ultraiectina, ISSN 0072-1026; no. 65)
Proefschrift Utrecht. – Met lit. opg. – Met samenvatting in het Nederlands.
ISBN 90-71577-18-X
SISO 562 UDC 549.6(043.3)
Trefw.: silicaten.

Aan mijn ouders

VOORWOORD

Allen die hebben bijgedragen aan de totstandkoming van het proefschrift wil ik hartelijk bedanken. In het bijzonder wil ik hierbij noemen :

Mijn promotor, Prof. Dr. R.D. Schuiling, voor reviews van manuscripten, discussies en suggesties, en voor stimulans in het laatste jaar.

Dr. J.B.H. Jansen, onder wiens leiding het onderzoek is uitgevoerd. Hij voorzag die vele versies van hoofdstukken en artikels van commentaar, en die niet aflatende kritiek is van groot nut geweest.

Ad van der Eerden, voor het uitvoeren van een aantal proeven en analyses, voor alle praktische lessen in het werken met de hoge druk apparatuur en de ovens, voor alle hulp bij het praktische chemische werk, voor vele suggesties, en voor een prettige werksfeer.

Drs. Rudy Konings en Drs. Cees Woensdregt, voor hun belangrijke bijdragen aan de kristallografische en morfologische beschrijvingen in de hoofstukken III en VI, voor reviews van manuscripten, en voor allerlei discussies en suggesties.

Drs. Ariejan Bos, voor vele discussies over experimenteel petrologisch werk en allerlei adviezen.

Maarten Broekmans voor een aantal inleidende experimenten m.b.t. Cs-mica.

Gert Kastelein, voor alle technische assistentie bij het werken met de hoge druk apparatuur.

Dr. R.C. Erd, U.S. Geological Survey, Menlo Park, for making available the original samples of buddingtonite, for advices and for reviews of the text of chapter III and IV.

Dr. C.S. Strom voor hulp bij de kristallografische berekeningen en het beschikbaar stellen van de benodigde computer programmas.

Drs. Joyce Wevers voor het mij leren omgaan met de IR-apparatuur en het mij leren interpreteren van de spectra. Ook ben ik haar erkentelijk voor allerlei discussies over de kristallografie van dioctahedrische micas.

P. van Krieken en T. Zalm voor de TGA en DTA analyses.

Charles Laman, Nellie Slaats en Vian Govers voor de Guinier opnamen en de diffractogrammen.

Frits Geelen voor een aantal SEM opnames.

Ir. B. Djie-Kwee, Giel Eussen en Theo van Zessen voor hun assistentie bij de mineraal ontsluitingen en de AAS en AES analyses.

Paul Anten voor ICPAES analyses.

Ing. Joop Pieters van het EMSA voor assistentie bij het werken met de SEM.

Dr. Herman van Roermund voor het TEM werk.

Dr. Renè Poorter voor het sporadische microprobe werk.

Drs. Luc Bol voor alle hulp en wetenswaardigheden op het gebied van microcomputers en software, voor discussies over allerhande onderwerpen, en voor een prettige tijd.

Dr. Anne Feenstra, voor alle discussies over dioctahedrische micas in de beginfase van het onderzoek, en voor reviews van hoofdstuk II.

Dirk Steenbeek en alle andere (oud)medewerkers van de instrumentmakerij voor de prettige sfeer gedurende al die jaren.

Je remerciee Prof. dr. A. Baronnet (Centre de la Recherche sur les Mècanismes de la Croissance Cristalline, CNRS, Marseille) pour le possibilitè d'un stage a son laboratoire. Voor het verblijf in Marseille werd financiele steun verkregen van NWO.

Alle medewerkers van de bibliotheek en van de tekenkamer en foto-afdeling van het IVAU voor de prettige samenwerking.

Mijn huidige werkgever, de vakgroep Anorganische Chemie, Materiaalkunde en Katalyse van de faculteit CT, Universiteit Twente, wil ik bedanken voor het gebruik van de repro-faciliteiten en de laserprinter.

En tenslotte wil ik mijn ouders bedanken voor alle steun die zij mij gedurende mijn studie en tijdens het werk aan dit proefschrift gegeven hebben.

CONTENTS

Chapter II of this thesis is published in Geologie en Mijnbouw, volume 66, 1987, page 259 - 269. Co-authors : J.M.A.R. Wevers, A.M.J. van der Eerden, A. Bos, J.B.H. Jansen.

Chapter III of this thesis is published in Physics and Chemistry of Minerals, volume 15, 1988, page 323 - 328. Co-authors : R.J.M. Konings, J.B.H. Jansen, C.F. Woensdregt.

Chapter V of this thesis is published in The America Mineralogist, volume 72, 1987, page 551 - 554. Co-authors are A.M.J. van der Eerden, and J.B.H. Jansen.

The Chapters IV, VI, VII and VIII are intended for publication in international journals.

SUMMARY

This thesis presents results of an experimental study on the incorporation of NH_4^+, Rb^+, and Cs^+ in micas and feldspars. The studied micas are dioctahedral. The feldspars are sanidine-like.

In chapter II it is shown that the ammonium analogue of muscovite, called tobelite, with the formula $NH_4Al_2Si_3AlO_{10}(OH)_2$ can be synthesized using NH_3 in water, sal volatile or urea as donors for NH_4^+. The synthesis conditions may be quite high, even 500 °C at a pressure of 4 to 5 kbar. These synthesis pressures are higher than ones reported up to now in the literature, and they demonstrate that tobelite is not necessarily a mineral that is restricted to low pressure and temperature environments. All tobelite found so far seem to have formed at low temperature and pressure. In the literature, tobelite is mentioned to occur in relationship to fossil fuel deposits, and in chapter II it is elucidated why such a relationship may occur.

The synthesis of $NH_4AlSi_3O_8$, its characterization with XRD, SEM and IR-spectroscopy, its study by thermal analyses, and its morphological description are reported in Chapter III. $NH_4AlSi_3O_8$ is very close in structure to sanidine ($KAlSi_3O_8$). The similarities of $NH_4AlSi_3O_8$ with the mineral buddingtonite ($NH_4AlSi_3O_8.½H_2O$) are so striking, that it is likely that buddingtonite and the ammonium analogue of sanidine are the same. The first description of buddingtonite reports that it has zeolitic properties. The half mole of lattice water in $NH_4AlSi_3O_8.½H_2O$ is, according to descriptions in the literature, not present in the structure in an ordered way.

A detailed study (Chapter IV) of the original samples of buddingtonite, kindly made available by the principal author of the article in which buddingtonite was described firstly, shows that the zeolitic properties, as well as the lattice water can be ascribed to an admixture of montmorillonite, a clay mineral, in the original samples. Buddingtonite is not redefined in chapter IV, but it is strongly suggested to consider buddingtonite and $NH_4AlSi_3O_8$ as the same silicates and to disregard the zeolitic half mole of water of buddingtonite.

Chapter V describes the synthesis and characterization of the Rb-analogue of $2M_1$-muscovite ($RbAl_2Si_3AlO_{10}(OH)_2$) and comparison of this silicate with muscovite and other dioctahedral micas. Chapter VI describes the synthesis, characterization, morphology and structure of the Rb-analogue of sanidine ($RbAlSi_3O_8$).

To get an indication of the influence of the incorporation of Rb in muscovite and sanidine on the reaction of muscovite to sanidine, corundum and water, the location of the equilibrium of the reaction of $RbAl_2Si_3AlO_{10}(OH)_2$ to $RbAlSi_3O_8$, corundum and water was studied at 2 kbar. The results are also given in chapter VI, and indicate that the temperature at which the equilibrium is probably situated is only slightly higher (probably maximal 20 °C) than for the reaction of the K-silicates. If complete replacement of K by Rb does not have much effect, incorporation of Rb in muscovite and sanidine on trace element level will probably not influence the position of the equilibrium at all.

In chapter VII, the incorporation of Rb in muscovite by ion-exchange is studied. Muscovite as well as its Rb-analogue are brought in contact with alkali chloride solutions to establish ion exchange of K and Rb. All exchange experiments are carried out at a pressure of 2 kbar. The most important result is that there exists a solvus between the endmembers $RbAl_2Si_3AlO_{10}(OH)_2$ and $KAl_2Si_3AlO_{10}(OH)_2$ (muscovite). The exact location of the solvus remains somewhat unclear, which is probably caused by the ability of micas to form intergrowths.

Chapter VIII gives an account of the synthesis and characterization of a Cs-containing mica with a structure resembling that of muscovite. On basis of the data it can not be proven that the mica is the Cs-analogue of muscovite, because no accurate chemical analyses could be gathered. The mica is formed at a temperature of 400 °C at 2 kbar and at 400 °C and 500 °C at pressures of 2 and 5 kbar. Investigated conditions are 300, 400, 500 and 600 °C at pressures of 0.5, 2, and 5 kbar. Pollucite ($CsAlSi_2O_6$) always occurs together with the mica, as well as another Al-containing phase (boehmite, or diaspore or corundum, depending on the conditions).

SAMENVATTING

Dit proefschrift doet verslag van een experimentele studie naar de inbouw van NH_4^+, Rb^+, en Cs^+ in micas en veldspaten. De bestudeerde micas zijn dioctahedrisch. De veldspaten lijken veel op sanidien.

In hoofdstuk II wordt aangetoond dat het ammonium analoog van muscoviet, genaamd tobeliet, dat de formule $NH_4Al_2Si_3AlO_{10}(OH)_2$ heeft, synthetisch bereid kan worden met NH_3 in water, vlugzout of ureum als donors voor NH_4^+. De synthese condities kunnen behoorlijk hoog zijn, zelfs 500 °C bij een druk van 4 of 5 kbar. Deze synthese drukken zijn hoger dan die, welke tot nu toe in de literatuur vermeld worden, en ze laten zien dat tobeliet niet noodzakelijkerwijs een mineraal is dat verwacht mag worden voor te komen in omgevingen met lage temperatuur en druk. De tot nu toe gevonden tobeliet lijkt te zijn gevormd bij lage temperatuur en druk. In de literatuur wordt vermeld dat tobeliet voorkomt in relatie tot fossiele brandstof afzettingen, en in hoofdstuk II wordt uitgelegd hoe een dergelijke relatie kan ontstaan.

Van de synthese van $NH_4AlSi_3O_8$, de karakterisering ervan met XRD, SEM en IR-spectroscopy, van de bestudering met thermische analyse, en van de morfologische beschrijving wordt verslag gelegd in hoofstuk III. $NH_4AlSi_3O_8$ lijkt structureel heel veel op sanidien ($KAlSi_3O_8$). De overeenkomsten tussen $NH_4AlSi_3O_8$ en het mineraal buddingtoniet ($NH_4AlSi_3O_8.½H_2O$) zijn zo sterk, dat het waarschijnlijk is dat buddingtoniet en het ammonium analoog van alkaliveldspaat hetzelfde zijn. De eerste beschrijving van buddingtoniet vermeldt dat het mineraal zeolitische eigenschappen bezit. De halve mol kristal water in ($NH_4AlSi_3O_8.½H_2O$) is volgens de literatuurbeschrijvingen niet op een geordende manier in de structuur aanwezig.

Een gedetailleerde studie (Hoofdstuk IV) van de oorspronkelijke monsters van buddingtoniet, welke vriendelijk ter beschikking werden gesteld door de eerste auteur van het artikel waarin buddingtoniet voor het eerst werd beschreven, laat zien dat de zeolitische eigenschappen alsook het kristalwater kunnen worden toegeschreven aan een bijmenging van montmorilloniet, een kleimineraal, in de oorspronkelijke monsters. Buddingtoniet wordt niet opnieuw gedefinieerd in hoofdstuk IV, maar het wordt sterk aanbevolen buddingtoniet en $NH_4AlSi_3O_8$ als dezelfde silikaten te beschouwen, en de zeolitische halve mol water niet meer in beschouwing te nemen.

Hoofdstuk V beschrijft de synthese en karakterisering van het Rb-analoog van $2M_1$-muscoviet ($RbAl_2Si_3AlO_{10}(OH)_2$) en vergelijk van dit silikaat met muscoviet en andere dioctahedrische micas. Hoofdstuk VI beschrijft de synthese en karakterisering, de morfologie en de structuur van van het Rb-analoog van sanidien ($RbAlSi_3O_8$).

Om een indicatie te krijgen van de invloed van de inbouw van Rb in muscoviet en sanidien op de reactie van muscoviet naar sanidien, korund en water, is de ligging van het evenwicht van de reactie van $RbAl_2Si_3AlO_{10}(OH)_2$ naar $RbAlSi_3O_8$, korund en water bestudeerd bij 2 kbar. De resultaten worden ook vermeld in hoofstuk VI, en wijzen erop dat de temperatuur waarbij het evenwicht ligt slechts weinig hoger is (vermoedelijk hooguit 20 °C) dan voor de reactie van de K-silikaten. Als complete vervanging van K door Rb niet veel effect heeft, zal inbouw van Rb op spore-element niveau vermoedelijk helemaal geen invloed hebben op de ligging van het evenwicht.

In hoofdstuk VII wordt de inbouw van Rb in muscoviet door middel van ionen-uitwisseling bestudeerd. Zowel muscoviet als zijn Rb-analoog worden in contact gebracht met alkali chloride oplossingen om uitwisseling van K en Rb te bewerkstelligen. Alle uitwisselingsproeven zijn bij een druk van 2 kbar uitgevoerd. Er bestaat een solvus tussen de eindleden $RbAl_2Si_3AlO_{10}(OH)_2$ en $KAl_2Si_3AlO_{10}(OH)_2$ (muscoviet). De exacte locatie van de solvus blijft ietwat onduidelijk, hetgeen vermoedelijk wordt veroorzaakt door de eigenschap van micas om vergroeiingen te vormen.

Hoofdstuk VIII beschrijft de synthese en karaktarisering van een Cs-houdende mica met een structuur welke op die van muscoviet lijkt. Het is op grond van de gegevens niet te bewijzen dat de mica het Cs-analoog van muscoviet is, omdat geen nauwkeurige chemische

analyses konden worden verkregen. De mica wordt gevormd bij een temperatuur van 400 °C bij 2 kbar en bij 400 °C en 500 °C bij drukken van 2 en 5 kbar. De onderzochte condities zijn 300, 400, 500 en 600 °C bij drukken 0.5, 2, en 5 kbar. Polluciet ($CsAlSi_2O_6$) komt altijd samen met de mica voor, evenals een tweede Al-houdende fase (boehmiet of diaspoor of korund, afhankelijk van de condities).

CHAPTER I.

INTRODUCTION

In the study of minerals and rocks, often considerable effort is given to determine their chemical composition in terms of trace elements. Trace elements may be specifically concentrated by geochemical processes. Trace element geochemistry may provide tools to trace the processes that led to the formation of the rocks, ores or minerals studied. Therefore, it is important to collect knowledge of the factors that govern the preference for or avoidance of a certain phase (melt, fluid or crystal) by a trace element. Besides the knowledge of element distribution, it is of importance to have insight in the physical conditions of mineral formation, and of the crystal structure and properties of the minerals of interest. To understand the crystal-chemical constraints on incorporation of a trace element in a mineral, it is useful to synthesize the trace element analogue of that mineral. Generally, these analogues will not occur in nature. This study will focus on the incorporation of nitrogen (in the form of NH_4^+), Rb^+ and Cs^+ in the common minerals muscovite ($KAl_2Si_3AlO_{10}(OH)_2$) and sanidine ($KAlSi_3O_8$). The ammonium analogue of muscovite is known as the (rare) mineral tobelite.

After the discovery of the ammonium silicate buddingtonite (Erd et al., 1964), and the discovery of incorporation of ammonium in muscovite (Vedder, 1965), for many years relatively little attention has been paid to the incorporation of ammonium in rockforming minerals. The presence of considerable amounts of ammonium in micas and feldspars was proven by Higashi (1978) and Honma and Itihara (1981). Recent discoveries of ammonium-bearing minerals and even ammonium endmember silicates in spatial relation to oil shales and coal (Loughnan et al., 1983; Juster 1984, 1987) as well as to Pb, Zn, (Ag) ores (Sterne et al., 1982, 1984; Williams et al., 1987) and gold deposits (Kydd and Levinson, 1986) led to a renewed interest in ammonium silicates. Some studies focused mainly on ammonium determination (Klock and Lamothke, 1986; Krohn and Altaner, 1987). Others were concerned with ammonium silicate synthesis (Bos et al., 1987), modeling of the behavior of ammonium in metamorphic fluids on basis of field data (Duit et al., 1986) or on basis of laboratory investigations (Bos et al., 1988). Studies on the origin of nitrogen in the Earth's Crust focused on whether the nitrogen is of sedimentary origin or mantle-derived (Eugster and Munoz, 1966; Hallam and Eugster, 1976; Kreulen and Schuiling, 1982; Hall, 1988a). Nitrogen gas occurs in fluid inclusions in high grade metamorphic terrains (e.g. Swanenberg, 1980), giving evidence that nitrogen occurs also in the lower crust. Crustal contamination of minette magmas, ultimately deriving from the upper mantle, is likely the explanation of their ammonium content (Hall, 1988a). NH_4^+-rich granitic magmas may be generated by

contamination with ammonium rich xenoliths (Hall, 1988b) or melting of precursor material of sedimentary origin, rich in ammonium, in the lower crust (Hall, 1987). Originally deriving from organic material, NH_4^+ might be fixed in ammonium- silicates like micas or feldspar. Knowledge of synthesis conditions and properties of ammonium silicates gives a background to the interpretation of data on nitrogen or ammonia occurrences in crustal rocks. Studies of synthetic ammonium-analogues of muscovite and sanidine gives information on the extent of structure modification of muscovite and sanidine lattices as a result of incorporation of NH_4^+. Furthermore, they shed new light on the structure of natural ammonium silicates like buddingtonite ($NH_4AlSi_3O_8.1/2H_2O$; Erd et al., 1964) or tobelite ($NH_4Al_2Si_3AlO_{10}(OH)_2$; Higashi, 1982).

Potassium in natural muscovite and sanidine may be replaced by other elements of similar chemical properties. Rubidium, and to a lesser extent cesium, are well known examples of substitutes. These substitutions are the result of partitioning between the mineral and another phase (fluid or melt). Substantial enrichment of Rb and Cs in rocks may be caused by the activity of postmagmatic fluids which are associated to acid magmatism. Also NH_4^+ may be enriched in such altered rocks. Enrichment of NH_4^+ in greisens may be explained by contamination of the postmagmatic metasomatizing fluids by hydrothermal waters having cycled through sedimentary country rocks (Hall, 1988b). These metasomatizing postmagmatic fluids are considered to be essential for the development of ores of Sn, W and/or Mo which often accompany hydrothermally altered granites (e.g. Tischendorf, 1977; Pollard, 1983). Metal complexes involving NH_4^+ may be important carriers of ore-metals. Knowledge on NH_4^+-, Rb- and Cs-incorporation in silicates is important for interpretation of field data from rocks rich in these elements. Rb- incorporation in minerals is also important for the interpretation of radiometric age determinations involving decay of ^{87}Rb to ^{87}Sr. (e.g. Andriessen, 1978; Majoor, 1988). Cesium incorporation in silicates has attracted new interest with recent research on immobilization of ^{137}Cs from radioactive wastes by incorporation in silicates (e.g. Gallagher and McCarthy, 1982). Komarneni and White (1981) studied the possible incorporation of this toxic isotope in rocks and soils in relation to unintentional release of ^{137}Cs from storage of nuclear wastes. Information on synthesis, structure and properties of Cs-silicates will be important for interpretation of the results of these investigations.

The main reason to combine studies on the incorporation of ammonium, rubidium and cesium in silicates is the similar geochemical behavior of Rb and Cs the similar ionic size of Rb^+ (1.52 Å, Shannon, 1976) and NH_4^+ (1.48 Å, Pauling, 1960), although ammonium in fact has no strictly defined radius due to its tetrahedral structure. The ionic radius of Cs^+ is slightly larger : 1.67 Å (Shannon, 1976). Very generally speaking, incorporation of 3 large monovalent ions on the alkali-sites of the common rock forming

minerals muscovite and sanidine is investigated. The studies are carried out in the framework of research within the Chemical Geology Department of the Utrecht University. Research topics involve investigations on the origin of nitrogen in the crust and the behavior of N_2 or NH_4^+ during metamorphism as well as the behavior of trace elements like rubidium and cesium in geochemical processes, for example those related to granitic magmatism.

The chapters II, III, and IV of this thesis deal with ammonium-silicates. Chapter II describes a study on the synthesis of tobelite from inorganic and an organic precursor material and gives an indication why the occurrence of tobelite could be spatially related to fossil fuel deposits. Chapter III describes the synthesis of $NH_4AlSi_3O_8$, and gives a characterization of the silicate. The question is raised whether it is identical to the mineral buddingtonite, which is considered to be an ammonium feldspar with zeolitic water. Ending the part on ammonium silicates, chapter IV gives a description of a renewed mineralogical study of the natural holotype specimen of the mineral buddingtonite, with emphasis on its zeolitic character and possible equivalence to the synthetic $NH_4AlSi_3O_8$.

The chapters V and VI are concerned with the synthesis and characterization of respectively the Rb-analogue of muscovite and of sanidine. Chapter VI also accounts of experiments at 2 kbar on the reaction $RbAl_2Si_3O_{10}(OH)_2 = RbAlSi_3O_8 + Al_2O_3 + H_2O$, which marks the upper stability of the Rb-analogue of muscovite. This could give information on the question whether the stability of muscovite is greatly affected by incorporation of extreme amounts of Rb. Chapter VII deals with ion exchange reactions of Rb^+ and K^+ between muscovite and (K,Rb)Cl solutions, and is primarily concerned with the extent of the solid solution between muscovite and its Rb-analogue.

The last part of the thesis is a study on the synthesis and characterization of a Cs-analogue of muscovite.

REFERENCES

Andriessen, P.A.M. (1978) Isotopic age relations within the polymetamorphic complex of the island Naxos (Cyclades, Greece). Verhandeling nr.3 ZWO laboratorium voor Isotopen Geologie. Thesis, Free University of Amsterdam, 1978, 71 p.

Bos.,A. De Haas, G.J., Voncken , J.H.L., Van der Eerden, A.M.J., Jansen, J.B.H. (1987) Hydrothermal synthesis of ammonium phlogopite. Geologie en Mijnbouw,66, 251 -258.

Bos, A., Duit, W., Van der Eerden, A.M.J., Jansen, J.B.H. (1988) Nitrogen storage in biotite : an experimental study on the ammonium and potassium partitioning between 1M-phlogopite and vapor a 2 kb. Geochimica et Cosmochimica Acta, 52, 1275 - 1283.

Duit, W., Jansen, J.B.H., Van Breemen, A., Bos, A. (1986) Ammonium micas in pelitic rocks as exemplified by Dôme de L'Agout (France). American Journal of Science, 286, 702 -732.

Erd, R.C., White, D.E, Fahey, J.J., Lee, D.E. (1964) Buddingtonite, an ammonium feldspar with zeolitic water. The American Mineralogist, 49, 831 - 850.

Eugster, H.P. and Munoz, J.L. (1966) Ammonium micas : possible sources of atmospheric ammonia and nitrogen. Science, 151, 683 - 686.

Gallagher, S.A. and McCarthy, G.J. (1982) High temperature thermal stability of $CsAlSiO_4$ and $CsAlSi_2O_6$. Materials Research Bulletin, 17, 89 - 94.

Hall, A. (1987) The ammonium content of Caledonian granites. Journal of the Geological Society, London, 144, 671 - 674.

Hall, A. (1988a) Crustal contamination of Minette magmas : evidence from their ammonium contents. Neues Jahrbuch für Mineralogie, Monatshefte, 3, 137 - 143.

Hall, A. (1988b) The distribution of ammonium in granites from SW England. Journal of the Geological Society, London, 145, 37 - 41.

Hallam, M. and Eugster, H.P. (1976) Ammonium silicate stability relations. Contributions to Mineralogy and Petrology, 57, 227 - 244.

Higashi, S.(1978) Dioctahedral mica minerals with ammonium ions. Mineralogical Journal of Japan, 9, 16-27.

Higashi, S. (1982) Tobelite, a new ammonium dioctahedral mica. Mineralogical Journal of Japan, 11, 138-146.

Honma, H. and Itihara, Y. (1981) Distribution of ammonium in minerals of metamorphic and granitic rocks. Geochimica et Cosmochimica Acta, 45, 983 - 988.

Juster T.C. (1984) Very low grade metamorphism of pelites, associated with coal, northeastern Pennsylvania. MSc-thesis, University of Wisconsin-Madison, 101 pp.

Juster T.C., Brown, P.E, Bailey, S.W. (1987) NH_4-bearing illite in very low grade metamorphic rocks, associated with coal, northeastern Pennsylvania. The American Mineralogist, 72, 555 - 565.

Klock, P.R. and Lamothke, P.J. (1986) Determination of ammonium in a buddingtonite sample by ion-chromatography. Talanta, 33, 495 - 498.

Komarneni, S. and White, W.B. (1981) Hydrothermal reactions of clay minerals and shales with cesium phases from spent fuel elements. Clays and Clay Minerals, 29, 299 - 308.

Kreulen, R. and Schuiling, R.D. (1982) N_2-CH_4-CO_2fluids during formation of the Dôme de L'Agout, France. Geochimica et Cosmochimica Acta, 46, 193 - 203.

Krohn, M.D. and Altaner, S.P. (1987) Near-infrared detection of ammonium minerals. Geophysics, 52, 924 - 930.

Kydd,R.A. and Levinson, A.A. (1986) Ammonium halos in lithogeochemical exploration for gold at the Horse Canyon carbonate hosted deposit, Nevada, USA. : Use and Limitations. Applied Geochemistry, 1, 407 - 417.

Loughnan, F.C., Roberts, F.I., Lindner, A.W. (1983) Buddingtonite, (NH_4-feldspar) in the Condor Oilshale Deposit, Queensland, Australia. Mineralogical Magazine, 47, 327 - 334.

Majoor, F.J.M. (1988) A geochronological study of the axial zone of the central Pyrenees, with emphasis on variscan events and Alpine resetting. Verhandeling nr. 6, ZWO Laboratorium voor Isotopen-Geologie. Thesis, Free University, Amsterdam, 117 pp.

Pauling, L. (1960) The nature of the chemical bond and the structure of molecules and crystals : an introduction to modern structural chemistry. 3rd edition. Cornell University Press, 644 pp.

Pollard, P.J. (1983) Magmatic and postmagmatic processes in the formation of rocks associated with rare element deposits. Transactions of the Institutions of Mining and Metallurgy, 92, B1 - B9.

Shannon R.D. (1976) Revised effective ionic radii and systematic studies of interatomic distances in halides and chalcogenides. Acta Crystallographica, A32, 751 - 767.

Sterne E.J., Reynolds, R.C.,Jr., Zantop, H. (1982) Natural ammonium illites from black shales hosting a stratiform, base metal deposit, Delong Mountains, Northern Alaska. Clays and Clay Minerals, 30, 161-166

Sterne E.J., Reynolds, R.C.,Jr., Zantop, H. (1984) Clay mineralogy and carbon nitrogen geochemistry of the Lik and Competition Creek zinc-lead-silver prospects, Delong Mountains, Alaska. Economic Geology, 79, 1406 - 1411.

Swanenberg, H.E.C. (1980) Fluid inclusions in high grade metamorphic rocks of SW Norway. Thesis, University of Utrecht, 147 pp.

Tischendorf G. (1977) Geochemical and petrographic characteristics of silicic magmatic rocks associated with rare element mineralization. Metallization Associated with Acid Magmatism, Vol. 2, M. Stemproc and L. Burnol, eds., 41 - 96, Geological Survey, Prague.

Vedder, W. (1965) Ammonium in muscovite. Geochimica et Cosmochimica Acta, 29, 221 - 228.

Williams, L.B., Zantop, H., Reynolds, R.C. (1987) Ammonium silicates associated with sedimentary exhalative ore deposits : a geochemical exploration tool. Journal of Geochemical exploration, 27, 125 - 141.

CHAPTER II.

Hydrothermal synthesis of tobelite, $NH_4Al_2Si_3AlO_{10}(OH)_2$, from various starting materials and implications for its occurrence in nature

J.H.L. Voncken[1], J.M.A.R. Wevers[2], A.M.J. van der Eerden[1], A. Bos[1] & J.B.H. Jansen[1]
[1] *Department of Geochemistry and Experimental Petrology, Institute for Earth Sciences, State University of Utrecht, Budapestlaan 4, 3524 CD Utrecht, The Netherlands;* [2] *Department of Mineralogy and Crystallography, Institute for Earth Sciences, State University of Utrecht, Budapestlaan 4, 3524 CD Utrecht, The Netherlands*

Received 13 March 1987; accepted in revised form 02 June 1987

Key words: hydrothermal ammonium mica synthesis, mica occurrences in fossil fuel deposits, thermal decomposition of ammonium micas

Abstract

Ammonium-bearing micas are prominent nitrogen containing minerals in the Earth's crust. Various starting materials and a range of conditions were applied for the hydrothermal synthesis of tobelite, the ammonium analogue of muscovite. The natural occurrence of the mineral is elucidated. The best crystallised tobelite is carefully investigated with XRD, SEM, DTA, TGA, and IR-spectroscopy. Cell parameters of the tobelite are a_0: 5.230 ± 0.007; b_0: 9.02 ± 0.01 Å; c_0: 10.55 ± 0.01 Å; β: 101.56° ± 0.01; V: 487.5 ± 0.7 Å^3. Tobelite is indexed on the basis of a 1M cell. Tobelite decomposes at temperature above 500° C in TGA/DTA studies, using heating rates of 10° C/min. Ammonia loss and dehydroxylation are separate processes. Ammonia loss proceeds relatively faster and it is a lower temperature process. In an IR spectrum of tobelite the NH_4^+-vibrations are readily perceivable, and they are determinative for tobelite with respect to other dioctahedral micas. Tobelite is easily identified by X-ray diffraction. The present synthesis results and literature data indicate that tobelite is readily formed in NH_3-rich environments. Such environments are likely to exist in fossil fuel deposits, where decomposition of amino-acids under reducing conditions normally yields NH_3-rich gas or fluid phases. Ammonium micas may be formed directly from ammonium bearing clay minerals, or by ammonia incorporation in pre-existing micas.

Introduction

Nitrogen within the lithosphere is concentrated in organic matter and in silicates. The genesis of nitrogen-bearing silicates is linked to questions concerning the origin and behaviour of nitrogen in the Earth's crust. In the last two decades, significant amounts of nitrogen have been detected in a wide variety of rocks, ranging from sediments to metamorphic rocks and even igneous rocks (Mylovskiy & Volynets, 1966; Wlotzka, 1961; Itihara & Honma, 1979; Honma & Itihara, 1981; Duit et al., 1986).

Occurrences of NH_4^+-bearing silicates (illite, mica, feldspar) are often related to deposits of organic matter. NH_4^+-muscovite is reported in low-grade pelitic rocks associated with coal-deposits (Juster, 1984). Ammonium-illite occurs in black shales associated with base metal deposits (Sterne et al., 1982). Cooper & Evans (1983) indicated that

41 to 84 percent of the nitrogen in 5 samples of oil shale is present as fixed NH_4^+ in silicates (illite and feldspar) The NH_4^+-feldspar buddingtonite was first reported to occur as a hydrothermal replacement of plagioclase in a hot spring environment (Erd et al., 1964). NH_4^+-feldspar is also encountered in oil shale deposits (Loughnan et al.,1983). Recently ammonioleucite was discovered in hydrothermally altered schists (Hori et al., 1986).

After the discovery of NH_4^+ in muscovite by Vedder (1965), increasing evidence has been gathered for the presence of NH_4^+ in phyllosilicates (Yamamoto & Nakahira, 1966; Higashi, 1978; Itihara & Honma, 1979; Cooper & Abedin, 1981; Norman & Palin, 1982). Duit et al. (1986) mentioned amounts up to 1140 ppm NH_4^+ in muscovite and up to 1880 ppm NH_4^+ in biotites from rocks of the Dome de l'Agout, France. Ammonium muscovite was first synthesized by Eugster & Munoz (1966) and Barrer & Dicks (1966). Since then several other authors have also synthesized NH_4^+-muscovites (Levinson & Day, 1968; Shigorova et al., 1981). NH_4^+-muscovite was discovered in nature by Higashi (1982), who named it tobelite after the type locality in the Tobe district, Japan.

The stability relations of NH_4^+-feldspar and NH_4^+-muscovite were investigated by Hallam & Eugster (1976). Hydrothermal synthesis of ammonium-muscovite from Al-Si-gels and amino-acids (Tsunashima et al., 1975) is particularly interesting with respect to fossil fuel deposits. Formation of NH_3-gas during the decomposition of amino-acids in an anoxic environment is very likely a common geological process.(c.f. Thorstenson & Mackenzie, 1971).

Ion exchange reactions of NH_4^+ and K^+ between phlogopite and alkali/ammonium chloride solutions have been experimentally investigated by Bos et al. (in prep.). They encountered a complete solid solution between the K^+ and NH_4^+-endmembers at 550° C and 2 kbar. Recently, during a study of very low grade metamorphic coal deposits, Juster (1984) found strong evidence for the existence of an asymmetrical solvus between muscovite and tobelite below 350° C at a pressure of about 1.5 kbar. The gradual slope on the tobelite side is sensitive to temperature, and if determined accurately, the solvus may be a useful geothermometer at very low grade metamorphic and even diagenetic conditions. Such a thermometer may prove to be a powerful tool in oil and gas exploration. Studies on exchange reactions of NH_4^+ and K^+ between muscovite and a chloride solution at relatively low hydrothermal conditions are in progress at our Institute's high pressure, high temperature laboratory.

In this paper we present results on the hydrothermal synthesis of tobelite ($NH_4Al_2Si_3AlO_{10}(OH)_2$) under a variety of conditions. The best crystallised micas were selected for XRD, TGA, DTA and IR -spectroscopy.

Some conclusions are drawn from our results and from literature data about the occurrence of tobelite.

Starting materials and experimental methods

In order to obtain the required ammonium-ion for the synthesis of tobelite, sal volatile, urea, and a NH_3-solution were used as starting materials. Mixtures of γ-Al_2O_3, cristobalite (SiO_2) and an Al-Si-gel of the required composition were selected. Cristobalite was synthetically prepared by heating purified quartz to 1500° C for 3 hours at 1 atm. Cristobalite is a more reactive component than quartz. An 1:1 Al-Si gel was prepared, from an Al $(NO_3)_3$-solution and TEOS, with application of ethanol (96%) according to the method of Hamil-

Table 1. List of used chemicals.

NH_4HCO_3-NH_2COONH_4	sal volatile, OPG.
NH_2CONH_2	urea, BDH Chemicals, no 30558, pro analysi
NH_3-solution (25%)	Merck, No. 5432, pro analysi
γ-Al_2O_3	Merck, No. 1095, pro analysi
SiO_2	quartz. Merck, No. 7536, pro analysi
Al $(NO_3)_3$	Merck, No. 1063, pro analysi
TEOS	Tetra-Ethyl-Ortho-Silicate, $(Si(OC_2H_5)_4)$ Merck-Schuchardt, No. 800658
Ethanol (96%)	Nedalco C.V.
H_2O	double distilled

ton & Henderson (1968). The chemicals used are listed in Table 1.

All experiments were carried out in gold capsules of 25–30 mm length and 5.4 or 4.1 mm internal diameter. The thickness of the tube-walls was 0.2 mm. The Al and Si compounds were first carefully mixed in an agate mortar and then transferred into the gold capsules separately from the easily decomposing NH_4^+-donors, which are either fluids or very rapidly dissolving solids. Stochiometric amounts of starting materials were calculated for the production of about 200 mg of tobelite per run. The capsules were welded and shut with a carbon arc. During the welding of the filled capsules the bottom was cooled with cold water or liquid nitrogen to prevent the escape of volatiles. The capsules were placed in cold seal pressure vessels of the Tuttle type (Tuttle, 1949). Argon was used as a pressure medium. The pressure was continuously read from a Bourdon-type pressure gauge, which was regularly calibrated against a Heise precision gauge. The accuracy was better than 10 bars at the pressures involved. The temperature was measured with chromel-alumel thermocouples, with an accuracy better than 5° C. After the runs, the pressure vessels were quenched isobarically to room temperature within a few minutes by blowing compressed cold air. A detailed technical description of hydrothermal equipment with special reference to the synthesis of NH_4^+-phlogopite is reported by Bos et al. (1987). All run products were examined with a polarising microscope, XRD, and SEM.

Syntheses of tobelite

Sal volatile (NH_4HCO_3-(NH_2COONH_4)) as starting material

The procedure is analogous to that of one of the methods applied by Eugster & Munoz (1966) where NH_4HCO_3 was used as NH_3-donor. On decomposition NH_4HCO_3 gives NH_3, H_2O and CO_2 in a ratio 1:1:1, whereas sal volatile decomposes in a ratio 3:2:1. Sal volatile was used in our experiments to obtain a higher P_{NH3}.

$$NH_4HCO_3\text{-}(NH_2COONH_4) \leftrightarrow 3\ NH_3 + 2\ CO_2 + H_2O \quad (1)$$

The formation of the ammonium-muscovite can be described by the reaction:

$$2\ NH_4HCO_3\text{-}(NH_2COONH_4) + 9\ \gamma\text{-}Al_2O_3 + 18\ SiO_2 + 7\ H_2O \leftrightarrow 6\ NH_4Al_2Si_3AlO_{10}(OH)_2 + 4\ CO_2 \quad (2)$$

Table 2. Selection of hydrothermal synthesis results.

Method	Starting materials	T (°C)	P_{tot} (kbar)	Run time (days)	Phases Produced
(1)	sal volatile, γ-Al_2O_3, cristobalite	550	2	36	tobelite, rare quartz and corundum
(2)	urea, Si-Al gel on muscovite composition	550	2	19	tobelite, minor buddingtonite and corundum
(3)	NH_3-solution γ-Al_2O_3, cristobalite	500	4	20	tobelite, rare quartz, corundum, very rare mullite-like phase.
		500	5	20	tobelite pure.

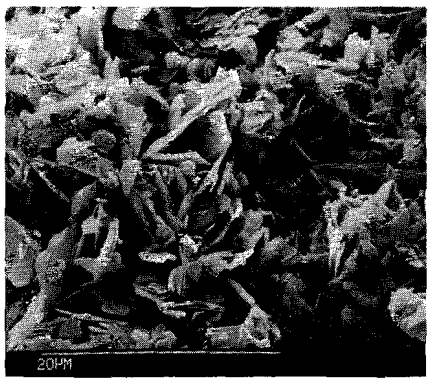

Fig. 1. SEM photograph of tobelite formed according to reaction (2).

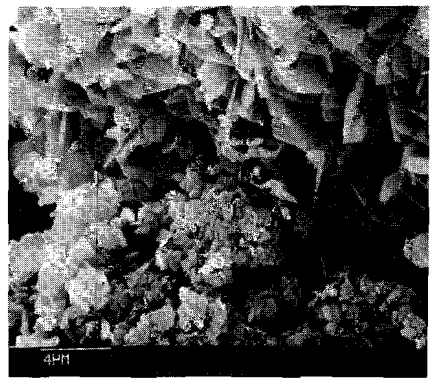

Fig. 2a. SEM photograph of tobelite formed according to reaction (4).

Eugster & Munoz (1966) reported good results for runs at 550° C and 2 kbar. Because sal volatile decomposes very rapidly on heating, it was always added in excess, in order to compensate for NH_3-loss during welding. Double distilled water acts as reactant and transport medium and was, therefore, also added in excess. Results of the syntheses are summarised in Table 2. The minimum time for the completion of reaction (2) was 3 weeks.

SEM-photographs of tobelites exhibit flakes which are about 4 micrometre in diameter and a few tenths of a micrometre in thickness (Fig. 1). Optically, the synthetic tobelites are colourless.

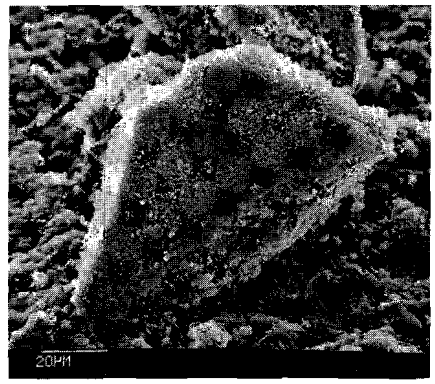

Fig. 2b. Tobelite, pseudomorph after a buddingtonite crystal.

Urea (NH_2CONH_2) as starting material

As CO_2 lowers the effective P_{NH3} and P_{H2O}, a decrease of the amount of CO_2 might improve the synthesis of tobelite. Urea (NH_2CONH_2) was tried as a NH_3-donor, following a suggestion of Aaftink (1985).

$$NH_2CONH_2 + H_2O \leftrightarrow 2NH_3 + CO_2 \qquad (3)$$

For comparative purposes, an Al-Si gel was used instead of the mixture of γ-Al_2O_3 and SiO_2 used in method (1). A gel was previously used by Tsunashima et al. (1975). The formation of tobelite from urea and an 1:1 Al-Si gel can be described by the reaction:

$$NH_2CONH_2 + 3H_2O + \text{Al-Si gel} \leftrightarrow 2 \text{ tobelite} + CO_2 \qquad (4)$$

SEM pictures of the run products (Figs 2a and 2b) show micas of extremely variable size; NH_4^+-feldspars covered with small tobelite crystals are occasionally visible. The occurrence of NH_4^+-feldspar was confirmed by XRD.

A 25% ammonia-bearing solution as starting material

As the methods described above gave no satisfactory results, we decided to try a NH_3-solution. NH_3-solutions in water were used as ammonium donors by Eugster & Munoz (1966) and Shigorova et al. (1981). The advantage of an NH_3-solution is that only the species NH_3 and H_2O are involved. A gel is probably not a very appropriate Al-Si-donor (see Discussion). Therefore, γ-Al_2O_3 and cristobalite were used again. The mica should form according to the reaction:

$$2NH_3 + 3\ \gamma\text{-}Al_2O_3 + 6\ SiO_2 + 3\ H_2O \leftrightarrow 2\ NH_4Al_2Si_3AlO_{10}(OH)_2 \quad (5)$$

Similarly as in the experiments with other starting materials the ammonium donor was added in excess. Liquid nitrogen was applied as cooling agent during welding. To obtain a higher increase of the effective P_{NH3} and P_{H20} relative to the experiments described above, pressures of 4 and 5 kbar were applied. Results of the synthesis are listed in Table 2.

SEM-photographs of the micas (Figs. 3a and b) show beautifully shaped crystals with a diameter to about 10 micrometres and a thickness of some tenths of a micrometre. Apparently, the increase of P_{H20} and P_{NH3} in the 4 and 5 kbar experiments, which is due to the absence of CO_2 and the increase of P_{total}, has a positive influence on the growth of the micas despite the slight decrease in temperature. Micas grown in one 4 kbar run show beautifully developed crystals which were therefore selected for determination of cell parameters and analysis with DTA and TGA/DTG.

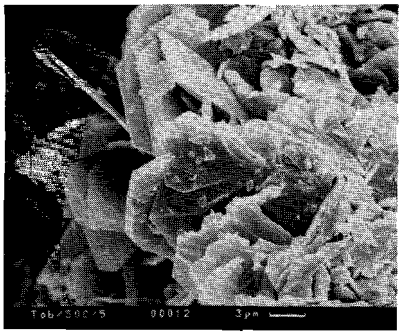

Fig. 3a. Tobelite forme according to reaction (5). The lines which are visible on the surface of the mica plates may represent cleavage lines or growth layer boundaries.

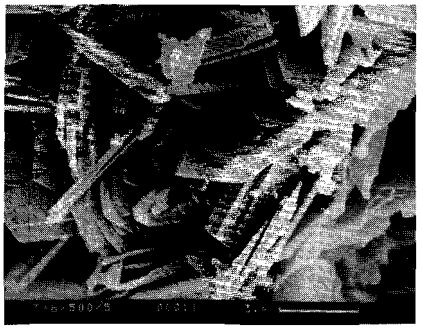

Fig. 3b. Tobelite made according to reaction (5). Note the almost euhedral crystals and their relative large dimensions, when compared to crystals shown in figs. 1 and 2a, 2b.

X-ray crystallography

The hydrothermally prepared NH_4^+-muscovites were investigated with a Philips PW1050 Diffractometer, connected to a PW1710 controlling device, and an Enraf Nonius FR552 Guinier Camera. $CuK_{\alpha 1}$-radiation ($\lambda = 1.54050$ Å) was used. To compare the crystallinity of the synthesised micas, the width of diffractometer peaks at half height was taken as a measure.

The X-ray diffraction pattern of our synthetic tobelite is similar to the patterns of the synthetic NH_4^+-muscovite reported by Eugster & Munoz (1966) and the natural NH_4^+-muscovite described by Higashi (1982). The small sizes of the crystals did not enable us to apply single crystal techniques. Silicon (JCPDS 27-1402) was used as an internal standard. The reflections were determined by densitometry from a Guinier film and the intensities were measured from a diffractogram. Cell parameters were calculated with a least squares refine-

ment program on 9 reflections. Computer calculated reflections are consistent with observations, and calculated hkl-values are in agreement with reported literature values (Eugster & Munoz, 1966; Higashi, 1982). However, Eugster & Munoz (1966) positioned the (110) reflection at 4.366 Å, while the reflection for natural 1M tobelite at 4.360 Å was interpreted as (11 −1) by Higashi (1982). The probably analogous reflection for 1M K-muscovite at d = 4.349 Å was indexed as (11 −1) by Yoder & Eugster (1955). Based on our results and on the pattern described by Higashi (1982), we conclude that the reflection may be better indexed as (11 −1). The tobelite can be indexed on the basis of a 1M cell implying a spacegroup Cm or C2. The X-ray pattern is listed in Table 3. The cell parameters are given in Table 4. The calculated specific gravity of tobelite calculated from our unitcell data is 2.57 g.cm^{-3}.

Table 3. X-ray pattern of synthetic tobelite.

hkl	d (calc.) (Å)	d (obs.) (Å) (Guinier)	I/I_0 (diffract.)
0 0 1	10.34	10.33	100
0 0 2	5.17	5.18	50
0 2 0	4.51	4.51	70
1 1 −1	4.38	4.38	33
0 2 1	4.13	4.13	16
−1 1 2	3.71	3.71	52
0 0 3	3.45	3.45	62
0 2 2	3.40	3.40	22
−1 1 3	2.989	2.991*	13
0 2 3	2.738	2.744*	16
1 3 0	2.593	2.594	10
0 0 4	2.584	2.582*	47
−1 3 1**	2.578		
2 0 0	2.562	2.564	13
−2 0 2	2.504	2.505*	21
1 3 1	2.457	2.457*	26
−1 3 2	2.418	2.418	22
2 0 1	2.378	2.379*	14
0 4 0	2.255	2.254*	9
1 3 2	2.229	2.228	9
2 2 0	2.228		
−1 3 3	2.181	2.184*	16
0 0 5	2.067	2.072*	21
−2 4 1	1.707	1.707	18
0 4 4	1.699	1.699	10
−3 3 1	1.507	1.508*	27
0 6 0	1.503	1.505*	

* reflections used in the least squares refinement.
** indices for this reflection used in the refinement.
The indexing is largely after Higashi (1982).

TGA and DTA

In the study of silicates with structurally bound ammonium the release of volatiles is an interesting topic. Cooper & Abedin (1981) suggested that thermal metamorphism at great depth of ammonium containing minerals is a possible source for nitrogen in metamorphic fluids. TGA and DTA are suitable techniques for such studies. An experimental setup for DTA at pressures up to 2000 bar will soon become available in our laboratory.

TGA was executed with a Dupont 1090 Thermal Analyser, using a heating rate of 10° C/min. Decomposition of tobelite ($NH_4Al_2Si_3AlO_{10}(OH)_2$) releases 1 mole of NH_3 and 1.5 mole of water. Tobelites formed according to reaction (2) and reaction (5) were analysed. The results are shown in Figs. 4a and 4b as solid lines. DTG-curves, calculated from the weight loss data are displayed in the same diagrams as dashed lines. The tobelites after reaction (2) and (5) loose 10.8 and 11.5 wt% respectively. The ideal tobelite should loose 11.7 wt%. The data demonstrate the improved purity of the syntesis products after reaction (5) with respect to that of reaction (2) (Table 2). In the DTG-curves two distinct peaks for each sample appear, representing the temperatures of maximum rate of weight loss. They are positioned at 600° and 750° C in Fig. 4a and at 650° and 850° C in Fig. 4b. The decomposition in two steps is consistent with the results of Higashi (1978), who ascribed the lower temperature step to the detachment of ammonia from the structure. It can be noted in Figs. 4a and 4b the peaks in the DTG-curve differ not only by the height of the maxima, but also by their sharpness. Even the H_2O-peaks show a difference in sharpness; the H_2O-peak in Fig. 4a is smoother than the one in Fig. 4b. It is suggested that the loss

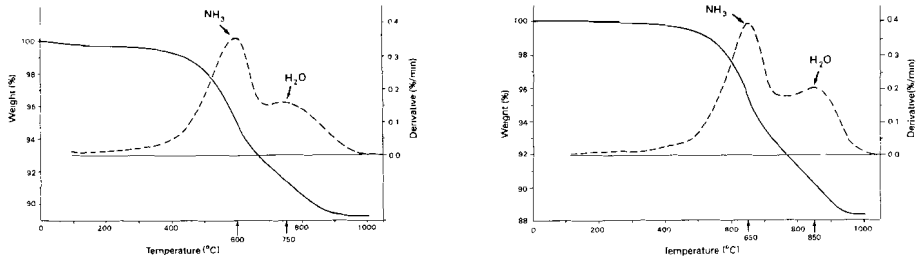

Fig. 4a (left) and Fig. 4b (right). TGA (solid line) and DTG (dashed line) plot of tobelite made according to reaction (2) (Fig. 4a) and made according to reaction (5) (Fig. 4b). Note that in each of the plots the peaks differ not only in height, but also in sharpness. The more flattened high-temperature curves indicate a more gradual loss of water relative to ammonia.

of H_2O proceeds more gradually than that of NH_3, and that the tobelite formed after reaction (2) loses its H_2O slower than the tobelite formed after reaction (5). The maxima of the NH_3- and H_2O-peaks are recorded with temperature intervals of 150° and 200° C in Figs. 4a and 4b.

DTA was performed applying the same heating rate as for the TGA. The DTA curves reveal two adjacent broad endothermic peaks for both micas, at 595° and 775° C for the tobelite fomed after reaction (2) and at 675° and 850° C for the one formed after reaction (5), respectively. The DTA temperatures are comparable with the TGA/DTG temperatures. Barrer & Dicks (1966), using a heating rate of 10° C/min., noted similar DTA peaks, but at temperatures of 500° and 600° C. Higashi (1982) described two endothermic DTA peaks for the decomposition of the well crystallised tobelite from the Horo locality at 575° and 605° C and for the tobelite from the Tobe deposit at 530° and 560° C, respectively; the difference in decomposition temperatures of the two micas is ascribed to variation in crystallinity and to interstratification of the Tobe material with some smectite. Unfor-

Table 4. Cell parameters of tobelites and of 1M muscovites and paragonite.

	This work Synthetic tobelite	Eugster and Munoz (1966) Synthetic tobelite	Higashi (1982) Natural 1M tobelite from the Tobe district
a_0(Å):	5.230 ± 0.007	5.217 ± 0.003	5.219 ± 0.004
b_0(Å):	9.02 ± 0.01	9.001 ± 0.003	8.986 ± 0.003
c_0(Å):	10.55 ± 0.01	10.540 ± 0.002	10.447 ± 0.002
β(°):	101.56 ± 0.01	101.37	101.31 ± 0.01
V(Å³):	487.5 ± 0.7	485.33	480.44

	Barrer and Dicks* (1966) Synthetic tobelite	Barrer and Dicks* (1966) Synthetic 1M muscovite	Yoder and Eugster (1955) Synthetic 1M muscovite	Chatterjee (1970) Synthetic 1M paragonite
a_0(Å):	5.18	5.214	5.208 ± 0.010	5.139 ± 0.003
b_0(Å):	8.96	8.994	8.995 ± 0.020	8.885 ± 0.002
c_0(Å):	10.49	10.278	10.275 ± 0.005	9.750 ± 0.003
β(°):	101.4	101.69	101.58 ± 0.08	98.87 ± 0.03
V(Å³):	–	–	–	439.8 ± 0.3

* no error values given by the authors.

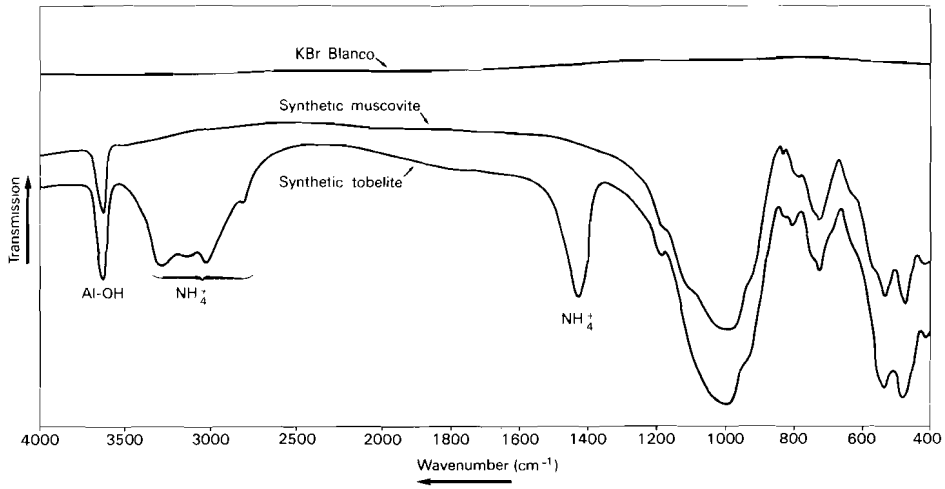

Fig. 5. IR-spectrum of synthetic tobelite. An IR-spectrum of synthetic muscovite, prepared in 3 weeks at 600° C and 5 kbar, is drawn for reference. A spectrum of a KBr blanco is displayed at the top of the figure.

tunately, heating rates were not specified, and this complicates the comparison of data.

IR-spectroscopy

IR-spectra of synthetic tobelites were reorded with a Perkin-Elmer 540 IR-Spectrometer, using KBr-tablets, which were dried for 24 hours at 300° C. The spectra reveal patterns of IR-vibrations which are consistent with data by Shigorova et al. (1981) and Higashi (1982). A typical pattern is displayed in Fig. 5. Band positions in the region 4000–1200 cm^{-1} are dominated by OH-stretching vibrations at about 3600 cm^{-1}, distinct NH_4^+-stretching vibrations between 3300–2800 cm^{-1}, and the NH_4^+-bending vibrations around 1430 cm^{-1}. From Fig. 5 and the literature data on the IR spectra of muscovite (Vedder, 1964; Velde, 1980; Langer et al., 1981), paragonite, margarite (Langer et al., ibid.), and the Rb-analogue of muscovite (Voncken et al., 1987) it is concluded that the NH_4^+-vibrations are readily perceived in dioctahedral micas. This makes IR-spectroscopy a very suitable technique for the determination of tobelite. The NH_4^+-vibration (ν_4) at 1430 cm^{-1} can be used for the ammonia analysis of micas (Shigorova, 1982; Duit et al., 1986). However, in unprepared whole rock analysis the 1430 cm^{-1} vibrations can be disturbed by carbonate vibrations. As a precaution acid treatment of the powdered whole rock sample is necessary.

Discussion

Our experiments show, that tobelite forms readily at temperatures of about 500° C and pressures up to 5 kbar in the presence of excess NH_3. In several runs with relatively low NH_3 fugacities, we encountered minor amounts of other products. The unexpected formation of feldspar after method (2) may be explained by the use of a Al-Si gel. It is possible that the three-dimensional framework-like structure of the gel leads to a metastable formation of feldspar instead of mica. An alternative explanation may be an initial high ammonia fugacity. According to Hallam & Eugster (1976), at 500° C buddingtonite may be stable at a NH_3 fugacity larger than 10^{-4}, whereas at lower fugacities tobelite is the

stable phase. The initial ammonia fugacity may be sufficiently high to form stable NH_4-feldspar. Because the runs were not buffered f_{NH3} will decrease as the reaction proceeds and finally tobelite will be the stable ammonium mineral. In the runs where a gel was applied the feldspars may grow to a rather large size and the run times were not long enough to let the feldspar disappear completely by the tobelite forming reaction. The buddingtonite crystal in Fig. 2b, which is covered with tiny tobelite crystals, illustrates the formation of feldspar prior to the crystallisation of the mica. Loss of NH_3 during welding may account for the presence of quartz and corundum or aluminosilicate in some of the runs. As quartz and corundum are incompatable with respect to each other, formation of andalusite could be expected. Perhaps the formation of a metastable mullite-like phase in a run after reaction (5) signifies the onset of aluminosilicate formation. The solubilities of alumina and silica are high under the chemical conditions of reaction (5) because the solution is very basic. This might have influenced the formation of an (unstable) aluminosilicate. The metastable aluminosilicate was, however, only detected in a 4 kbar run.

A temperature as high as 500° C was necessary to speed up reaction rates to run times of 3 weeks. In natural environments tobelite may occur at much lower temperatures (Juster, 1984).

From the unit cell data it is evident that our 1M tobelite cell is relatively large. Eugster & Munoz (1966) did not state explicitly that the micas which they describe are of the 1M polytype, but it is tentatively suggested by the quotation of the c-axis. The natural 1M tobelite has a fine scale interlayering of smectite, and small amounts of potassium are present in the crystal structure (Higashi, 1982). Both observations may account for the variation in the until cell parameters. Higashi (1982) reported a $2M_2$ polytype of natural tobelite from the Horo locality, and Juster (1984) reported a natural $2M_1$ polytype. No cell parameters were reported for these micas.

Micas crystallised after reaction (5) show the highest decomposition temperatures. The maximum of H_2O-loss occurs at a higher temperature than the maximum of NH_3-loss. H_2O will have more difficulty to escape than NH_3 because the hydroxyl groups are more strongly bound than the ammonium groups. Barrer & Dicks (1966) as well as Higashi (1982) obtained their results from mica fractions of about 1 micrometre. The sizes of the tobelites in our TGA/DTA studies are in general larger than 4 micrometres (Figs. 1, 3a, 3b). Crystal size may explain the differences between our results and those of Barrer & Dicks (1966) and Higashi (1982), as well as the difference between our samples. Differences in crystallinity may provide an other explanation for the differences between our results and literature data. However, if the width of diffractometer peaks at half height is taken as a measure of crystallinity, our samples may be considered to show a similar crystallinity. Another explanation for the differences between our results and those of Higashi (1982) may be that his natural tobelite contains some potassium and is interlayered with smectite.

In natural environments, buddingtonite is encountered about as frequently as tobelite. We suggest that the NH_4^+-mica may be a rather common mineral, especially in NH_3-rich environments. Fossil fuel deposits are very interesting in this context, because in these environments NH_3 is likely to be produced by the decomposition of amino-acids. Clay minerals (vermiculite, kaolinite) may serve as precursors for ammonium mica formation (Gruner, 1939; Levinson & Day, 1968; Shigorova et al., 1981).

Although up to now tobelite seems to be rather rare, it may have been mostly overlooked in mineralogical studies. Generally, routine chemical analyses of minerals and rocks do not include standard NH_4^+-analyses. Microprobe analyses of silicates with unexpected NH_4^+-incorporation yield too low totals and the analyses would tend to be discarded, rather than complemented with mineral separation and wet chemical analyses, or other analytical methods (e.g. IR-spectroscopy).

Pure tobelite separates can be readily distinguished from muscovite and paragonite by their X-ray pattern. The intensity of the (0 0 1) reflection of muscovite is relatively increased by ammonium incorporation (Higashi, 1978). Comparison of the cell parameters of synthetic or natural 1M dioc-

tahedral micas with those of tobelite makes it apparent that tobelite has the largest unit cell, as is to be expected from the relative size of the ionic radii of Na^+, K^+, and NH_4^+. IR-spectrometry executed with KBr-tablets offers a simple and quick method for detecting NH_4^+-incorporation, which is determinative for tobelite with respect to other dioctahedral micas.

Conclusions

1. Tobelite is formed relatively easy at temperatures of about 500° C and pressures up to 5 kbar in the presence of excess NH_3.
2. Tobelite may be a rather common mineral in fossil fuel deposits where the decomposition of amino-acids may lead to the formation of a NH_3-rich environment.
3. Tobelite can be readily identified using X-ray diffraction combined with IR-spectroscopy.
4. Tobelite, synthesised in our experiments, can be indexed on the basis of a 1M unit cell. The cell parameters are larger than those reported in the literature for natural and synthetic 1M tobelites.
5. Thermal decomposition temperatures of the tobelite are above 500° C at 1 atm.
6. During decomposition of tobelite in TGA and DTA, ammonia is released at a faster rate and at a lower temperature than water.
7. The choice of starting materials is of influence on the formation of stable and metastable phases.
8. Liquid nitrogen as cooling agent during welding of capsules is advisable when easily volatised starting materials are used.

Acknowledgements

G. Kastelein is thanked for his technical assistance in the high pressure laboratory. C. Laman made the diffractometer recordings and the Guinier films. G.P.J. Geelen performed a part of the SEM-work. P. van Krieken and A. Romeyn (Department of Geography, University of Utrecht) performed the TGA/DTG and the DTA analyses. A. Feenstra and A. Senior critically reviewed the text. The IR-spectrometer is financially supported by Z.W.O-W.A.C.O.M. The Dr. Schürmann Foundation is thanked for financial support for the purchase of the noble metals required for the experiments.

References

Aaftink, G. 1985. Ion echange of K^+ and NH_4^+ in synthetic muscovites – Internal report, (in Dutch), State University of Utrecht· 23 p

Barrer, R.M. & Dicks, L.W.R. 1966. Chemistry of Soil Minerals, Part III. Synthetic micas with substitutions of NH_4 for K, Ga for Al and Ge for Si – J. Chem. Soc. A: 1379–1385

Bos, A., De Haas, G.J., Voncken, J.H.L., Van der Eerden, A.M.J. & Jansen, J.B.H. 1987. Hydrothermal synthesis of ammonium phlogopite – Geol. Mijnbouw, 66: 251–258 (this issue)

Chatterjee, N.D. 1970. Synthesis and upper stability of paragonite – Contrib. Mineral. Petrol. 27: 244–257

Cooper, J.E. & Abedin, K.Z. 1981. The relationship between fixed ammonium-nitrogen and potassium in clays from a deep well in the Texas Gulf Coast – Tex. J. Sci. 33: 103–111

Cooper, J.E. & Evans, W.S. 1983. Ammonium-nitrogen in Green River Formation Oilshale – Science 219: 492–493

Duit, W., Jansen, J.B.H., Van Breemen, A. & Bos, A. 1986. Ammonium micas in metamorphic rocks as exemplified by Dome de L'Agout (France) – Am. J. Sci. 286: 702–732

Erd, R.C., White, D.E., Fahey, J.J. & Lee, D.E. 1964. Buddingtonite, an ammonium feldspar with zeolitic water – Am. Mineral. 49: 831–850

Eugster, H.P. & Munoz, J.M. 1966. Ammonium micas: possible sources of atmospheric ammonia and nitrogen – Science 151: 683–686

Gruner, J.W. 1939. Ammonium mica synthesized from vermiculite. – Am. Mineral. 24: 428–433

Hallam, M. & Eugster, H.P. 1976. Ammoniumsilicate stability relations – Contrib. Mineral. Petrol. 57: 227–244

Hamilton, D.L. & Henderson, C.M.B. 1968. The preparation of silicate compositions by a gelling method – Mineral. Mag. 36: 832–838

Higashi, S. 1978. Dioctahedral mica minerals with ammonium ions – Mineral. J. (Tokyo) 9: 16–27

Higashi, S. 1982. Tobelite, a new ammonium dioctahedral mica – Mineral. J. (Tokyo) 11: 138–146

Honma, H. & Itihara, Y. 1981. Distribution of ammonium in minerals of metamorfic and granitic rocks – Geochim. Cosmochim. Acta 45: 983–988

Hori, H., Nagashima, K., Yamada, M., Miyawaki, R. & Marubashi, T. 1986. Ammonioleucite, a new mineral from Tatarazawa, Fujioka, Japan – Am. Mineral. 71: 1022–1027

Itihara, Y. & Honma, H. 1979. Ammonium in biotite from metamorphic and granitic rocks in Japan – Geochim. Cosmochim. Acta 43: 503–509

Juster, Th. C. 1984. Very low grade metamorphism of pelites, associated with coal, Northeastern Pennsylvania – MSc thesis, University of Wisconsin-Madison: 101 pp

Langer, K., Chatterjee, N.D. & Abraham, K. 1981. Infrared studies of some synthetic and natural $2M_1$ dioctahedral micas – Neues Jahrb. Mineral. Abh. 142: 91–110

Levinson, A.A. & Day, J.J. 1968. Low temperature hydrothermal synthesis of montmorillonite, ammonium-micas and ammonium-zeolites – Earth Planet. Sci. Lett. 5: 52–54

Loughnan, F.C., Ivor-Roberts, F. & Lindner, A.W. 1983. Buddingtonite (NH_4-feldspar) in the Condor Oilshale Deposit, Queensland, Australia – Mineral. Mag. 47: 327–334

Milovskiy, A.V. & Volynets, V.F. 1966. Nitrogen in metamorphic rocks – Geochem. Int. 3: 752–758

Norman, D.I. & Palin, J.M. 1982. Volatiles in phyllosilicate minerals – Nature 296: 551–553

Shigorova, T.A., Kotov, N.V., Kotel'nikova, Ye.N., Shmakin, B.M. & Frank-Kamenetzkiy, V.A. 1981. Synthesis, diffractometry and IR-spectroscopy of micas in the series from muscovite to the ammonium analogue – Geochem. Int. 18: 76–82

Shigorova, T.A. 1982. The possibility of determining the ammonium cntent of mica by IR spectroscopy – Geochem. Int. 19: 110–114

Sterne, E.J., Reynolds, R.C. Jr & Zantop, H. 1982. Natural ammonium illites from black shales hosting a stratiform base metal deposit, Delong Mountains, Northern Alaska – Clays Clay Miner. 30 161–166

Thorstenson, D.C. & Mackenzie, F.T. 1971. Experimental decomposition of algae in seawater and early diagenesis – Nature 234: 543–545

Tsunashima, A., Kanamaru, F., Ueda, S., Koizumi, M. & Matshushita, T. 1975. Hydrothermal syntheses of amino acid-montmorillonites and ammonium micas – Clays Clay Miner. 23: 115–118

Tuttle, O.F. 1949. Two pressure vessels for silicate water-studies – Geol. Soc. Am. Bull. 60: 1727–1729

Vedder, W. 1965. Ammonium in muscovite – Geochim. Cosmochim. Acta 29: 221–228

Vedder, W. 1964. Correlations between infrared spectrum and chemical composition of micas – Am. Mineral. 49: 736–768

Velde, B. 1980. Cell dimensions, polymorph type, and infrared spectra of white micas: the importance of ordening – Am. Mineral. 65: 1277–1280

Voncken, J.H.L., Van der Eerden, A.M.J. & Jansen, J.B.H. 1987. Synthesis of a Rb analogue of $2M_1$ muscovite – Am. Mineral. 72: 551–554

Wlotzka, F. 1961. Unterzuchungen zur Geochemie des Stickstoffs – Geochim. Cosmochim. Acta 24: 106–154

Yamamoto, T. & Nakahira, M. 1966. Ammonium in sericites – Am. Mineral. 51: 1775–1778

Yoder, H.S. & Eugster, H.P. 1955. Synthetic and natural muscovites – Geochim. Cosmochim. Acta 8: 225–280

CHAPTER III.

Hydrothermally Grown Buddingtonite, an Anhydrous Ammonium Feldspar ($NH_4AlSi_3O_8$)

J.H.L. Voncken, R.J.M. Konings*, J.B.H. Jansen, and C.F. Woensdregt
Institute for Earth Sciences, University of Utrecht, Budapestlaan 4, P.O. Box 80.021. 3508 TA Utrecht, The Netherlands

Abstract. Ammonium feldspar was grown hydrothermally from a gel, having a stöchiometric $Al_2O_3 \cdot 6SiO_2$ composition. As a source for NH_4^+, a 25 percent NH_3 solution was used. Internal Cr/CrN and graphite/methane buffers fixed the fugacity of NH_3 during the experiments. Unit cell parameters of the synthetic ammonium feldspar are *a*: 0.8824 (5) nm, *b*: 1.3077 (8) nm, *c*: 0.7186 (4) nm, β: 116.068 (12)°, *V*: 0.7448 (34) nm^3. The X-ray powder diffraction pattern is measured and indexed in accordance to the space group *C2/m*. Infrared and thermal gravimetric analyses provide no evidence for the presence of structurally bound water molecules in the crystal structure of synthetic ammonium feldspar. Hydrothermally grown anhydrous ammonium feldspar is shown to be identical to the mineral buddingtonite by the similarity of the data between the synthetic and natural materials. There may be justification for considering natural buddingtonite as an anhydrous feldspar with the ideal formula $NH_4AlSi_3O_8$. Reexamination of natural specimens is desirable.

Introduction

The mineral buddingtonite ($NH_4AlSi_3O_8.1/2H_2O$) was first described by Erd et al. (1964) as a monoclinic ammonium feldspar with zeolitic water. It occurs as a replacement of plagioclase in an ammonium rich hot spring system of Sulphur Bank, Lake County, California. Wet chemical, infrared, thermogravimetric and differential thermal analyses provided supportive evidence for the presence of zeolitic water in natural buddingtonite. Erd et al. (1964) stated that the mineral is an anhydrous phase above 430° C. Gulbrandsen (1974) found buddingtonite in the Meade Peak Member of the Phosphoria Formation, SE Idaho, USA, where it is the principal constituent of a mudstone interval between two phosphate rich beds. It is probably of diagenetic origin. Kimbara and Nishimura (1982) found buddingtonite in the Tōshichi Spa, Iwate Prefecture, Japan. The mineral occurs as a replacement of plagioclase in a hydrothermally altered pyroclastic rock. Loughnan et al. (1983) described the occurrence of uniformly distributed buddingtonite throughout the upper part of the Condor Oilshale Deposit in Queensland, Australia. The buddingtonite in the Condor Deposit is also thought to be of a probable diagenetic origin.

Synthetic ammonium feldspar is reported in only a few studies. Barker (1964) synthesized a nearly pure buddingtonite (97.3 percent of the theoretical NH_4^+) through a cation exchange reaction between NH_4Cl and synthetic alkali feldspar (Or_5Ab_{95}) at 550° C and 2000 bar. Hallam and Eugster (1976) determined the stability relations of the ammonium silicates buddingtonite and tobelite, the ammonium analogue of muscovite (Higashi 1982). They used the Cr/CrN and graphite/methane buffers and proved that relatively high values of f_{NH3} are necessary for the formation of ammonium feldspar.

Because the presence of structurally bound water molecules remains questionable, we have examined synthetic ammonium feldspar by means of X-ray diffraction, thermal analysis, infrared absorption and scanning electron microscopy.

Experimental Techniques

The starting material for the ammonium feldspar synthesis consisted of coprecipitated gels, with a composition of $Al_2O_3.6SiO_2$, prepared according to the method of Hamilton and Henderson (1968). The chemicals used for the gel preparations were $Al(NO_3)_3$ (Merck no. 1063, p.a.) and T.E.O.S. (Merck-Schuchardt No. 800658, p.a.). A 25 percent NH_3 solution (Merck No. 5432, p.a.) was the ammonium source. Ammonia was added in excess. Chromium powder (Ventron No. 00672), chromium nitride powder (Ventron No. 49112) and graphite (Norit) were applied for the buffering of the ammonia fugacity during the reaction, following the method described by Hallam and Eugster (1976).

The Al–Si gel was placed in an unsealed platinum tube. This tube was tightly crimped on both sides and placed in a larger platinum tube, welded on one side, and containing Cr and CrN in known amounts. Subsequently, the ammonia was added. The outer tube was welded with a carbon-arc while it was constantly cooled in a water bath. The platinum capsule was placed in a larger gold capsule, welded on one side and containing a known amount of graphite. The gold capsule was welded under cooling from a water bath. The synthesis experiments were carried out in externally heated cold seal pressure vessels (Tuttle 1949). Argon gas was the pressure medium. The experiments were

* Present address: Netherlands Energy Research Foundation ECN, P.O. Box 1, 1755 ZG Petten, The Netherlands

Table 1. Experimental results. $P = 2$ Kbar

Run nr.	T in °C	Run time in days	Quench time in min[a]	Phases produced
RK18	550	10	15	buddingtonite + minor tobelite[b]
RK21[c]	590–550	5	15	buddingtonite + minor tobelite[b]
RK33[c]	660–570	10	15	tobelite + quartz
JV85A-E88	600	14	15	buddingtonite + minor tobelite
JV85B-E89	600	14	15	buddingtonite + minor tobelite
JV110-E205	600	18	15	buddingtonite + minor tobelite
JV110-E206	600	18	15	buddingtonite + minor tobelite
JV110-E207	600	18	15	buddingtonite + minor tobelite
JV96A-E127	600	14	5	buddingtonite
JV96B-E128	600	14	5	buddingtonite
JV96C-E129	600	14	5	buddingtonite

[a] times by approximation for cooling to room temperature. Quench times differ slightly for different run temperatures
[b] SEM-photographs of the run products are shown in Figure 3a and b
[c] slow cooling to the lower temperature

run at 2 kbar total pressure in the temperature range region of 660–550° C at either constant or decreasing temperature. For the latter experiments a programmable temperature controller (Eurotherm) was used. The experimental conditions and results are summarised in Table 1. Temperatures were measured with chromel-alumel thermocouples and are considered to be accurate to ±5° C. The pressure was read from a bourdon-type pressure gauge which was calibrated against a Heise precision gauge of which the accuracy is ±10 bar. After quenching with compressed cold air the capsules were reweighed to check for leakage. The buffer materials were checked by XRD and appeared never to be exhausted. Optical examination with a polarising microscope showed ammonium feldspar as colourless grains, generally about 10–30 µm length. The largest crystals appeared to be too small for a well oriented determination of the optical properties. In general, the yield of successful ammonium feldspar synthesis runs was at least about 98 percent. If no other phases could be identified with XRD, optical microscope and SEM, the sample was considered to be pure buddingtonite. Tobelite is often found as a minor phase (Table 1) and it is considered to occur as a run product from insufficiently rapid quenching, because its stability field is traversed during cooling.

Analytical Methods

The X-ray powder diffraction patterns have been obtained with a Guinier FR552 (Enraf Nonius) focussing camera using Cu$K\alpha$1 radiation. Heating stage X-ray diffraction was carried out using a HT Guinier Cu$K\alpha$1 (Enraf Nonius FR553) focussing powder camera. A heating rate of 25° C per h was applied from 20° C to 1020° C. For determination of the unit cell parameters, silicon powder was taken as internal standard. Peak positions and intensities have been recorded in this procedure with a double beam recording microdensitometer (MK IIICS; Joyce and Loebl & Co Ltd). The unitcell refinements were made with the computer program UNITCELLC (Strom 1976a). Thermogravimetric analysis were made in air with a Dupont 1090 Thermal Analyser with a heating rate of 10° C per minute. Infrared absorption spectra were measured from powdered samples in KBr disks, with a Perkin Elmer 580 IR spectrophotometer. For morphological analysis, the run products were examined by means of a Cambridge S150 or M600 scanning electron microscope.

Table 2. X-ray powder diffraction data of hydrothermally grown buddingtonite

hkl	d_{hkl} obs (Å)	I/I_o	*hkl*	d_{hkl} obs (Å)	I/I_o
110	6.78	25	022	2.899	20
020	6.54	35	$\bar{3}11$	2.870	15
001	6.47	25	$\bar{1}32$	2.776	10
$\bar{1}11$	5.93	50	$\bar{3}12$	2.656	20
$\bar{2}01$	4.336	100	$\bar{2}41$	2.611	30
111	3.989	45	240	2.522	15
130	3.820	75	$\bar{1}51$	2.434	12
$\bar{1}31$	3.643	15	330	2.260	15
$\bar{1}12$	3.470	40	060	2.180	18
220	3.390	90	241	2.154	12
$\bar{2}02$	3.323	60	$\bar{1}52$	2.116	8
040	3.269	40	$\bar{4}22$	2.056	15
002	3.234	90	222	1.994	15
131	3.020	40	400	1.982	15
$\bar{2}22$	2.963	25			
041	2.918	20			

Results

X-ray Powder Diffraction

The d_{hkl} values of buddingtonite, given by Erd et al. (1964), Gulbrandsen (1974), Kimbara and Nishimura (1982) and Loughnan et al. (1983) are indexed according to a primitive *P*-cell. Kimball and Megaw (1974) suggest a *C*-cell symmetry for the holotype buddingtonite. We have indexed the pattern of synthetic ammonium feldspar according to a *C* centered unit cell, as in the case of high sanidine (Ribbe 1963). The d_{hkl} values of the hydrothermal ammonium feldspar and their intensities are listed in Table 2. The lattice

Table 3. Unit cell parameters of hydrothermally grown buddingtonite

Space group	a (nm)	b (nm)	c (nm)	β(°)	V (nm^3)
$C2/m$	0.8824 (5)	1.3077 (8)	0.7186 (4)	116.068 (12)	0.7448 (34)[a]
	0.8804 (2)	1.3024 (3)	0.7183 (1)	116.105 (18)	–[b]

[a] This work
[b] D.E. Appleman in Kimbal and Megaw (1974). Natural holotype buddingtonite from the Sulphur Bank Deposit. Figures in parentheses represent the estimated standard deviation and refer to the last decimal place

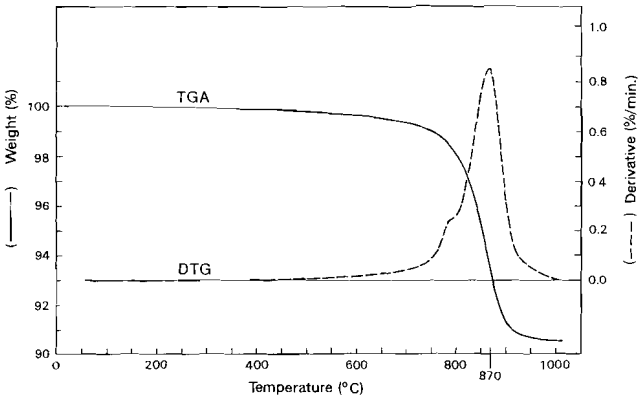

Fig. 1. TGA (solid line) and DTG (dashed line) curve of ammonium feldspar

parameters are given in Table 3. They are in good agreement with the values reported by Kimball and Megaw (1974) for natural buddingtonite from the Sulphur Bank Deposit.

In HT-XRD, the ammonium feldspar pattern does not change up to approximately 650° C. Above this temperature many lines grow weaker and eventually fade in the temperature region of 770 to 830° C. Above 830° C the structure is amorphous. These results agree with those of Loughnan et al. (1983). They mention that the XRD-pattern of a heated natural buddingtonite from the Condor Oilshale Deposit remains virtually unaffected up to 500° C. Remnants of the feldspar pattern could be traced by them to about 750° C. The temperature interval of 770 to 830° C found for the breakdown of the synthetic ammonium feldspar in HT-XRD marks the onset of its decomposition in the thermogravimetric analysis of Figure 1. In the TGA the silicate decomposed between 800 and 900° C. In a TGA applying the same heating rate as in the HT-XRD, the decomposition took place between 750 and 850° C.

Thermogravimetric Analysis

The decomposition reaction of anhydrous ammonium feldspar may be written as follows:

$$2\,NH_4AlSi_3O_8 \rightarrow 2\,NH_3 + H_2O + 6\,SiO_2 + Al_2O_3$$

Taking the formula as $NH_4AlSi_3O_8$, the ideal weight loss should be 10.1 weight percent. Figure 1 shows a thermogravimetric analysis of pure ammonium feldspars. Below 400° C no weight losses are detected. At about this temperature, the sample starts to lose weight very slowly. The total weight loss is approximately 9.5 weight percent and it occurs mainly between 800 and 900° C. It is in good agreement with the ideal value. A DTG-curve, calculated from the weight loss data shows a large peak at 870° C with a small shoulder at about 800° C. The peak and the shoulder may be attributed to the loss of $2NH_3 + H_2O$ according to the above reaction. A TGA (not shown), with the same heating rate as the HT-XRD, yielded a loss of 9.6 weight percent. If we assume that ammonium feldspar is represented by the formula $NH_4AlSi_3O_8 \cdot 1/2H_2O$, like natural buddingtonite, the ideal weight loss would be 13.1 weight percent. This value diverges strongly from the experimental results. Erd et al. (1964) report, however, a weight loss of 12.0 weight percent for natural holotype buddingtonite. Loughnan et al. (1983) recorded a total weight loss of 11.7 weight percent for natural buddingtonite, heated to 600° C.

IR-Spectroscopy

Figure 2 shows the spectra of the KBr carrier material, at 20° C and when dried at 120° C and the spectra of ammonium feldspar from the run JV110-E206 (Table 1) at 20, 120 and 450° C in the spectral range of 4000–400 cm^{-1}. A spectrum of synthetic tobelite, $NH_4Al_2Si_3AlO_{10}(OH)_2$, (Voncken et al. 1987) is added for reference. The absorption

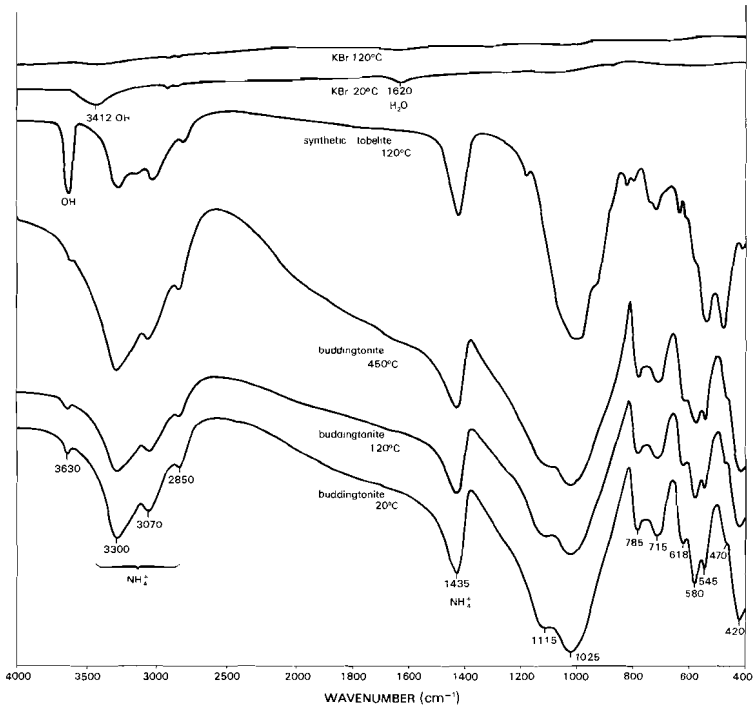

Fig. 2. IR spectra of KBr blank at 20° C and 120° C, and of ammonium feldspar (run JV110-E206) at 20, 120 and 450° C. The ammonium feldspar spectrum at 20° C was correcte d for the KBr spectrum at 20° C by placing the blanc KBr disk in the reference beam. A spectrum of synthetic tobelite is added for reference

maxima of synthetic ammonium feldspar are listed in Table 3, together with the IR data given by Erd et al. (1964). The maxima at 3300, 3070, 2850 and 1435 cm^{-1} are due to the stretching and bending vibrations of ammonium (Shigorova et al. 1981; Hori et al. 1986). An excellent agreement exists between the absorption maxima of the synthetic and natural buddingtonite, except for the absorption maxima at 3412, 1620 and 731 cm^{-1}, which occur in the natural buddingtonite spectrum. Erd et al. (1964) assigned the 3412 cm^{-1} frequency to residual water in stretching mode and the 1620 cm^{-1} to the bending mode vibrations of water. They attributed the band at 3650–3500 cm^{-1} to structurally bound water as a results of a comparison between the IR-spectra of buddingtonite and NH_4^+-montmorillonite. Even though the maximum at 3630 cm^{-1} in our buddingtonite spectra could be explained by the presence of water molecules (Hofmeister and Rossman 1985; Beran 1986), there exists another and more plausible explanation. The mineral tobelite has one of its strongest absorption maxima at 3630 cm^{-1} (Voncken et al. 1987). As tobelite occurs in several runs as a secondary phase (Table 1), the absorption maximum at 3630 cm^{1} in our ammonium feldspar spectra can better be explained by the presence of small amounts of the ammonium mica.

Crystal Morphology

The structure of the feldspars is formed by tetrahedra of $(Si, Al)O_4$, linked to each other in three dimensions. Large cations fill the open spaces in the tetrahedral network. The crystal faces of high sanidine can be classified by the PBC method into relatively slow growing *F*-faces and others, less important for the crystal morphology. The most important of the *F*-faces (F_1 faces) are parallel to at least two PBC's of strong Si, Al-bonds. They are {*110*}. {*001*}, {*010*}, {$\bar{2}01$}, {*111*}. F_2 faces which are parallel to one PBC with only Si, Al bonds and one PBC with additional weaker K–O bonds, are {*130*}, {*021*}, {$\bar{2}21$}, {$\bar{1}12$}, {*100*} and {$\bar{1}01$} (Woensdregt 1982).

The crystals shown in the Figures 3a and 3b could be indexed either by direct measurement of interfacial angles or by means of the computer program CAMERA (Strom 1976b). The pictures display characteristic habits of hydrothermally grown buddingtonite crystals. The experiments were made at either constant (550° C) or decreasing temperature (10° C per day, from 590 to 550° C), but no difference in crystal morphology was observed. The tiny euhedral crystals (up to 0.05 mm) show {*010*}, {*110*}, {*100*}, {*001*} and {$\bar{1}01$}, while {*130*} is occasionally observed.

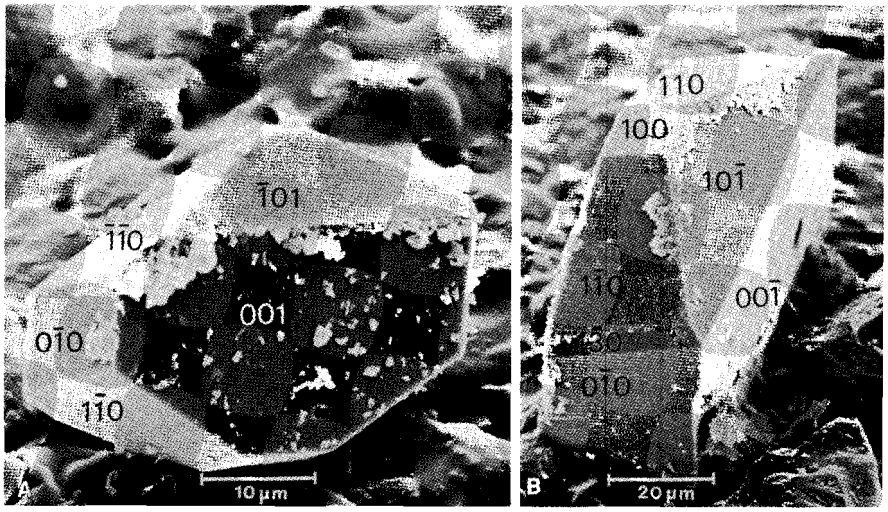

Fig. 3. **(A)** Buddingtonite crystal, grown at 550° C, 2 kbars. **(B)** Buddingtonite crystal, grown at 590–550° C, 2 kbars. The white flakes on the crystal faces are small NH_4-mica crystals (tobelite), believed to have been formed during quenching

Table 4. IR absorption maxima of hydrothermally grown and natural buddingtonite in cm^{-1}

(1)[a]	(2)[b]	(1)[a]	(2)[b]
3630[c]	3650–3600	785	785
–	3412	–	731
3300	3296	715	711
3070	3068	618	621
2850	2848	580	583
–	1620	545	546
1435	1419	470	466
1115	1117	420	425
1025	1034		

[a] This study
[b] Erd et al. (1964)
[c] attributed to tobelite impurity

The morphology of hydrothermally grown ammonium feldspar does not essentially differ from that of natural buddingtonite (Erd et al. 1964), and the agreement between the habits of buddingtonite and high sanidine is an indication that their crystal structures are very similar.

Discussion

In the feldspar structure little space is left for structural water, the cations occupy the main part of the cavities in the tetrahedral framework. Erd et al. (1964) reported for natural buddingtonite the chemical composition $NH_4AlSi_3O_8 \cdot 1/2H_2O$, suggesting a zeolitic nature for the half mole of water. Kimball and Megaw (1974) stated in their interim report on the X-ray structural investigations of the holotype buddingtonite specimen: "If the chemical formula proposed for buddingtonite by Erd et al. (1964) is correct, the half mole of water would appear to be completely disordered."

The X-ray powder diffraction pattern of synthetic ammonium feldspar can be indexed satisfactorily on the basis of the *C2/m* space group symmetry. There are some slight differences between the X-ray powder diffraction pattern of the synthetic ammonium feldspar and reported patterns of natural buddingtonites. The 6.47 and 2.116 Å reflections in the pattern of the synthetic material have not been observed in patterns of natural material. A reflection at 3.60 Å, observed in all natural buddingtonite patterns, except the one given by Loughnan et al. (1983), could not be identified with certainty in the pattern of the synthetic silicate. The 3.129 Å reflection reported by Erd et al. (1964) does not belong to buddingtonite and represents an impurity (R.C. Erd, pers. comm., 1987). The differences observed in the X-ray powder diffraction patterns may be caused by differences in the techniques applied. We used a Guinier powder camera, in contrast to the other workers mentioned above, who used a diffractometer. The X-ray diffraction and morphological data indicate a close similarity between synthetic ammonium feldspar and high sanidine.

The calculated density from our unit cell volume is 2.29 $g \cdot cm^{-3}$. From the unit cell data of Erd et al. (1964), using the anhydrous formula, a value of 2.31 $g \cdot cm^{-3}$ can be calculated, and similarly, a value of 2.30 $g \cdot cm^{-3}$ is obtained from the data of Kimbara and Nishimura (1982). Erd et al. (1964) calculated a value of 2.38 $g \cdot cm^{-3}$, using the hydrous formula. These authors measured, however, a specific gravity of 2.32 $g \cdot cm^{-3}$ for the holotype material. Gulbrandsen (1974) measured a specific gravity of 2.36 $g \cdot cm^{-3}$, but stated that the analysed grains were typically clouded with minute inclusions, that are presumed to be mostly organic matter, illite and iron oxide. Its appears, that our calculated density is in good agreement with values

calculated for natural buddingtonites and the measured value for the holotype material.

HT-XRD analysis of synthetic ammonium feldspar gives no indication of a significant change in the crystal structure upon heating. The TGA curve shows the absence of zeolitic water since no weight loss is observed beneath 400° C. Structural water in alkali feldspar may however persist up to 900° C (Beran 1986). Volatiles are slowly released between 400 and 800° C, whereas the decomposition of ammonium feldspar takes place very rapidly at higher temperatures. The maximum rate of weight loss is reached at 870° C. The total weight loss is in accordance with the formula $NH_4AlSi_3O_8$. Although we explain the 3630 cm^{-1} band in the IR-spectra by the presence of secondary tobelite, very minor replacement of *M*-site ammonium by structural water remains possible. As the molecular weights of water and ammonia are very similar, this would result in only a very minor change in the TGA data.

The DTA curves of Erd et al. (1964) show 2 broad exothermic peaks, the first one at 608 and the second one at 814° C. They state: "the larger broad exothermic peak at 608° C probably represents loss of ammonia, and the significance of the smaller exothermic peak at 814° C is not known." These authors attribute a small endothermic band at 119° C to loss of water. The unexplained DTA peak suggests the presence of an unidentified phase in the original sample. The occurrence of an unidentified ammonium-bearing phyllosilicate could explain the larger weight loss recorded for natural type buddingtonite with respect to its synthetic counterpart in TGA. If we take, on the basis of our experimental results, tobelite as a possible impurity, about 30 percent by weight of this mineral would be necessary to explain the difference in weight loss between the holotype buddingtonite and our synthetic material. There is no sign of any of the tobelite reflections in the XRD-pattern of the holotype buddingtonite. Small amounts of montmorrillonite are present, but do not show on the X-ray diffraction pattern of the type material (R.C. Erd, pers. comm., 1987).

At present, the large differences in TGA results between synthetic and natural material can not be explained. Re-examination of natural buddingtonite might shed more light on this subject.

Conclusions

1) Hydrothermally grown anhydrous ammonium feldspar is shown to be identical to the mineral buddingtonite as is borne out by the similarity of the data between the synthetic and natural materials.

2) Synthetic ammonium feldspar and high sanidine have similar crystal structures, as is evidenced by X-ray diffraction and crystal morphology data.

3) There may be justification for considering natural buddingtonite as an anhydrous feldspar with the ideal formula $NH_4AlSi_3O_8$.

Acknowledgements. The authors thank A. van der Eerden for his advice and help in the laboratory, G. Kastelein for his technical assistance, C. Laman for the (HT) X-ray powder diffraction analyses, F. Geelen for his help with the electron microscopy, P. van Krieken for the TGA analyses and C. Strom for corrections of the English text. Dr. R.C. Erd is thanked for his valuable suggestions and stimulating comments.

References

Barker DS (1964) Ammonium in alkali feldspars. Am Mineral 49:851–858

Beran A (1986) A model for the allocation of water in alkali feldspars, observed from infrared spectroscopy investigations. Phys Chem Minerals 13:306–310

Erd RC, White DE, Fahey JJ, Lec DE (1964) Buddingtonite, an ammonium feldspar with zeolitic water. Am Mineral 49:831–857

Gulbrandsen RA (1974) Buddingtonite, ammonium feldspar in the Phosphoria Formation, Southeastern Idaho. J Res US Geol Survey, Vol. 2, nr. 6:693–697

Hallam M, Eugster HP (1976) Ammonium silicate stability relations. Contrib Mineral Petrol 57:227–244

Hamilton DL, Henderson CMB (1968) The preparation of silicate compositions by a gelling method. Mineral Mag 36:832–838

Higashi S (1982) Tobelite, a new ammonium dioctahedral mica. Mineral J 11:138–146

Hofmeister AM, Rossman GR (1985) A spectroscopic study of irradiation coloring of amazonite: structurally hydrous, Pb bearing feldspar. Am Mineral 70:794–804

Hori H, Nagashima K, Yamada M, Miyawaki R, Marubashi T (1986) Ammonioleucite, a new mineral from Tatarazawa, Fujioka, Japan. Am Mineral 71:1022–1027

Kimball MR, Megaw HD (1974) Interim report on the crystal structure of buddingtonite. In: MacKenzie WS, Zussman J (eds) Feldspars. Proc. NATO ASI on Feldspars, Manchester. Manchester Press, pp 81–86

Kimbara K, Nishimura T (1982) Buddingtonite from the Tōshichi Spa, Iwate Prefecture, Japan. Kobutsugaki Zasshi, J Mineral Soc Jpn 15:207–216 (In Japanese, with English Abstract)

Loughnan FC, Roberts FI, Lindner AW (1983) Buddingtonite (NH_4-feldspar) in the Condor Oilshale Deposit, Queensland, Australia. Mineral Mag 47:327–334

Ribbe PH (1963) A refinement of the crystal structure of sanidinized orthoclase. Acta Crystallogr 16:426–427

Shigorova TA, Kotov NV, Kotel'nikova YeN, Shmakin BM, Frank-Kamenetzkiy VA (1981) Synthesis, diffractometry and IR-spectroscopy of micas in the series from muscovite to the ammonium analogue. Geochem Int 18:76–82

Strom C (1976a) UNITCELLC, An interactive APL program for computing cell constants. Geol Mineral Institute, State University of Leiden, The Netherlands

Strom C (1976b) Indexing crystal faces on SEM photographs. J Appl Crystallogr 9:291–297

Tuttle OF (1949) Two pressure vessels for silicate-water studies. Geol Soc Am Bull 60:1727–1729

Voncken JHL, Wevers JMAR, Van der Eerden AMJ, Bos A, Jansen JBH (1987) Hydrothermal synthesis of tobelite, $NH_4Al_2Si_3Al0_{10}(OH)_2$, from various starting materials and implications for its occurrence in nature. Geol Mijnbouw 66:259–269

Woensdregt CF (1982) Crystal morphology of monoclinic potassium feldspars. Z Kristallogr 161:15–33

Received July 14, 1987

CHAPTER IV.

HOLOTYPE BUDDINGTONITE FROM THE SULPHUR BANK QUICKSILVER DEPOSIT, CALIFORNIA : AN AMMONIUM FELDSPAR WITH ASSOCIATED MONTMORILLONITE

ABSTRACT

An amount of approximately 70 mg of the holotype buddingtonite mineral separate DW1 from the Sulphur Bank Quicksilver Deposit, Lake County, California, is studied with respect to its water content. This and another type mineral separate are compared with synthetic anhydrous ammonium feldspar. The samples were studied with XRD, IR-spectroscopy STEM, SEM, TGA, DTA and analyzed chemically. It is shown that the holotype buddingtonite sample DW1 contains admixtures of FeS_2, a Ti-containing phase, and, most important, montmorillonite. The presence of minor amounts of this clay mineral influences the IR-spectrum, TGA and DTA of the holotype buddingtonite. SEM illustrates that montmorillonite may occur as overgrowths on feldspar crystal faces. Montmorillonite is capable of reversible dehydration, and its admixture can explain the zeolitic behavior previously ascribed to buddingtonite. When occurring as overgrowths, even small amounts of montmorillonite result in a large active surface for (de)hydration. Buddingtonite can be considered as an ammonium feldspar without zeolitic water.

INTRODUCTION

Buddingtonite was first described by Erd et al. (1964) as an ammonium feldspar with zeolitic water, for which the formula $NH_4AlSi_3O_8.1/2H_2O$ was proposed. Evidence for this formula was provided by chemical analysis, XRD, thermal analysis, and IR-spectroscopy. The holotype buddingtonite was found as a hydrothermal replacement of plagioclase in certain parts of the Sulphur Bank Quicksilver Deposit, Lake County, California (White and Robertson, 1962). Several other occurrences of buddingtonite have been discovered since its first description (Gulbrandsen, 1974; Kimbara and Nishimura, 1982; Loughnan et al., 1983). These authors all accepted the hydrous formula that was proposed for buddingtonite.

Experimental studies on ammonium feldspars (Barker, 1964; Hallam and Eugster, 1976) were not conclusive either with respect to the zeolitic character of buddingtonite. A crystallographic study of holotype buddingtonite by Kimball and Megaw (1974) led to the conclusion that the buddingtonite structure can be regarded as a feldspar structure, in which the water was not present in an ordered way. The structure and properties of synthetic ammonium feldspar represent the anhydrous formula $NH_4AlSi_3O_8$ (Voncken et al.,(1988). Lattice parameters and X-ray diffraction pattern display a striking similarity with those of the natural ammonium feldspar. A possible explanation for the remaining differences in properties between natural and synthetic ammonium feldspar may be the presence of minor amounts of admixtures of other phases in the natural material. Erd et al. (1964) mentioned already in their original description of buddingtonite that the mineral was not completely mechanically separated from its impurities. Marcasite, anatase and montmorillonite were found in DW1 (Erd et al., 1964, p. 840). The amount of FeS_2-impurity was checked by them with chemical analysis, and it was found to be less that 3 percent. Montmorillonite did not show in the XRD-analysis of the material, which led them to conclude that its amounts were negligible. Buddingtonite has recently gathered importance because of spatial relations to oil shales (Loughnan et al., 1983) and Au-deposits (Kydd and Levinson, 1986).

This study presents the results of a new investigation of natural holotype buddingtonite, with appropriate comparisons with synthetic ammonium feldspar, in order to understand the nature of its zeolite-like behavior.

SAMPLE DESCRIPTION

About 70 mg of the holotype buddingtonite separate DW1, originally described by Erd and coworkers (1964) and about 100 mg of another type separate, indicated as 2821, which is not previously described, are studied. The latter sample contains some montmorillonite (R.C. Erd, pers. comm., 1988). The separation of the sample DW1 and subsequent treatments are described in Erd et al., (1964). The sample 2821 was additionally treated with 1 : 1 HCL and 1 : 1 HNO_3 and sedimented in water (R.C. Erd, pers. comm., 1987). A thin section was made from a chip of the original rock sample, labeled 582-K, of which the tube sample DW1 and the sample 2821 were separated by Erd et al. (1964). With respect to DW1, sample 2821 represents a more impure separate from the original untreated holotype rock sample.

Synthetic buddingtonite was prepared from NH_3 and an Al-Si-gel, at 600 ^oC and 2 kbar after the method of Voncken et al. (1988). A rapid quench pressure vessel was used, making cooling to room temperature within 2 seconds possible. If quenching is insufficiently rapid, secondary tobelite is developed (Voncken et al., 1988). The samples were studied by means of an optical microscope, XRD, IR-spectroscopy and SEM. With SEM only small feldspar crystals were visible on the faces of the larger feldspars. A typical picture of an euhedral synthetic ammonium feldspar is illustrated in figure 1.

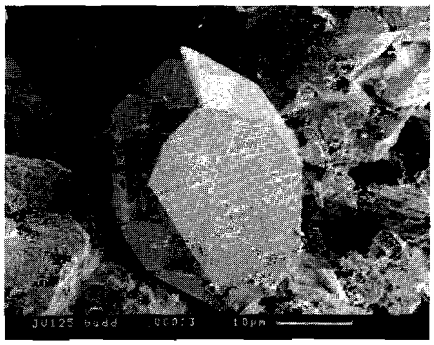

Figure 1. SEM photograph of a synthetic ammonium feldspar crystal grown at 600 ^oC and 2 kbar.

ANALYTICAL TECHNIQUES

X-ray powder diffraction photographs were taken with an Enraf Nonius FR552 powder diffraction camera, using CuKα1-radiation. For SEM, the samples were coated with gold. A Cambridge Stereoscan was operated at an accelerating voltage of 10 KeV. For STEM, the samples were ground for 5 minutes in alcohol in an agate mortar, and a drop of the suspension was transferred to a copper grid, bearing a carbon film on one side. STEM was performed with a JEOL 200C Transmission Electron Microscope at 120 or 200 KeV. The microscope has

analytical facilities (Link Systems Ltd.). For IR-spectroscopy, equal amounts of sample (2.5 mg) were mixed in a dry state with 250 mg of KBr. Tablets were pressed in vacuum, and subsequently dried for 1 night at 120 ^{o}C. Subsequently IR-spectra were recorded with a Perkin Elmer 580 IR-spectrometer. Thermal analysis (TGA and DTA) were executed with Dupont thermal analyzers in air at a heating rate of 10 ^{o}C/min. Due to the limited amount of sample, only relatively small amounts of DW1 and 2821 were used for analyses. Wet chemical analyses of DW1 were carried out for NH_4^+ and Sr, Ba, Mn, Fe, P, S, Mg, V, Na, Al, Ca, Zn, Cu, Li, Zr, Ni, Ti, K, and Cr. NH_4^+ was determined by colorimetry after acid decomposition and Kjehldahl distillation. Other main and trace elements were detected with ICPAES after acid decomposition. On the thin section from a chip from the rock sample 582-K, preliminary microprobe analyses for nitrogen were carried out.

RESULTS

The XRD-pattern of the holotype sample DW1 only showed buddingtonite lines. In the pattern of sample 2821 vague broad lines were visible at 4.45 Å, 3.04 Å, 2.92 Å, 2.59 Å and 1.50 Å, which can be ascribed to the presence of montmorillonite, although tobelite is also a possibility. For detailed descriptions of the X-ray diffraction patterns and lattice parameters of holotype and synthetic buddingtonite, the reader is referred to specific publications dealing with these subjects (Erd et al., 1964; Kimball and Megaw, 1974; Voncken et al., 1988).

In the IR-spectra of the natural ammonium feldspars (figure 2), two distinct bands in the spectral range 3750 - 3600 cm^{-1} are conspicuous. These bands are most clearly visible in the spectrum of the buddingtonite 2821. KBr-disks with synthetic and natural ammonium feldspars, containing equal amounts of sample were prepared. The KBr-tablet with the synthetic feldspar was put in the reference beam, thus subtracting ammonium feldspar vibrations from the spectra of the natural buddingtonite and highlighting vibrations from admixtures. The resulting spectra, obtained with DW1 and 2821, display the same vibrations, but the clearest result is obtained with 2821. The spectrum is given in figure 3. The vibrations of the spectrum obtained with 2821 are listed in table 1. By comparison with literature spectra (see footnote of table 1) many bands can be ascribed to montmorillonite. Therrefore, tobelite is ruled out as a possible admixture. Two bands of feldspar still persist. The NH_4^+-bands in the spectrum of figure 3 suggest that the montmorillonite may contain ammonium.

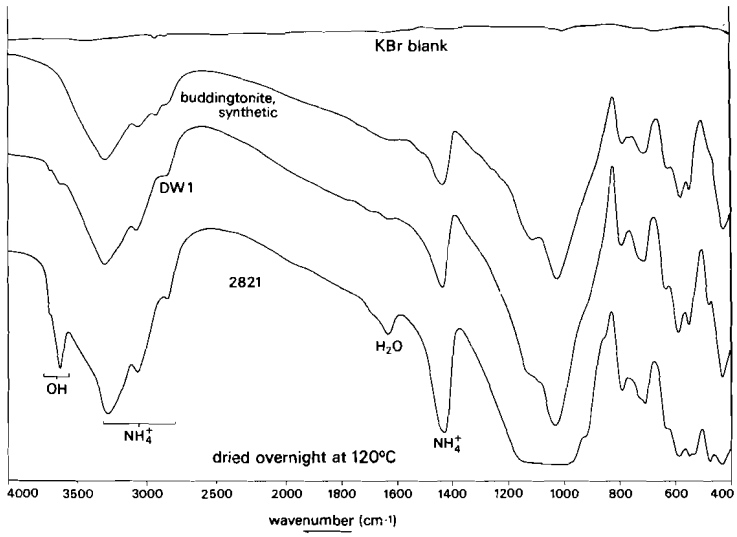

Figure 2. IR-spectra in the spectral range 4000- 400 cm^{-1} for DW1, 2821 and synthetic buddingtonite.

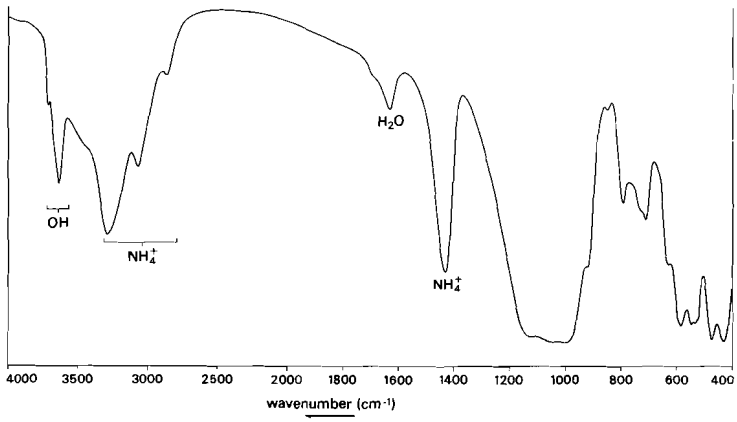

Figure 3. IR-spectrum obtained from buddingtonite separate 2821, with a sample of synthetic buddingtonite in the reference beam of the spectrometer. See table 2.

Table I. IR-vibrations of DWI and 2821. A sample of synthetic buddingtonite was in the reference beam during the analysis.

cm^{-1}	Intensity	Interpretation		Reference
3710	sh	3703	OH-stretch montmorillonite	1
		3655	OH-stretch montmorillonite	1
3630	s	3640	OH-stretch montmorillonite	2
		3630	OH-stretch, tobelite	3
3400	sh	3410	H_2O (montmorillonite)	2
3290	s	3290-3300	NH_4^+	
3070	s	3070	NH_4^+	4-10
2850	m	2850	NH_4^+	
1640	m	1630	H_2O (montmorillonite)	2
1430	s	1430-1435	NH_4^+	4-10
1130	vs	1120	montmorillonite	2
1050	vs			
		1035	montmorillonite(broad band)	2
1000	vs			
920	sh	915	montmorillonite	2,11
895	w	880	montmorillonite	2
785	m	795	montmorillonite	2
735	sh	731	buddingtonite or sanidine	2,4
705	m	711, 715	buddingtonite	4,5 or
		692	montmorillonite	2
630	sh	626	montmorillonite	2
580	st	575	montmorillonite	2
540	st	520	montmorillonite	2
470	st	464	montmorillonite	2
430	st	425	montmorillonite	2

1) Mortland et al., 1963
2) Van der Marel and Beutelspacher, 1976
3) Voncken et al., 1987
4) Erd et al., 1964
5) Voncken et al., 1988
6) Shigorova et al., 1981
7) Vedder, 1965
8) Solomon and Rossman, 1988
9) Chourabi and Fripiat, 1981
10) Krohn and Altaner, 1987
11) Serratosa, 1962

Abbreviations :
s = strong
m = medium
w = weak
sh = shoulder

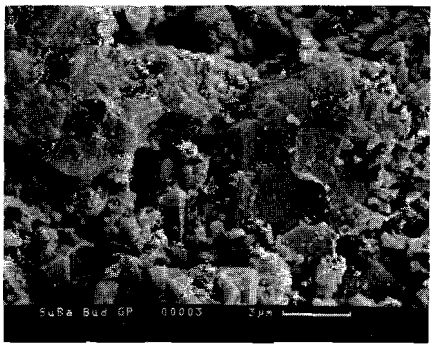

Figure 4a. SEM photograph of a buddingtonite-bearing aggregate in holotype separate DW1.

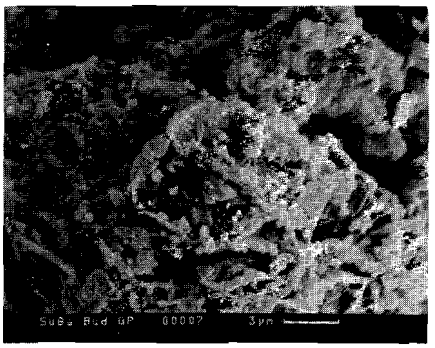

Figure 4b. SEM-photograph of thick platy and some thin flaky material in holotype separate DW1.

Figure 4a, b, and c display parts of the samples DW1 and 2821. Feldspar morphologies of buddingtonite are visible (figure 4a). Figure 4b illustrates thick plates from DW1. Thin flakes are visible as overgrowths on feldspar faces in sample 2821 (figure 4c). The thicker plates have sizes in the order of magnitude of that of the feldspar crystals or somewhat smaller. The grainsize of the thin flakes is $\leq$ 1 micrometer. The estimated amount of the flaky material in DW1 is probably less than 1 percent. This material is present in larger quantities (estimated 4 to 5 times as much) in 2821, where it may be developed on cleavage and twinning planes within the buddingtonite crystals. Optical examination of DW1 in the thin section of the 582-K rock sample gave no conclusive results with respect to this, due to the small grain size of the buddingtonite crystals. A STEM-study of the separates DW1 and 2821 confirms the presence of plates and flakes in both the samples. The small thin flakes are extremely unstable under the electron beam. They

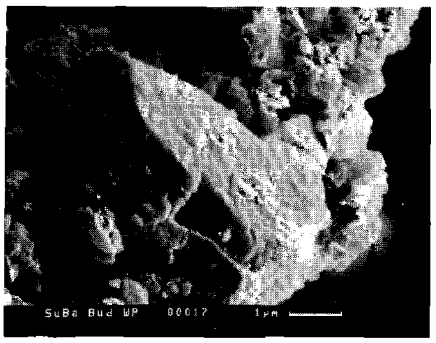

Figure 4c. SEM-photograph of a buddingtonite crystal, of type separate 2821. Overgrowth with what is probably a phyllosilicate, is visible.

decompose within about 30 seconds, even at 120 KeV. No diffraction pattern or even a good photograph of this material could be taken. The larger and thicker plates were by means of electron diffraction patterns identified as buddingtonite. The thick plates are probably formed during grinding of the material. Buddingtonite has good {001} and distinct {010} cleavage (Erd et al. 1964). A qualitative chemical analysis showed an Al/Si peak ratio that is reasonably consistent with a feldspar (figure 5a). A similar pattern for synthetic buddingtonite is given in figure 5b. Only in DW1 rare pyrite (or marcasite) was encountered as well as a Ti-containing phase, which is likely the anatase mentioned by Erd et al. (1964).

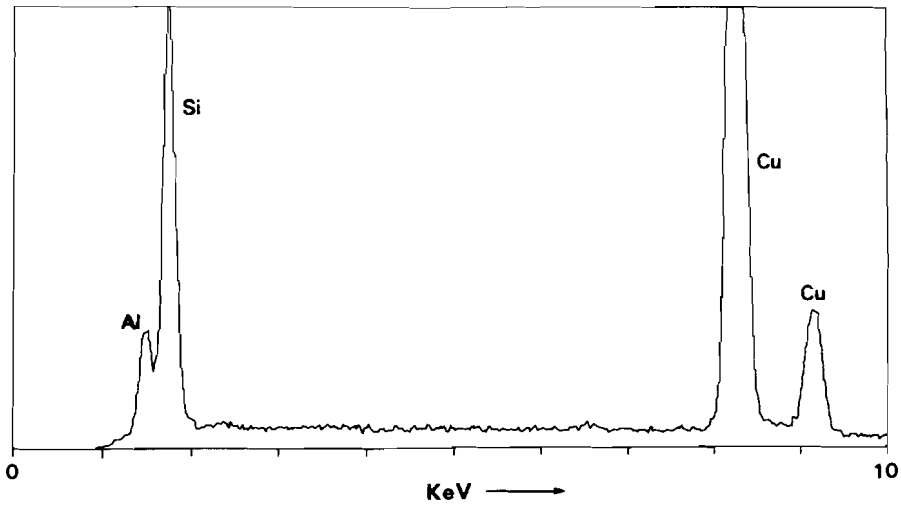

Figure 5a. E.D.S. spectrum of a grain of natural buddingtonite from DW1, obtained with STEM coupled to an analytical system. Cu-lines are from the sample grid.

If buddingtonite has the chemical formula $NH_4AlSi_3O_8$, the amount of ammonium, expressed as $(NH_4)_2O$, would have to be 10.1 weight percent. Wet chemical determination of NH_4^+, and trace element analyses by ICPAES must be considered qualitative due to the small amounts of sample available for the analyses. If the amounts of NH_4^+ in weight percent, determined wet chemically, are recalculated to $(NH_4)_2O$, values of 8.5 and 8.3 weight percent are found for DW1. This agrees very well with the results of Erd et al. (1964, table 3), who mention 8.34 weight percent $(NH_4)_2O$. Small amounts of Na or K are still present and explain the deviation of natural buddingtonite from the ideal composition (cf. Erd et al., 1964).

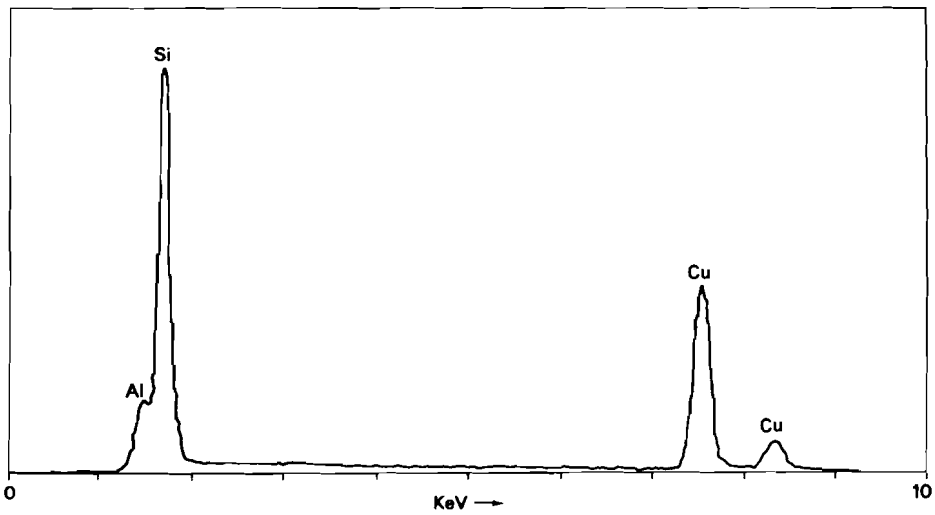

Figure 5b. E.D.S. spectrum of a grain of synthetic buddingtonite, obtained with STEM coupled to an analytical system. Cu-lines are from the sample grid.

Generally the wet chemical analyses of main and trace elements do not indicate strong deviations from the values of Erd and his coworkers. As their chemical data are based upon analyses of larger amounts of sample, their data must be preferred. Microprobe analysis of the nitrogen content of buddingtonite from the thin section of the 582-K sample (from which DW1 was prepared by Erd et al., 1964), are only semiquantitative. Reference materials for the nitrogen analyses were synthetic $NH_4AlSi_3O_8$ or AlN, but calibration was not optimal. If the analyzed nitrogen is expressed as $(NH_4)_2O$, the weight percentages are between 6.25 and 6.65.

Ideally, on thermal decomposition a feldspar with the formula $NH_4AlSi_3O_8$ would lose 10.1 weight percent according to the reaction :

$$2NH_4AlSi_3O_8 \rightleftharpoons 2NH_3 + H_2O + Al_2O_3 + SiO_2$$

Erd et al. (1964) recorded a weight loss of 12 percent for the DW1 sample, whereas our TGA shows a weight loss of 10.8 weight percent (figure 6a). The rise of the curve above 850 ^oC is due to the rise of the baseline as was proven with a corundum blank (not shown). In the

TGA of DW1 and 2821, several stages of weight loss can be recognized. They are summarized in table 2. Figure 6b shows the TGA of sample 2821. The total weight loss is 14 percent, and it is lost in two main stages. The most remarkable is the strong weight loss below 150 °C (5.0 percent). The TGA data (9.6 weight percent) for synthetic ammonium feldspar are taken from Voncken et al. (1988).

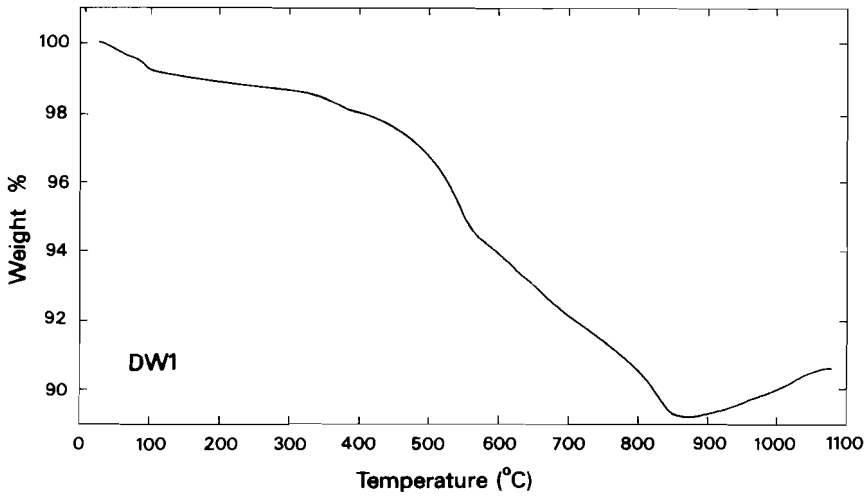

Figure 6a. TGA curve of sample DW1.

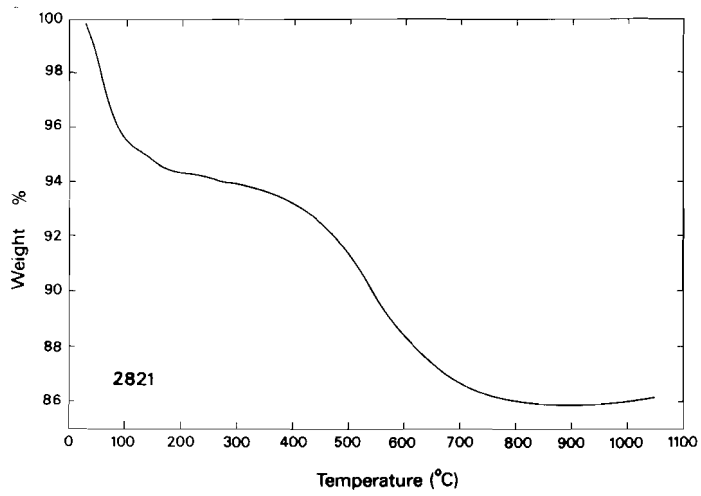

Figure 6b. TGA curve of sample 2821.

Table II. TGA results

Synthetic $NH_4AlSi_3O_8$		DW1		2821	
T °C	weight loss	T °C	weight loss	T °C	weight loss
		0 - 150	1.0	0 - 150	5.0
		150-360	0.6	150-850*	9.0
		360-410	0.5		
		410-550	3.0		
		550-800	4.2		
800-900	9.6	800-850	1.5		
Total	9.6	Total	10.8	Total	14.0

* : Main stage around 550 °C.

Table III. DTA results

Synthetic $NH_4AlSi_3O_8$		DW1		2821	
T °C	type	T °C	type	T °C	type
		100	endo*	60	endo
				110	endo
				150	endo
		350-490	exo		
		550	endo or exo	550	endo or exo
800	exo	±850	exo		
875	exo	980	exo		

* : endo = endotherm, exo = exotherm.

In a DTA analysis of synthetic ammonium feldspar (figure 7a), a large positive undulation is present between 25 and 700 °C. The same undulation is present in the DTA-curves of DW1 and 2821. It is due to a difference in thermal conductivity between the silicate and the reference material (corundum). It does not represent a thermal decomposition. The DTA results are summarized in table 3. Although the distinction between exothermic and endothermic peaks is mostly rather straight forward, at 500 °C in the spectrum of the separates DW1 and 2821 2821, it is ambiguous whether there are endothermic or possibly also exothermic peaks present. The derivative is not conclusive here due to a high noise level.

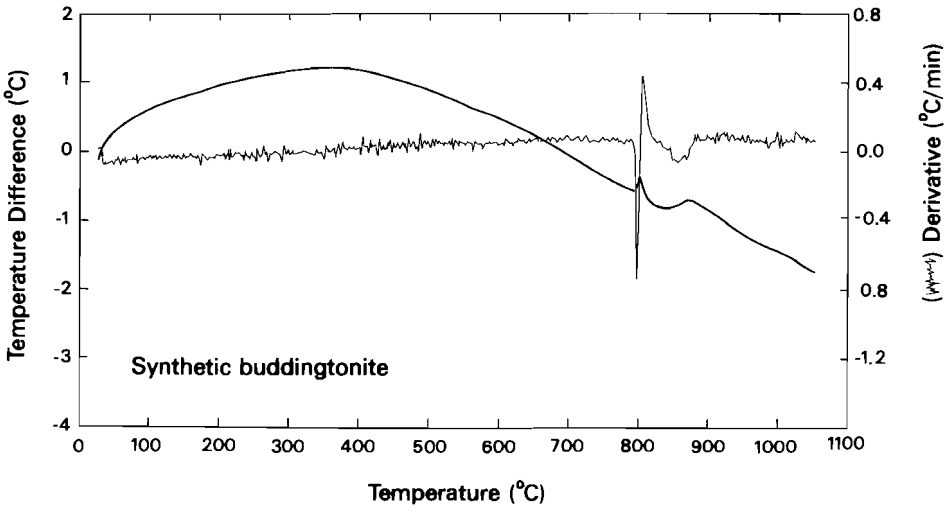

Figure 7a. DTA-curve of synthetic ammonium feldspar.

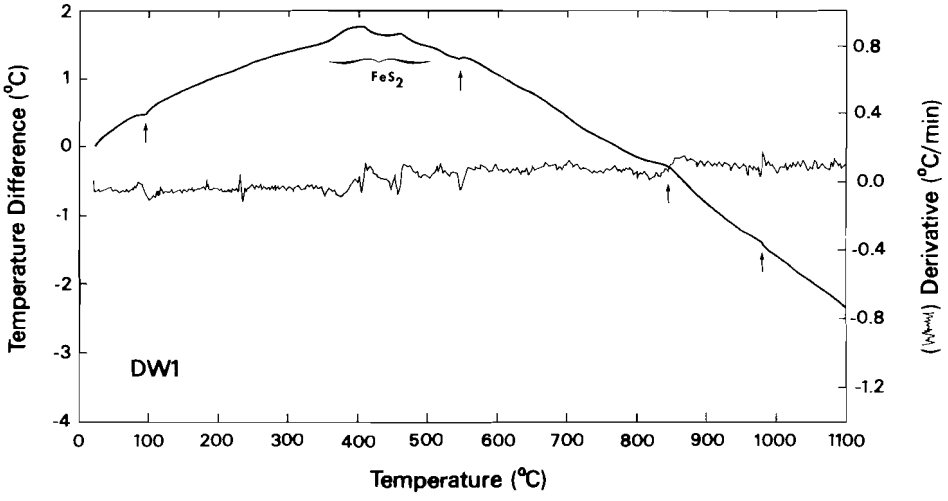

Figure 7b. DTA-curve of sample DW1. Peaks marked with an arrow are listed in table 3.

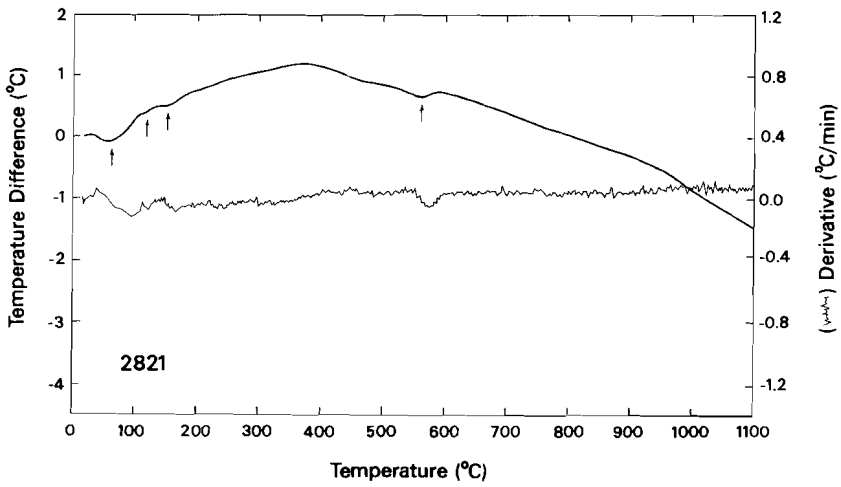

Figure 7c. DTA-curve of separate 2821. Peaks marked with an arrow are listed in table 3.

DISCUSSION

Iron sulfide (likely marcasite) and a Ti-phase (likely anatase), which were mentioned to be epresent in DW1 by Erd and his co-workers, are observed in DW1 by STEM. The presence of FeS_2 is consistent with DTA results. Exothermic peaks between 350 and 490 °C can be attributed to decomposition of pyrite or marcasite (Smykatz-Kloss, 1974). Absence of these peaks in the DTA of type sample 2821 agrees with the absence of FeS_2 observed in electron microscopical analysis and with the preparation history of 2821 (treatment with acids). The small exothermic peak at 980 °C in the DTA of DW1 may possibly be attributed to the transition of anatase to rutile.

With XRD, montmorillonite is not found in DW1. XRD-results suggest its presence in 2821. IR-vibrations in the range 3750 - 3600 cm^{-1} are crucial. Vibrations of OH in phyllosilicates are well known to occur in this region (e.g. Farmer, 1974). However, hydrous species are common as minor impurities in feldspar (Rossman, 1988). Structurally incorporated water and hydroxide ions may result in vibrations in this region of the IR-spectrum (Hofmeister and Rossman, 1985; Beran, 1986). Our IR-data, however, leave little doubt that both DW1 and 2821 contain

montmorillonite. It is possibly ammonium-bearing. The precise amount of montmorillonite in DW1 is somewhat problematical. Erd et al. (1964) believe the total amount of impurities in DW1 to be less than 5 percent, of which less than three percent is FeS_2. Calculation of the amount of montmorillonite on the basis of the chemical analyses is dubious, as the analysis of DW1 includes buddingtonite and montmorillonite and the latter mineral may have a wide range of compositions. Intensities of the IR-bands at 3710 and 3630 cm^{-1} can be taken to calculate the relative amounts of montmorillonite in these samples. I/I_0 of the 3710 and 3630 cm^{-1} bands are for DW1 8.3 and 16.7 respectively, and for 2821 they are 31.3 and 63.8 respectively. This suggests that 2821 contains about 4 times as much montmorillonite as DW1, which agrees reasonably with the estimates from SEM-photographs. Under the electron microscope, two types of platy material were visible. One type, consisting of very thin flakes, decomposes very quickly, and is interpreted as being montmorillonite. Ammonium-bearing ill-crystallized montmorillonite can be expected to be very unstable under the electron beam. Thermal analysis gives confirmation of the presence of montmorillonite in DW1 and 2821. Loss of interlayer water may take place in several steps up to 200 ^{o}C (cf. Koster van Groos and Guggenheim, 1987a). In the DTA of the montmorillonite rich sample 2821, peaks are found at 60, 110, and 150 ^{o}C. In the DTA of DW1, which contains only small amounts of montmorillonite, only a peak is found at 100 ^{o}C. The three peaks in 2821 can be explained by the loss of adsorbed and interlayer water in three steps. The amount of montmorillonite in DW1 is very small, and only one dehydration step is visible. Release of NH_3 from NH_4^+-bearing montmorillonite takes place gradually between 200 and 600 ^{o}C (Chourabi and Fripiat, 1981). Loss of NH_3 and H_2O from buddingtonite starts at 500 ^{o}C (figure 6b) with an optimum at about 550 ^{o}C. An exothermic and an endothermic process may take place here. The exothermic process can be explained by the de-ammoniation of buddingtonite, whereas the endothermic process can be explained by dehydroxylation of montmorillonite. Erd et al. (1964) mention a temperature of 608 ^{o}C for the exothermic loss of NH_3 and H_2O from DW1, but applied a different heating rate (12 ^{o}C/min) in thermal analysis. Dehydroxylation of montmorillonite is an endothermic reaction between 500 and 700 ^{o}C (Chourabi and Fripiat, 1981; Koster van Groos and Guggenheim, 1987b). In comparison with the results of Koster van Groos and Guggenheim (1987b), 550 ^{o}C is relatively low, but, as pointed out by Chourabi and Fripiat (1981), if the montmorillonite contains ammonium, protons left after de-ammoniation of montmorillonite may catalyze the dehydroxylation which as a result takes place at a lower temperature. The additional weight loss produced by the dehydroxylation of montmorillonite reaction explains the steeper weight loss curve of DW1 between 500 and 550^{o}C with respect to the following part. At about 800 ^{o}C, no clear reaction takes place in the DTA of 2821, but in the DTA of DW1 a sign of an exothermic reaction is visible at about 850 ^{o}C. This broad peak may represent the breaking up of the Al-O-Si lattice

which remains after de-ammoniation of buddingtonite, but also the lattice remaining after decomposition of montmorillonite. Any residual volatile compounds in these structures will be released more quickly. The absence of any sign of reaction at high temperatures in 2821 may perhaps be the result of a very gradual decomposition of the remains of composites of ill crystallized montmorillonite and buddingtonite.

If the weight losses of the DW1 separate below 100 ^{o}C are to not taken into account, a loss of 10.1 weight percent remains for the rest of the temperature range. If also 0.5 percent is subtracted for the loss of volatiles from FeS_2, occurring between 350 and 490 ^{o}C, 9.6 percent remains for buddingtonite and dehydroxylation of montmorillonite. Even if the amount of montmorillonite in DW1 is around 1 percent, this weight loss agrees very well with the value of 9.6 weight percent found for synthetic $NH_4AlSi_3O_8$ (Voncken et al., 1988). Also the value of 10.8 weight percent is close to the ideal value of 10.1 weight percent. As montmorillonite will regulate its water content according to the degree of humidity, laboratory conditions will have an influence on the weight losses detected. The difference between the value found by Erd et al. (1964) for DW1 and the present one is therefore considered not to be of importance. Montmorillonite is notorious for its capacity of reversible dehydration (e.g. Serratosa, 1962) and this ability can perfectly explain the zeolitic behavior previously described of DW1 and considered to belong to buddingtonite. When the montmorillonite occurs as overgrowths on buddingtonite crystal faces, only a small amount is needed to form a large active surface for (de)hydration.

CONCLUSIONS

1) The holotype buddingtonite separate DW1 from the Sulphur Bank, California contains admixtures of montmorillonite, FeS_2 and a Ti-containing phase (likely anatase).

2) The presence of montmorillonite affects the IR-spectrum and the TGA and DTA.

3) Due to its ability of reversible dehydration, montmorillonite can perfectly explain the zeolitic behavior previously ascribed to buddingtonite.

4) In TGA, a total weight loss of 10.8 weight percent, due to volatile loss is found. After correction for the contribution of adsorbed water and FeS_2, 9.6 percent remains. Although there exists a minor contribution to this value by dehydroxylation of montmorillonite, this value agrees very well with the value of 9.6 percent of synthetic $NH_4AlSi_3O_8$.

5) Buddingtonite can be considered as an ammonium feldspar without zeolitic water.

ACKNOWLEDGMENTS

R.C. Erd kindly made available the samples of natural buddingtonite used in this study. P. van Krieken and T. Zalm are thanked for executing for the thermal analysis. A. van der Eerden analyzed the buddingtonite separates chemically. R. Poorter assisted with the electron microprobe analyses for nitrogen. The X-ray diffraction photographs were taken by N. Slaats. H. van Roermund of the Faculty of Geology and Geophysics and J. Pieters of the Electron Microscopy Section of the Faculty of Biology of the University of Utrecht are thanked for the STEM-work.

REFERENCES

Barker, D.S. (1964) Ammonium in alkali feldspars. American Mineralogist, 49, 851-858.

Beran, A. (1986) A model for the allocation of water in alkali feldspars, observed from infrared spectroscopy investigations. Physics and Chemistry of Minerals, 13, 306 - 310.

Chourabi, B. and Fripiat, J.J. (1981) Determination of tetrahedral substitutions and interlayer surface heterogeneity from vibrational spectra of ammonium in smectites. Clays and Clay minerals, 29, 260-268.

Erd R.C., White D.E., Fahey J.J., Lee D.E. (1964) Buddingtonite, an ammonium feldspar with zeolitic water. American Mineralogist, 49, 831-857

Farmer, V.C. (1974) The infrared spectra of minerals. Mineralogical Society Monograph 4, 331 - 363.

Gulbrandsen, R.A. (1974) Buddingtonite, ammonium feldspar in the Phosphoria Formation, Southeastern Idaho. Journal of Research of the US Geological Survey, Vol.2, nr.6, 693-697.

Hallam M., and Eugster H.P. (1976) Ammonium silicate stability relations. Contributions to Mineralogy and Petrology, 57, 227-244.

Hofmeister, A. M. and Rossman, G.R. (1985) A spectroscopic study of irradiation coloring of amazonite : Structurally hydrous Pb-bearing feldspar. American Mineralogist, 70, 794 - 804.

Kimball M.R., and Megaw H.D. (1974) Interim report on the crystal structure of buddingtonite. In: MacKenzie W.S. and Zussman J. (eds) Feldspars. Proc. NATO ASI on Feldspars, Manchester. Manchester Press, pp 81-86

Kimbara K., and Nishimura. T. (1982) Buddingtonite from the Toshichi Spa, Iwate Prefecture, Japan. Kobutsugaki Zasshi, Journal of the Mineralogical Society of Japan, 15, 207-216 (In Japanese, with English Abstract)

Koster van Groos, A. F., and Guggenheim, S. (1987a) Dehydration of a Ca- and a Mg-exchanged montmorillonite (SWy-1) at elevated pressures. American Mineralogist, 72, 292-298.

Koster van Groos, A. F., and Guggenheim, S. (1987b) High pressure differential thermal analysis (HP-DTA) of the dehydroxylation of Na-rich montmorillonite and K-exchanged montmorillonite. American Mineralogist, 72, 1170-1175.

Krohn, M.D. and Altaner, S.P. (1987) Near Infrared detection of ammonium minerals. Geophysics, 52, 924-930.

Kydd, R.A. and Levinson, A.A. (1986) Ammonium halos in lithogeochemical exploration for gold at the Horse Canyon carbonate hosted deposit, Nevada, USA : use and limitations. Applied Geochemistry, 1, 407 - 417.

Loughnan F.C., Roberts F.I., and Lindner A.W. (1983) Buddingtonite (NH_4-feldspar) in the Condor Oilshale Deposit, Queensland, Australia. Mineralogical Magazine, 47, 327-334

Mortland, M.M., Fripiat, J.J., Chaussidon, J., and Uytterhoeven, J. (1963) Interaction between ammonia and the expanding lattices of montmorillonite and vermiculite. Journal of Physical Chemistry, 67, 248-258.

Rossman G.R. (1988) Vibrational spectroscopy of hydrous components. In : Vol. 18 of Reviews in Mineralogy : "Spectroscopic Methods in Mineralogy and Geology", F.C. Hawthorne, editor, 193 - 206, Mineralogical Society of America.

Serratosa, J.M. (1962) Dehydration and rehydration studies of clay minerals by infrared spectra. International Series of Monographs on Earth Sciences, Monograph II (Earl Ingerson, editor), 1962, 412 - 418, Pergamon Press, New York.

Shigorova, T.A., Kotov N.V., Kotel'nikova Ye.N., Shmakin B.M., and Frank-Kamenetzkiy V.A. (1981) Synthesis, diffractometry and IR-spectroscopy of micas in the series from muscovite to the ammonium analogue. Geochemistry International, 18, 76-82.

Smykatz-Kloss, W. (1974) Differential Thermal Analysis. Applications and Results in Mineralogy. Springer Verlag, Berlin, Heidelberg, New York, 185 pp.

Solomon, G.C. and Rossman, G.R. (1988) NH_4^+ in pegmatitic feldspars from the southern Black Hills, South Dakota. American Mineralogist, 73, 818-821.

Van der Marel. H. W., and Beutelspacher, H. (1976) Atlas of Clay Minerals and their Admixtures. Elsevier, Amsterdam, Oxford, New York, 1976.

Vedder, W. (1965) Ammonium in muscovite. Geochimica et Cosmochimica Acta, 29, 221-228.

Voncken, J.H.L., Wevers, J.M.A.R., Van der Eerden, A.M.J., Bos, A., and Jansen, J.B.H. (1987) Hydrothermal synthesis of tobelite, $NH_4Al_2Si_3AlO_{10}(OH)_2$, from various starting materials and implications for its occurrence in nature. Geologie en Mijnbouw, 66, 259-269.

Voncken, J.H.L., Konings, R.J.M., Jansen, J.B.H., and Woensdregt, C.F (1988) Hydrothermally grown buddingtonite, an anhydrous ammonium feldspar ($NH_4AlSi_3O_8$). Physics and Chemistry of Minerals, 15, 323- 328.

White, D.E. and Robertson, C.E. (1962) Sulphur Bank, California, a major hot-spring Quicksilver Deposit. In : Petrologic studies : a volume to honor A.F. Buddington. Geological Society of America, Special Paper, 397-428.

CHAPTER V.

Synthesis of a Rb analogue of $2M_1$ muscovite

JACK H. L. VONCKEN, AD M. J. VAN DER EERDEN, J. BEN H. JANSEN
Department of Geochemistry and Experimental Petrology, State University of Utrecht, Budapestlaan 4, 3524 CD Utrecht, the Netherlands

ABSTRACT

In the course of a study on the incorporation of Rb in muscovite, the Rb analogue of muscovite was synthesized at 600°C and 5 kbar. Rb_2CO_3, γ-Al_2O_3, and SiO_2 (cristobalite) were used as starting materials. Wet-chemical analyses and TGA data of the run products indicate that the composition is consistent with the ideal Rb end member. SEM photographs display well-crystallized micas as run products. The X-ray powder pattern can be satisfactorily indexed on the basis of a $2M_1$ cell, having $a = 5.215 \pm 0.003$, $b = 9.059 \pm 0.005$, $c = 20.59 \pm 0.01$ Å, $\beta = 96.540° \pm 0.003°$. The most likely space group is $C2/c$. The calculated density is 3.06 $g \cdot cm^{-3}$. Compared with muscovite, the unit cell is enlarged mainly in the direction of the c axis, and the cell volume is enlarged by 3.3%. The IR-band positions of the Rb analogue of muscovite are similar to those of muscovite. On the basis of d spacings, the Rb end member can be easily distinguished from muscovite. By means of IR spectrophotometry, it can be easily distinguished from the NH_4 analogue of muscovite.

INTRODUCTION

Over the past 20 years, several studies on K-Rb exchange in rock-forming minerals have been reported. Several minerals have been studied: feldspars and feldspathoids (Lagache, 1968; Iiyama, 1968; Roux, 1971; Lagache and Sabatier, 1973), and phlogopite (Beswick, 1973; Volfinger, 1974). For muscovite, only the introduction of Rb as a trace element has been studied intensively (Volfinger, 1969, 1976).

Rb is often found in considerable amounts in hydrothermally altered granitic rocks and their aureoles (Vriend et al., 1985; Bussink, 1984) as well as in pegmatites (Černý and Burt, 1984). Muscovite, biotite, and feldspars are the most important host minerals for Rb in these rocks. Rb contents of several thousands of parts per million in pegmatitic muscovites are not uncommon. Luecke (1981) reported amounts up to 1 wt%. Khanna (1977) reported 6.98 wt% Rb in a muscovite from a pegmatite. K-Rb partition coefficients between micas and vapor depend on temperature (Beswick, 1973; Volfinger, 1976), and they may be of use as a geothermometer (De Albuquerque, 1975; Bernotat et al., 1976).

In the course of an investigation on the incorporation of Rb in muscovite, a Rb analogue of muscovite was synthesized. It is the purpose of this paper to describe the properties of this phase, herein informally referred to as Rb-muscovite, with SEM, chemical analyses, TGA, XRD, and IR spectrophotometry.

SYNTHESIS AND EXPERIMENTAL METHODS

For the synthesis of muscovite, several procedures are described in the literature. A variety of starting materials have been used, for example, KCl, $Al(OH)_3$, and $SiO_2 \cdot xH_2O$ (Gruner, 1939); $K_2O \cdot 6SiO_2$ and γ-Al_2O_3 (Yoder and Eugster, 1955; Chatterjee and Johannes, 1974); natural kaolinite and KOH (Velde, 1965, 1966); and K_2CO_3, γ-Al_2O_3, and SiO_2 (Chatterjee and Johannes, 1974).

Since the synthesis of muscovite from K_2CO_3, γ-Al_2O_3, and SiO_2 seems to be little problematic (Chatterjee and Johannes, 1974), we chose Rb_2CO_3, γ-Al_2O_3, and SiO_2 for starting materials for the synthesis of Rb-muscovite. Dried, extra pure Rb_2CO_3 (Merck, no. 7612), analytical grade γ-Al_2O_3 (Merck, no. 1095), and quartz (Merck, no. 7536) were used. The quartz was purified by hand-picking, because it contained small impurities of feldspars and mica. The pure quartz was heated for 3 h at 1500°C and 1 atm, resulting in a well-crystallized cristobalite. The starting materials were finely ground and mixed in an agate mortar, under acetone.

The synthesis of the Rb-muscovite was performed at 600°C and 5 kbar. The formation of the mica is according to the following reaction:

$$Rb_2CO_3 + 3\ \gamma\text{-}Al_2O_3 + 6\ SiO_2 + 2\ H_2O = 2\ RbAl_2Si_3AlO_{10}(OH)_2 + CO_2.$$

The synthesis was carried out in sealed Au capsules, containing about 200 mg of carbonate and oxide mixture and 50 μL of double-distilled water. Conventional cold-seal pressure vessels were used. The pressure medium around the Au capsule was Ar. The temperature is considered to be accurate to 1%, the pressure to 5%. Isobaric quenching to room temperature within a few minutes was achieved by blowing on the vessel compressed cold air. Run times of about 3 weeks produced well-crystallized micas. No other products were encountered. In a short run at 600°C and 15 kbar with a piston-cylinder apparatus, the Rb-muscovite can be formed besides appreciable amounts of corundum and Rb-feldspar.

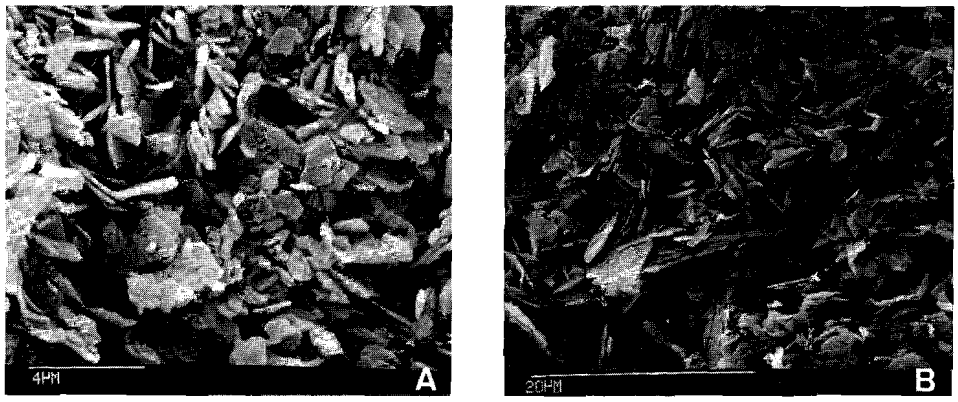

Fig. 1. (A) and (B) SEM photographs of synthetic Rb-muscovite.

DESCRIPTION OF THE MICA

Optical and SEM description

Run products were examined under a polarizing microscope, which revealed very small, colorless mica flakes. The run products were too small for a well-oriented determination of the optical properties. SEM was used to get an impression of the morphology of the synthesized micas. Typical SEM pictures are given in Figures 1A and 1B. The crystals are usually thin, more or less hexagonal platelets, with a diameter of 1 to 4 μm, and a thickness of some tenths of a micrometer.

Chemical analyses

Rb, Si, and Al have been determined after a HF-$HClO_4$-HNO_3 and a $LiBO_2$-melt decomposition. Only samples composed of pure mica were used, and run products containing other phases (piston-cylinder runs) were not analyzed. Rb, Al, and Si were all determined by AAS. The results are given in Table 1. The values are in good agreement with ideal Rb, Al, and Si contents. Microprobe analyses (not reported here) gave semiquantitative results, owing to the small size of the micas.

Thermogravimetric analyses

To check for the presence of hydroxyl in the crystal and of H_3O^+ (which may be present in the interlayer), TGA analyses were executed. For comparison, an analysis of a synthetic muscovite (synthesized from K_2CO_3, γ-Al_2O_3, and SiO_2 at 600°C and 5 kbar) also was made. The muscovite loses 4.30 ± 0.2 wt% at temperatures up to 1000°C. The ideal weight loss of muscovite should be 4.52 wt%. Yoder and Eugster (1955) found values of 4.27 and 4.52 wt% for samples of a synthetic muscovite. For Rb-muscovite, a loss of 3.95 ± 0.2 wt% was recorded at temperatures up to 1000°C. The ideal weight loss of Rb-muscovite should be 4.05 wt%.

The TGA analyses are thus consistent with the presence of hydroxyl. The presence of significant amounts of H_3O^+ is not indicated. The hydroxyl groups of Rb-muscovite decompose mainly between 400 and 750°C.

TABLE 1. Chemical analyses (wt%) of the synthesized Rb-muscovite

	Ideal Rb end member	Acid decomposition (AAS)	$LiBO_2$-melt decomposition (AAS)
Rb	19.22	18.9 ± 0.3	19.4 ± 0.3
Si	18.95	—	19.0 ± 0.5
Al	18.20	—	18.3 ± 0.5

X-ray diffraction

The X-ray investigation of the Rb-muscovite was made with a Philips PW1050 diffractometer and an Enraf Nonius FR552 Guinier camera. Cu$K\alpha_1$ radiation was used (λ = 1.540 50).

The X-ray pattern of the Rb-muscovite resembles that of $2M_1$ muscovite in great detail. The Rb-muscovite was indexed on the basis of a $2M_1$ cell, which implies a space group $C2/c$ (Güven, 1971). Owing to the small size of the crystals, single-crystal techniques could not be applied. Cell parameters were calculated with a least-squares refinement program, on nine reflections. Si (JCPDS 27-1402) was used as an internal standard. Prediction by computer calculations of other reflections, which were not used in the refinement program, gave results that were in good agreement with observation, and calculated *hkl* values were consistent with values expected from the analogous muscovite reflections. It was concluded that it is possible to index the mica on a $2M_1$ cell with space group $C2/c$. The indexed X-ray diffraction pattern is given in

TABLE 2. X-ray pattern of Rb-muscovite

hkl	d_{calc} (Å)	d_{obs} (Å)	I/I_0 Diffractometer	I/I_0 Guinier
002	10.23	10.40	4	
004	5.12	5.20	4	12
020	4.53	4.52	16	30
110	4.50	4.48*	9	
022	4.14	4.13*	26	26
113	3.94	3.92	17	
023	3.77	3.73*	61	37
114	3.56	3.56	6	
006	3.409	3.41*	33	21
024	3.391			
025	3.036	2.99	15	
131	2.607			
116	2.596	2.590*	53	85
200	2.591			
202	2.582	2.580*	100	100
131	2.570			
204	2.425	2.430	6	
133	2.391	2.390	4	
040	2.265	2.261*	19	32
221	2.260			
222	2.152	2.155	16	
223	2.075	2.070	27	
044	2.071			
0,0,10	2.046	2.038	6	
046	1.887	1.885	2	
2,0,10	1.703	1.704	14	
060	1.510	1.509*	32	53
331	1.506	1.506	22	
262	1.303	1.300*		20

* Reflections used in the least-squares refinement.

Table 2. I/I_0 of the Guinier camera recording was determined with a densitometer of Joyce and Loebl, Inc. It may be noted here that the basal reflections are remarkably weak, especially for the diffractogram. A comparable observation was made by Chatterjee (1974). He noted that the basal reflections of synthetic, very fine grained (up to 2 μm) margarite were weaker than the equivalent reflections of coarser-grained natural margarite. He ascribed the effect to the very small grain size of the synthetic mica. It may be that the very fine grain size of the Rb-muscovite is also responsible for its relatively weak basal reflections. Incorporation of H_3O^+ would have the same effect, but TGA data showed that the presence of H_3O^+ is unlikely. As muscovite that was synthesized at the same conditions and with comparable grain size gives clearly stronger basal reflections, an effect of Rb in the alkali sites on the intensity of the X-ray lines cannot be ruled out.

IR spectrophotometry

An IR spectrum of Rb-muscovite was made with a Perkin-Elmer 580 IR spectrophotometer, using dried KBr tablets. In Table 3, the band positions for the Rb-muscovite are given and compared with published values for muscovite (Langer et al., 1981). The band positions of muscovite and Rb-muscovite are very similar. Band assignments (Langer et al., 1981) are also given.

TABLE 3. IR absorption maxima for synthetic Rb-muscovite and comparison with literature values for muscovite

Rb-muscovite wavenumber (cm^{-1})	Intensity*	Muscovite wavenumber** (cm^{-1})	Muscovite band assignments**
3630	vs	3637	Al–OH
1065	w	1065	Si–O
1040–1000	vs	1028–996	Si–O and Si–O–Si
929	ms	937	Si–O–^{VI}Al
829	ms	831	^{VI}Al–O?
800	ms	805	^{VI}Al–O–^{VI}Al
750	s	751	^{VI}Al–O–^{IV}Al
725	w	727	Si–O–^{VI}Al
690	w	700	Si–O–^{IV}Al
615	w	619	Si–O
530	vs	539	Si–O–^{IV}Al
475	vs	480	Si–O
410	s	410	
351	ms	353	

* w = weak; ms = medium strong; s = strong; vs = very strong.
** Langer et al. (1981).

Comparison with other muscovites

From the list of *d* values it appears that Rb-muscovite can be distinguished easily from muscovite. Observed *d* spacings are generally larger than those of muscovite (Yoder and Eugster, 1955; Chatterjee and Johannes, 1974). In Table 4 a comparison is made between published values of cell dimensions for muscovite and the obtained values for the Rb-muscovite. Compared with muscovite, the unit-cell of the Rb-muscovite is enlarged mainly in the direction of the c axis. Analogous behavior was noted by Hazen and Wones (1972) and Beswick (1973) for Rb-phlogopite. The increase in cell volume of Rb-muscovite relative to muscovite is 3.3%. The corresponding increase for Rb-phlogopite is 2.9% [as can be calculated from data of Beswick (1973)]. The NH_4-muscovites of Eugster and Munoz (1966) and Higashi (1982) are 1M micas, and the unit cells of these micas cannot be compared directly to the Rb-muscovite cell. The *d* spacings of basal reflections of these micas are, however, similar to those of Rb-muscovite basal reflections.

By means of IR spectrophotometry, Rb-muscovite can be distinguished easily from NH_4-muscovite (Eugster and

TABLE 4. Comparison between the cell dimensions of synthetic muscovites and Rb-muscovite

	1	2	3	4
a (Å)	5.189	5.1871	5.1883	5.215 ± 0.003
b (Å)	8.995	8.9927	8.9898	9.059 ± 0.005
c (Å)	20.097	20.1490	20.1516	20.59 ± 0.01
β	95°11′	95°46.78′	95°46.28′	96.540° ± 0.003°
V (Å^3)	—	935.09	935.14	966.4 ± 0.5

Note: Columns are (1) Yoder and Eugster (1955), synthetic muscovite; (2) Chatterjee and Johannes (1974), synthetic muscovite; (3) Chatterjee and Johannes (1974), synthetic muscovite; (4) This work, synthetic Rb-muscovite.

Munoz, 1966; Higashi, 1982), because of the absence of the characteristic NH_4-vibrations.

Calculated densities for muscovite from Table 4 are 2.83 $g \cdot cm^{-3}$. The calculated density of Rb-muscovite is 3.06 $g \cdot cm^{-3}$, an increase of 8.1%. For phlogopites, the corresponding increase is 8.2%, as can be calculated from data by Hazen and Wones (1972).

Conclusions

1. The Rb-muscovite is simple to synthesize at 600°C and 5 kbar and with the preparation of the starting mixture given in this paper.

2. Chemical analyses and hydroxyl content are in good agreement with values expected for the ideal Rb end member.

3. The X-ray pattern of the Rb-muscovite is analogous to that of $2M_1$ muscovite. The *d* spacings are generally larger. Rb-muscovite can be indexed on the basis of a $2M_1$ cell, and the space group is very likely *C*2/*c*.

4. In comparison with muscovite, the substitution of Rb for K results in lattice expansion mainly in the direction of the c axis. The cell volume is enlarged by 3.3%. The calculated density increases by 8.1% to 3.06 $g \cdot cm^{-3}$.

5. The IR spectrum shows a great similarity between the band positions of muscovite and Rb-muscovite.

6. Rb-muscovite can be distinguished easily from muscovite on basis of *d* spacings and from NH_4-muscovite by IR spectrophotometry.

Acknowledgments

C. Laman made the diffractograms and Guinier films. C. Strom assisted with the cristallographic calculations. P. Van Krieken made the TGA analyses. G.P.J. Geelen took the SEM photos. J. Wevers gave many helpful suggestions concerning the crystallographic part. G. Kastelein is acknowledged for his technical assistance in the high-pressure laboratory. Messrs. A. Feenstra, A. Bos, P. Hartman, and C. Peach critically reviewed the text. The Dr. Schürmann Foundation is gratefully acknowledged for financial support of HPT equipment. WACOM (research group for analytical chemistry of rocks and minerals, supported by the Netherlands Organisation of Pure Research, Z.W.O.) is gratefully acknowledged for financial support of the IR spectrophotometry.

References

Bernotat, W.H., Carron, J.P., and Lagaehe, M. (1976) K/Rb and Rb/Cs partitioning between K-feldspars and biotites of Precambrian granites from Sinai. Tschermaks Mineralogische und Petrographische Mitteilungen, 23, 23–38.

Beswick, A.E. (1973) An experimental study of alkali metal distributions in feldspars and micas. Geochimica et Cosmochimica Acta, 37, 183–208.

Bussink, R.W. (1984) Geochemistry of the Panasqueira tungsten-tin deposit, Portugal. Ph.D. thesis, State University of Utrecht, the Netherlands, 170 p.

Černý, P., and Burt, D.M. (1984) Paragenesis, crystallochemical characteristics and geochemical evolution of micas in granite pegmatites. Mineralogical Society of America Reviews in Mineralogy, 13, 257–299.

Chatterjee, N.D. (1974) Synthesis and upper thermal stability limit of 2M margarite, $CaAl_2[Al_2Si_2O_{10}(OH)_2]$. Schweizerische Mineralogische und Petrographische Mitteilungen, 54, 753–767.

Chatterjee, N.D., and Johannes, W. (1974) Thermal stability and standard thermodynamic properties of synthetic $2M_1$-muscovite, $KAl_2[Si_3AlO_{10}(OH)_2]$. Contributions to Mineralogy and Petrology, 48, 89–114.

De Albuquerque, C.A.R. (1975) Partitioning of trace elements in coexisting biotite, muscovite and potassium feldspar of granitic rocks, northern Portugal. Chemical Geology, 16, 89–108.

Eugster, H.P., and Munoz, J. (1966) Ammonium micas: Possible sources of atmospheric ammonia and nitrogen. Science, 151, 683–686.

Gruner, J.W. (1939) Formation and stability of muscovite in acid solutions at elevated temperatures. American Mineralogist, 24, 624–628.

Güven, N. (1971) The crystal structures of $2M_1$-phengite and $2M_1$-muscovite. Zeitschrift für Kristallographie, 134, 196–212.

Hazen, R.M., and Wones, D.R. (1972) The effect of cation substitutions on the physical properties of trioctahedral micas. American Mineralogist, 57, 103–129.

Higashi, S. (1982) Tobelite, a new ammonium dioctahedral mica. Mineralogical Journal, 11, no. 3, 138–146.

Iiyama, J.T. (1968) Étude expérimentale de la distribution d'éléments en traces entre deux feldspaths. Feldspath potassique et plagioclase coexistant. I. Distribution de Rb, Cs, Sr et Ba à 600°C. Bulletin de la Société française de Mineralogie et Cristallographie, 91, 130–140.

Khanna, V.K. (1977) Note on the unusually high concentration of rubidium in a lithium mica from Govindpal area of Bastar district. Journal of the Geological Society of India, 18, 500–502.

Lagache, M. (1968) Étude expérimentale de la répartition des éléments-traces entre la leucite, l'orthose et des solutions hydrothermales. Le rubidium à 600°C. Comptes Rendus, Academie des Seiences, Paris, 267, D141–D144.

Lagache, M., and Sabatier, G. (1973) Distribution des éléments Na, K, Rb, et Cs à l'état de trace entre feldspaths alcalins et solutions hydrothermales à 650°C, 1 kbar: Données expérimentales et interpretation thermodynamique. Geochimica et Cosmochimica Acta, 37, 2617–2640.

Langer, K., Chatterjee, N.D., and Abraham, K. (1981) Infrared studies of some synthetic and natural $2M_1$ dioctahedral micas. Neues Jahrbuch für Mineralogie, Abhandlungen, 142, 1, 91–110.

Luecke, W. (1981) Lithium pegmatites in the Leinster granite (southeast Ireland). Chemical Geology, 34, 195–233.

Roux, J. (1971) Fixation du rubidium et du cesium dans la néphéline et dans l'albite à 600°C dans les conditions hydrothermales. Comptes Rendus, Academie des Sciences, Paris, D1469–D1472.

Velde, B. (1965) Experimental determination of muscovite polymorph stabilities. American Mineralogist, 50, 436–449.

——— (1966) Upper stability of muscovite. American Mineralogist, 51, 924–929.

Volfinger, M. (1969) Partage de Rb et Cs entre sanidine, muscovite et solution à 600°C–1000 bars. Comptes Rendus, Academie des Sciences, Paris, 269, D1–D3.

——— (1974) Effet de la composition des micas trioctaedriques sur les distributions de Rb et Cs a l'état de traces. Earth and Planetary Science Letters, 24, 299–304.

——— (1976) Effet de la température sur les distributions de Na, Rb et Cs entre la sanidine, la muscovite, la phlogopite, et une solution hydrothermale sous une pression de 1 kbar. Geochimica et Cosmochimica Acta, 40, 267–282.

Vriend, S.P., Oosterom, M.G., Bussink, R.W., and Jansen, J.B.H. (1985) Trace element behaviour in the W-Sn granite of Regoufe, Portugal. Journal of Geochemical Exploration, 23, 13–25.

Yoder, H.S., and Eugster, H.P. (1955) Synthetic and natural muscovites. Geochimica et Cosmochimica Acta, 8, 225–280.

Manuscript received August 25, 1986
Manuscript accepted January 17, 1987

CHAPTER VI.

CHARACTERIZATION OF THE Rb-ANALOGUE OF SANIDINE AND ITS LOW TEMPERATURE STABILITY RELATIONS AT 2 KBAR WATER PRESSURE

ABSTRACT

This study gives an account of the hydrothermal synthesis and characterization of the Rb-analogue of sanidine, $RbAlSi_3O_8$. The phase is described morphologically and studied with XRD. Unit cell parameters are a: 8.837(5) Å; b: 13.035(7) Å; c: 7.187(4) Å; β : 116.27(1) °. An indexed powder X-ray diffraction pattern, based on the space group C2/m, is given. The crystal structure $RbAlSi_3O_8$ is similar to that of buddingtonite ($NH_4AlSi_3O_8$), which is evidenced by unit cell parameters and crystal morphology. The reaction $RbAl_2Si_3AlO_{10}(OH)_2 \rightleftharpoons RbAlSi_3O_8 + Al_2O_3 + H_2O$, is studied by means of reversal experiments at 2 kbar. Although the bracket is not uniquely defined, it is proposed that the reaction takes largely proceeds between 660 and 680 °C. The bracket agrees with $RbAlSi_3O_8$ synthesis experiments. From molar volumes of the Rb-analogues with respect to those of muscovite and sanidine, it can be concluded that the slope of the equilibrium curve in the P,T-diagram for the reaction involving the Rb-silicates will be steeper than the corresponding one for muscovite and sanidine + corundum + H_2O. Our experimental data are consistent with this conclusion.

INTRODUCTION

Rb-endmember silicates are unknown from nature. Rb often replaces K in silicates like feldspars and micas. The minerals are important constituents of igneous rocks, and magmatic differentiation trends are established on basis of K/Rb-variations in these rocks (Shaw, 1968). Substantial enrichment of Rb in K-silicates may be caused by the activity of postmagmatic fluids associated with acid magmatism. Such fluids play an essential role in the formation of ore deposits of Sn, W, and/or Mo, which are often associated with granitic magmatism. (e.g. Tischendorf, 1977; Pollard, 1983). Rb-distributions in these rocks are occasionally extensively mapped and eventually correlations with other elements or minerals are studied statistically (e.g. Vriend et al., 1985). Radiometric age determinations based on the ^{87}Rb to ^{87}Sr decay are widespread. For both whole rock and mineral age determinations, knowledge of the incorporation of Rb in rockforming silicates and its possible consequences for mineral stability and crystal structure is of interest.

Hydrothermal synthesis of Rb-feldspar is reported by Barrer and McCallum (1953), Ghelis and Gasperin (1970), Ghelis (1971), and Pentinghaus and Bambauer (1971). Bruno and Pentinghaus (1974) reviewed much of the literature, in which only monoclinic Rb-feldspars were mentioned. Grove and Ito (1973), and McMillan et al. (1980) discussed triclinic Rb-feldspars, which are structurally analogous to low-microcline. Henderson (1979) considered thermal expansion of alkali-feldspars, including $RbAlSi_3O_8$.

In this study we will focus on characterization of $RbAlSi_3O_8$ by X-ray Powder Diffraction, on its morphology and on the relation to the Rb-analogue of muscovite in the reaction : $RbAl_2Si_3AlO_{10}(OH)_2 \rightleftarrows RbAlSi_3O_8 + Al_2O_3 + H_2O$. This reaction is analogous to the reaction muscovite sanidine + corundum + water, which is studied for example by Chatterjee and Johannes (1974).

EXPERIMENTAL METHODS

Rb-feldspar was grown hydrothermally from a gel with a composition $Rb_2O.Al_2O_3.6SiO_2$, prepared after the method of Hamilton and Henderson (1968), or from a stoichiometric mixture of dried, extra pure Rb_2CO_3 (Merck, no. 7612), analytical grade γ-Al_2O_3 (Merck, no. 1095) and cristobalite (synthesized by heating purified quartz to 1500°C). The quartz was transformed to cristobalite because the latter compound is more reactive. The carbonate and oxides were finely ground and mixed in an agate mortar, under acetone. About 200 mg of gel or carbonate-oxide mixture was sealed with double distilled water into gold capsules, which were subsequently placed into a cold seal pressure vessel or an internally heated pressure vessel. For experimental conditions see table I.

The synthesis of the Rb-analogue of muscovite was carried out according to the method of Voncken et al. (1987). Corundum was made by heating γ-Al_2O_3 at 1000°C for 48 hours.

Experiments for the reaction $RbAl_2Si_3AlO_{10}(OH)_2 \rightleftarrows RbAlSi_3O_8 + Al_2O_3$ (corundum) + H_2O were carried out as follows : Rb-muscovite was sealed in gold capsules, with double distilled water. For the reversal runs the charges consisted of a stoichiometric mixture of $RbAlSi_3O_8$ and α-Al_2O_3 (corundum), seeded with $RbAl_2Si_3AlO_{10}(OH)_2$ in an amount of 10 percent of weight of the charge, and excess double distilled water. The 10 percent of weight of mica was added to provide nuclei for the mica formation (c.f. Chatterjee and Johannes, 1974).

Table I. Synthesis experiments

Run Nr.	T °C	P_{H2O} kbar	Time days	App.*	Starting Materials	Results
RK13	680	3	11	E	gel	$RbAlSi_3O_8$
JV95	700	5	7	I	gel	$RbAlSi_3O_8$
E412	700	2.5	14	E	carb./oxide	$RbAlSi_3O_8$**
JV133a	600	5	31	E	carb./oxide	$RbAl_2Si_3AlO_{10}(OH)_2$
JV133b	600	5	31	E	carb./oxide	$RbAl_2Si_3AlO_{10}(OH)_2$

* : E = Externally heated, I = Internally heated pressure vessel.

** : also trace mica detected, probably $RbAl_2Si_3AlO_{10}(OH)_2$

In the runs in which Rb_2CO_3 is used CO_2 will be formed during the run. Therefore P_{H2O} will in fact be slightly lower then the values in table 1. At the synthesis conditions of table 1 the pressure of CO_2 will be not larger then 50 to 60 bars for run E412 and 180 - 200 bars for JV133a and JV133b. The exact pressure depends on the amount of carbonate used in the specific runs and on the temperature. P_{H2O} will be almost equal to P_{total}.

The runs to determine the bracket for the reaction $RbAl_2Si_3AlO_{10}(OH)_2 \rightleftharpoons RbAlSi_3O_8 + Al_2O_3$ (corundum) + H_2O were conducted at 620, 640, 660, 680 and 700 °C and 2 kbar total pressure (See table IV, V and VI). After the run, the capsules were checked for leakage, and subsequently cleaned and dried. The capsule was placed in a ceramic dish and immersed in double distilled water. Then it was cut open and the solid and solution were washed out. The solid and diluted solution were separated by centrifuging. The fluid was diluted to a known volume and analyzed with AAS or ICPAES. The solid was washed thoroughly, dried and studied with optical microscopy, XRD- and IR- spectroscopy.

Conventional cold seal vessels and an internally heated pressure vessel were used (Table I). The pressure medium was argon. The temperature is considered to be accurate to 1 % , the pressure to 5 % . Quenching of the internally heated pressure vessel to room temperature was achieved in a few seconds. For the cold seal vessels, isobarical quenching to room temperature within a few minutes was achieved by blowing compressed cold air. In the externally heated rapid quench vessel, cooling to room temperature proceeds in a few seconds.

ANALYTICAL TECHNIQUES

X-ray powder photographs and diffractograms were obtained with an Enraf Nonius FR552 focusing camera (CuKα1-radiation) and a Philips PW1730 Powder Diffractometer (CuKα-radiation). For determination of unit cell parameters, silicon was taken as an internal standard. Peak intensities and positions on Guinier photographs have been determined with a double beam recording microdensitometer (MKIIICS; Joyce and Loebl & Co, Ltd.). Unit cell refinements were made with the program UNITCELLC (Strom, 1976a). Scanning electron microscopy for morphological analysis was carried out with a Cambridge M600 or Cambridge Stereoscan microscope. Thermogravimetric analyses were made in air with Dupont 1090 thermal analyzer with a heating rate of 10°C/minute. IR-spectra were made from powder samples in pressed KBr-disks, with a Perkin Elmer 580 IR-spectrometer. Chemical analyses (AES) of Rb were carried out with a Perkin Elmer 460 AAS/AES spectrometer, and analyses of Si and Al were made with ICPAES on an ARL 34000 spectrometer.

RESULTS

1) $RbAlSi_3O_8$ characterization

The Rb-feldspar crystals from the run products were generally about 50 micrometer in length, although occasionally crystals of about 80 micrometer length occurred. On large crystals, some of the optical properties of $RbAlSi_3O_8$ could be observed. Rb-feldspar is colorless, optically biaxial, with an estimated optical angle of 40 - 50 degrees. The optical sign is negative. These properties agree with those reported for $RbAlSi_3O_8$ by Winchell and Winchell (1964).

It is possible that during hydrothermal synthesis some water or H_3O^+ becomes incorporated into the synthesized feldspar. Thermogravimetric analyses on approximately 15 mg of sample was executed to investigate this. $RbAlSi_3O_8$ shows no weight loss on heating to 1000°C.

With scanning electron microscopy, generally very euhedral crystals were observed. On the faces of the feldspar crystals formed in an cold seal pressure vessel, regularly small white flakes are observed. These are very likely micas, generated because during cooling the stability field of the Rb-analogue of muscovite is traversed. The presence of mica is also indicated by XRD- and IR-data. These micas were rarely observed on crystals from the experiment in an internally

heated vessel, due to the rapid quenching.

The morphology of Rb-feldspar, $RbAlSi_3O_8$, is exemplified by figure 1, which shows a crystal grown in a run at 680 °C and 3 kbars. The crystal could be indexed by means of the computer program CAMERA (Strom, 1976b). Crystals formed from a gel have a morphology identical with those grown from a carbonate-oxide mixture.

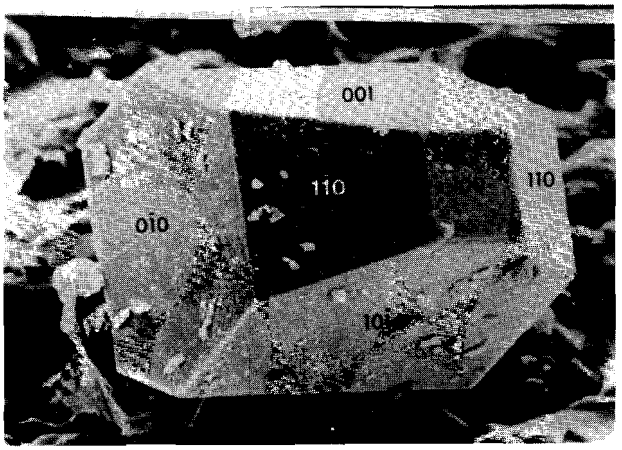

Figure 1. Indexed SEM-picture of a Rb-feldspar.

The dominating crystal faces of $RbAlSi_3O_8$ are {110}, {100}, {001}, {$\bar{1}$01} and minor {$\bar{2}$01}. The morphology of $RbAlSi_3O_8$ is similar to that of high sanidine. Applying the PBC theory, the crystal faces of high sanidine can be classified by the PBC-method into relatively slow growing F-faces and others, less important for the morphology (Woensdregt, 1982). The most important F-faces (F_1-faces) are parallel to at least 2 PBC's of strong (Si,Al)-O bonds. They are {110}, {001}, {010}, {$\bar{2}$01} and {$\bar{1}$11}. F_2-faces are parallel to one PBC with only (Si,Al)-O bonds and one PBC with additional weaker K-O-bonds. These faces are {130}, {021}, {$\bar{2}$21}, {$\bar{1}$12}, {100} and {$\bar{1}$01} (Woensdregt, 1982). The Rb-sanidine morphology is also similar to that of $NH_4AlSi_3O_8$, which is described by (Voncken et al., 1988). The {$\bar{1}$01}, {100},{010} and {110} faces dominate for both feldspars, whereas {130} and {$\bar{2}$01} are developed less often and as minor faces in the Rb-feldspar morphology.

The XRD-pattern of Rb-sanidine was indexed on the basis of the space group C2/m, which is proposed for monoclinic $RbAlSi_3O_8$ (Ghelis, 1971). Unit cell parameters are given in table II. The dimensions of the unit cell of buddingtonite are similar to those of Rb-feldspar. The indexed powder X-Ray diffraction pattern of $RbAlSi_3O_8$ is listed in Table III.

Table II. Unit cell dimensions.

Phase	Space Group	a (Å)	b (Å)	c (Å)	β (°)	V (Å^3)	Reference
$RbAlSi_3O_8$	C2/m	8.837(5)	13.035(7)	7.187(4)	116.27(1)	742.4(4)	(1)
$RbAlSi_3O_8$	C2/m	8.839(1)	13.034(1)	7.182(1)	116.29(1)	741.8(2)	(2)
$RbAlSi_3O_8$	C2/m	8.834(4)	13.042(5)	7.195(3)	116.42(3)	-	(3)
$NH_4AlSi_3O_8$	C2/m	8.824(5)	13.077(8)	7.186(4)	116.068(12)	744.8(34)	(4)
$KAlSi_3O_8$	C2/m	8.5642	13.0300	7.149	115.994	-	(5)

(1) This Work; (2) : Bruno and Pentinghaus (1974); (3) : Ghelis and Gasperin (1970)
(4) : Voncken et al., (1988); (5) Cole et al. (1949).

Table III. X-Ray Powder Diffraction Pattern of $RbAlSi_3O_8$

hkl	d(Å) (obs)	I/I_0	hkl	d(Å) (obs)	I/I_0
0 2 1	4.59	24	$\bar{1}$ 1 2	2.565	23
$\bar{2}$ 0 1	4.35	31	$\bar{3}$ 3 1	2.432	22
1 1 1	3.970	34	$\bar{1}$ 1 3	2.320	23
1 3 0	3.816	74	$\bar{3}$ 3 2	2.308	24
$\bar{1}$ 3 1	3.643	67	3 3 0	2.263	13
$\bar{2}$ 2 1	3.619	72	1 3 2	2.243	11
$\bar{1}$ 1 2	3.469	85	1 5 1	2.216	12
2 2 0	3.393	12	$\bar{4}$ 0 1	2.189	26
$\bar{2}$ 0 2	3.328	100	0 6 0	2.177	68
0 4 0	3.265	10	2 4 1	2.153	9
0 0 2	3.230	74	$\bar{1}$ 5 2	2.123	10
1 3 1	3.016	85	$\bar{2}$ 0 2	2.093	6
$\bar{2}$ 2 2	2.965	8	$\bar{1}$ 3 3	2.074	6
0 4 1	2.914	66	$\bar{4}$ 2 2	2.063	50
0 2 2*	2.896	19	2 2 2	1.993	24
$\bar{1}$ 3 2	2.774	76	4 0 0	1.986	25
$\bar{2}$ 4 1	2.613	68	* not used in the unit cell determination		
2 2 1*					
3 1 0	2.594	79			

2) Reversal experiments at 2 kbar with respect to the reaction

$RbAl_2Si_3AlO_{10}(OH)_2 \rightleftharpoons RbAlSi_3O_8 + Al_2O_3 + H_2O$

In the remainder of this work, $RbAl_2Si_3AlO_{10}(OH)_2$ will also be indicate as RbM (Rb-muscovite), $RbAlSi_3O_8$ also as RbF (Rb-feldspar), and α-Al_2O_3 also as C (corundum).

XRD and IR-spectroscopy were applied to monitor the progress of the reaction. XRD enables the detection of all the phases of interest. The strongest line in the XRD-pattern of RbF -202 was taken to examine the amount of RbF. C was found to be always present in the products of the reversal experiments. The intensity of the basal reflection of the Rb-analogue of muscovite (RbM) is very low compared to that of other dioctahedral micas (Voncken et al. ,1987). To determine the amount of the RbM, instead of the basal reflections 00l, with l = 1 or 2, which are usually the strongest reflections for dioctahedral micas, the characteristic doublet at 1.507 Å (composed of 060 at 1.506 Å and $\bar{3}31$ at 1.509 Å) was applied. Both reflections are often indistinguishable. Because the strongest Rb-mica line is at 2.580 Å, is very close to a rather strong RbF reflection, this line was considered less appropriate to determine the amount of mica. Other strong Rb-mica lines were also close to feldspar lines, which made their usage doubtful.

To establish the amount of mica in another way, also IR-spectroscopy was used. The OH-stretching vibration of the mica, at 3260 cm^{-1} (Voncken et al., 1987) is suitable to determine the presence of mica. Unfortunately, typical IR-vibrations of the feldspar and of corundum below 1200 cm^{-1} are masked by strong mica-vibrations. Therefore, detection of the presence of feldspar and corundum will be very difficult with IR-spectroscopy. In table IV, V,and VI, and in figure 2 to 4, the data provided by IR-spectroscopy and XRD are given.

Chemical analyses of the quenched fluids of these experiments are listed in table VII. The results are evaluated with the aid of figure 5 and 6. The level of the Al-concentrations was below or slightly above the detection limit, so only data for Rb and Si are considered.

Table IV. RbM determination by XRD

Starting Mixture : RbM + H_2O				Starting Mixture : RbF + C + H_2O			
Run no	Run Time (days)	T (°C)	I/I_o	Run no	Run Time (days)	T (°C)	I/I_o
140	14	620	21	145	14	620	21
141	14	640	21	146	14	640	14
142	28	660	26	147	28	660	13
143	28	680	25	148	28	680	16
144	14	700	15	149	14	700	8

Table V. Determination of RbF by XRD.

Starting Mixture : RbM + H_2O				Starting Mixture : RbF + C + H_2O			
Run no	Run Time (days)	T (°C)	I/I_o	Run no	Run Time (days)	T (°C)	I/I_o
140	14	620	53	145	14	620	16
141	14	640	47	146	14	640	14
142	28	660	56	147	28	660	13
143	28	680	61	148	28	680	32
144	14	700	100	149	14	700	100

Table VI. RbM determination by IR

Starting Mixture : RbM + H_2O				Starting Mixture : RbF + C + H_2O			
Run no	Run Time (days)	T (°C)	I/I_o	Run no	Run Time (days)	T (°C)	I/I_o
140	14	620	55	145	14	620	93
141	14	640	100	146	14	640	93
142	28	660	67	147	28	660	100
143	28	680	12	148	28	680	92
144	14	700	1	149	14	700	42

Table VII. Chemical analyses of quenched fluids

Run	Rb (ppm)	Si (ppm)
140	1.23	2.08
141	1.26	0.85
142	0.56	2.61
143	0.25	1.53
144	0.59	1.06
145	1.88	1.84
146	4.11	1.97
147	4.78	1.72
148	2.27	1.28
149	1.39	1.37

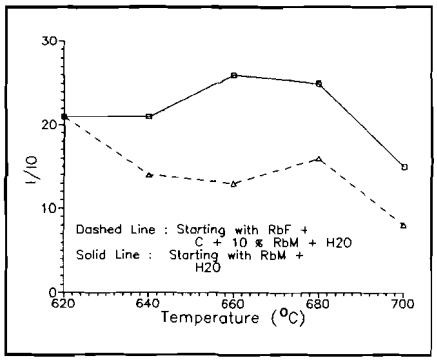

Figure 2. RbM detection with XRD on basis of the $\bar{3}31$ and 060 reflections.

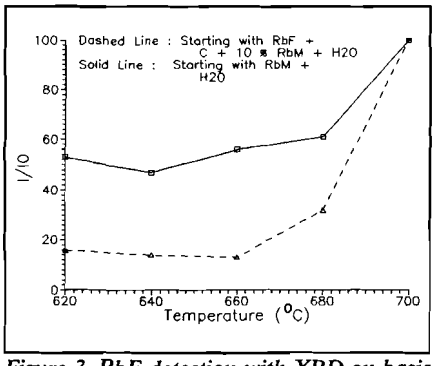

Figure 3. RbF-detection with XRD on basis of the $\bar{2}02$ reflection.

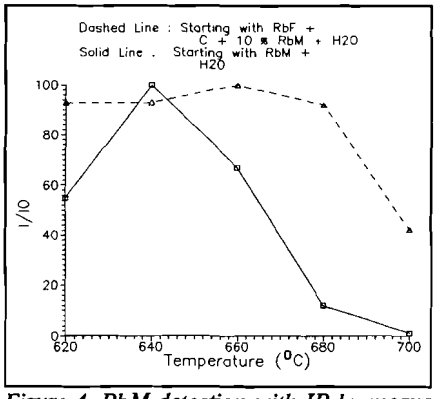

Figure 4. RbM detection with IR by means of the 3620 cm^{-1} vibration.

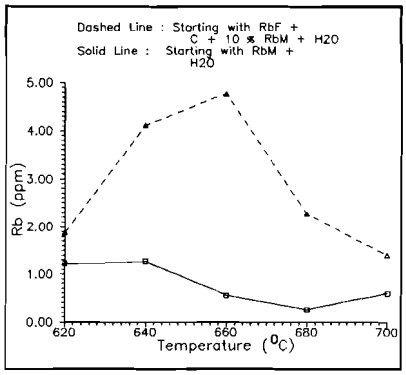

Figure 5. Rb-analyses of the quenched fluids.

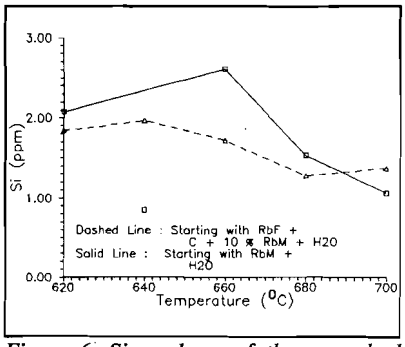

Figure 6. Si analyses of the quenched fluids.

DISCUSSION

The ionic radii of Rb^+ and NH_4^+ are very similar, and it is therefore interesting to compare the feldspars $RbAlSi_3O_8$ and $NH_4AlSi_3O_8$. Our unit cell parameters for $RbAlSi_3O_8$ agree very well with literature results. In comparison with $NH_4AlSi_3O_8$ there are only minor differences, mainly in the dimensions of the a and b-axes. The morphology of the monoclinic $RbAlSi_3O_8$ is very similar to the observed morphology of synthetic buddingtonite and high sanidine. A $RbAlSi_3O_8$ is anhydrous and these observations may be additional arguments for the non-zeolitic character of synthetic ammonium feldspar, $NH_4AlSi_3O_8$ (Voncken et al. (1988).

The reversal experiments for the reaction :

$$RbAl_2Si_3AlO_{10}(OH)_2 \rightleftharpoons RbAlSi_3O_8 + Al_2O_3 + H_2O$$

have been monitored by XRD and IR-spectroscopy. After the experiments, all phases of interest (Rb-muscovite, Rb-feldspar, corundum) are present in each run. Only the mutual proportions of phases will yield some indication about the conversion progress. The general picture is that a decrease of the amount of Rb-muscovite correlates with an increase of the amount of Rb-feldspar above 680 °C. The XRD- and IR-investigations of the products of the entire set of experiments do not uniquely indicate where the equilibrium is located in the temperature range. Taking into account the IR-data, a zone of 60 °C, from 640 to 700 °C is suggested in which the equilibrium could be situated.

The chemical analyses of the quenched fluids of the experiments display patterns for both the Rb-and Si-concentrations which show generally a lowering of concentrations between 660 and 680 °C. One Si-concentration, which is much lower than the rest of the values is measured at 640 °C for the reaction starting with RbM + H_2O (figure 6). It is likely that this concentration is an outlier, because such a lowering in the Si-content would likely be accompanied by precipitation of an Si-containing phase and no Si-containing phase was found other than the already mentioned silicates. Interpretation of the fluid analyses is complicated because by the fact that all phases of interest are involved in every experiment. The low solubility of corundum will probably be the cause of the very low concentrations of Al in the quenched fluids. In the literature (Holdren and Speier, 1985; Chou and Wollast, 1984, 1985) it is indicated that the dissolution of alkali-feldspar is incongruent at low temperatures (25 °C) and near neutral or slightly acidic conditions, and also at high temperatures (Anderson and Burnham, 1983). Solubility data for muscovite in slightly acid or near neutral solutions are scarce. A dissolution experiment (JV82a) with muscovite in double distilled water at 500 °C and 2 kbar (run time 2 weeks) indicated non-stoichiometric dissolution of muscovite. It is assumed that this is also the case for Rb-muscovite. When dissolution is incongruent, it will be difficult to interpret the solubility data clearly. In figure 5 and 6, it can be observed that concentrations are generally lower above 680 °C than below 660°C. This may be an indication that there is a change of the phase dominating the composition of the solution in this interval. Therefore the range 660 - 680 °C is supposed to be the best choice for the experimental bracket with the present data set. In that case the reaction bracket is tightened to a 20 °C range.

Chatterjee and Johannes (1974) established a bracket of 640-660 °C at 2 kbar total pressure for the reaction : $KAl_2Si_3AlO_{10}(OH)_2 \rightleftharpoons KAlSi_3O_8 + Al_2O_3 + H_2O$.
This bracket is slightly lower in temperature than our results for the Rb-analogues. From the change in volume of the reaction, it may be estimated that the slope of the equilibrium curve in the P,T field for the reaction of the Rb- analogues may be steeper than that of the muscovite-sanidine-corundum-water equilibrium.

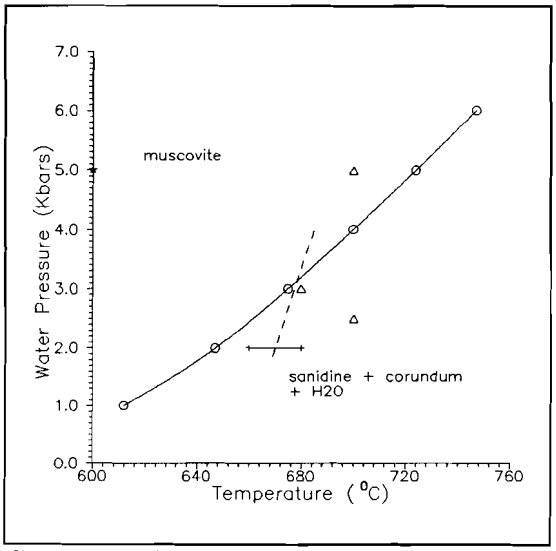

Figure 7. P,T-diagram showing the bracket suggested by the reversal experiments and an inferred part of the equilibrium line (dashed). Triangles : RbF-syntheses. Star : RbM-syntheses. Circles : data from Chatterjee and Johannes (1974).

For the reaction of the K-silicates ΔV_R = 109.5 + 25.58 + V_{H2O} - 140.71 = -6.08 cm^3 + V_{H2O}. For the reaction of the Rb-silicates, ΔV_R = 111.73 + 25.58 + V_{H2O} - 145.44 = -8.13 cm^3 + V_{H2O}. Assuming that the entropy change ΔS_R is equal for both reactions, as very similar crystal structures are involved, the equilibrium line for the reaction of the Rb-analogues in the P, T-field will be steeper than that of K-silicates. This fact agrees with the conditions of the RbF synthesis experiments at 680 °C at 3 kbar and 700 °C at 5 kbar. If the equilibrium temperature would be situated above 680 °C, then a negative slope for the equilibrium line would result, assuming that the feldspars in the mentioned synthesis experiments are stable. The negative slope is unlikely for a dehydration reaction.

In figure 7 the equilibrium curve for the reaction of muscovite is drawn after Chatterjee and Johannes (1974). The feldspar synthesis experiments are plotted and our bracket for the equilibrium of the Rb-silicates data is indicated. The conditions of synthesis experiments imply a steeper equilibrium curve for the reaction of the Rb-analogues, as a reaction of a starting

mixture with the stoichiometry of feldspar in the stability field of muscovite leads to formation of muscovite + quartz. In figure 7 an inferred part of the equilibrium curve for the reaction of the Rb-analogues is indicated (dashed line).

In natural muscovites and K-feldspars Rb occurs only in low amounts. Concentrations are seldom higher than several hundreds of ppm and are occasionally in the range of a few weight percent (e.g. Heier and Billings, 1973; Cerny and Burt, 1984). Our experimental data indicate that the effect of 100 % exchange of Rb for K on the reaction involved is very small. Natural Rb-incorporation, in sanidines and muscovites will evidently not affect the stability relations.

CONCLUSIONS

1) Monoclinic $RbAlSi_3O_8$ is structurally and morphologically very similar to synthetic buddingtonite ($NH_4AlSi_3O_8$) and to high sanidine. The anhydrous nature of $RbAlSi_3O_8$ and high sanidine may be an additional argument for the anhydrous nature of buddingtonite.

2) For the reaction $RbAl_2Si_3AlO_{10}(OH)_2 \rightleftharpoons RbAlSi_3O_8 + Al_2O_3 + H_2O$ at 2 kbar a experimental bracket between 660 and 680 °C is suggested. This implies that the equilibrium line at 2 kbar is situated at a slightly higher temperature that the corresponding reaction of muscovite to sanidine + corundum + water at that temperature.

3) The equilibrium curve of the Rb-analogues will probably have a steeper slope in the P_{H2O},T diagram than the corresponding one for the reaction muscovite to sanidine + corundum + H_2O.

ACKNOWLEDGMENTS : G. Kastelein is thanked for technical assistance in the laboratory, and F. Geelen for the SEM-picture. X-Ray Diffractograms and Guinier photographs were made by C. Laman. Mrs. Dr. C.S. Strom kindly provided the CAMERA and UNITCELLC computer programs.

REFERENCES

Anderson, G.W. and Burnham, C.W. (1983) Feldspar solubility and the transport of aluminium under metamorphic conditions. American Journal of Science, 283A, 2283- 297.

Barrer R.M. and McCallum, N. (1953) Hydrothermal chemistry of silicates. Part IV. Rubidium and Caesium aluminosilicates. Journal of the Chemical Society, 4029 - 4035.

Bruno E. and Pentinghaus H. (1974) Substitutions of cations in natural and synthetic feldspars. In : The Feldspars, proceedings of a NATO-ASI, Manchester, 1972, W.S. Mackenzie and J. Zussmann, eds., Manchester University Press, 574-610.

Cerny, P. Burt, D.M. (1984) Paragenesis, crystallochemical characteristics and geochemical evolution of micas in granitic pegmatites. In : Reviews in Mineralogy, 13, "Micas", S.W. Bailey, editor. Mineralogical Society of America, pp. 257 - 292

Chatterjee, N.D. and Johannes, W. (1974) : Thermal stability and standard thermodynamic properties of synthetic $2M_1$ muscovite, $KAl_2Si_3AlO_{10}(OH)_2$. Contributions to Mineralogy and Petrology, 48, 89-114.

Chou, L. and Wollast, R. (1984) Study of the weathering of albite at room temperature and pressure with a fluidized bed reactor. Geochimica et Cosmochimica Acta, 48, 2205-2217.

Chou, L. and Wollast, R. (1985) Steady-state kinetics and dissolution mechanism of albite. American Journal of Science, 285, 963-993.

Cole, W.F., Sörum, H., Kennard, O. (1949) The crystal structure of orthoclase and sanidinized orthoclase. Acta Crystalographica, 2, 280 - 287.

Heir, K.S., Billings, S.K. (1973) Rubidiumj. In : Handbook of Geochemistry, Vol. II-4.(K.H. Wedepohl, ed.) Springer Verlag, Berlin, Heidelberg, New York, D1 -D4.

Ghelis M. and Gasperin M. (1970) Evolution des paramètres dans le système $KAlSi_3O_8$ - $RbAlSi_3O_8$. Comptes Rendus de la Academie des Sciences, Paris, 271, D1928 - 1929.

Ghelis M. (1971) Structure crystalline de $RbAlSi_3O_8$. Acta Crystallographica, B27, 854-855.

Grove, T. and Ito, J. (1973) High temperature displacive transformations in synthetic feldspars. Transactions of the American Geophysical Union, 54, 499.

Hamilton D.L. and Henderson C.M.B. (1968) The preparation of silicate compositions by a gelling method. Mineralogical Magazine, 36, 832 - 838.

Henderson, C.M.B. (1979) An elevated temperature X-ray study of synthetic disordered Na-K alkalifeldspars. Contributions to Mineralogy and Petrology, 70, 71-79.

Holdren, G.H. and Speyer, P.M. (1985) ph dependent changes in the rate and stoichiometry of dissolution of alkalifeldspar at room temperature. American Journal of Science, 285, 994-1026.

McMillan, P.F., Brown, W.F. Openshaw, R.E. (1980) The unit cell parameters of and ordered K-Rb- feldspar series. The American Mineralogist, 65, 458-464.

Pentinghaus H. and Bambauer, H. (1971) Substitution of AL(III), Ga(III), Fe(III), Si(IV), and Ge(IV) in synthetic alkalifeldspars. Neues Jahrbuch für Mineralogie, Monatshefte, 417-418.

Pollard, P.J. (1983) Magmatic and postmagmatic processes in the formation of rocks associated with rare element deposits. Transactions of the Institutions of Mining and Metallurgy, 92, B1 - B9.

Shaw, D.M. (1968) A review of K-Rb-fractionation trends by covariance analysis. Geochimica et Cosmochimica Acta, 32, 573 - 601.

Strom, C.S. (1976a) UNITCELLC, an interactive APL-program for computing cell constants. Geological and Mineralogical Institute, Leiden University, The Netherlands.

Strom, C.S. (1976b) Indexing crystal faces on SEM-photographs. Journal of Applied Crystallography, 9, 291-297.

Tischendorf, G. (1977) Geochemical and petrographic characteristics of silicic magmatic rocks associated with rare-element mineralisation. In : Metallisation Associated with Acid Magmatism, Vol. 2, M. Stemproc and L. Burnol, eds., Geological Survey, Prague, 41 - 96.

Voncken J.H.L., Van der Eerden, A.M.J. Jansen, J.B.H. (1987) Synthesis of a Rb-analogue of $2M_1$ muscovite. The American Mineralogist, 72, 551-554.

Voncken J.H.L., Konings, R.J.M., Jansen, J.B.H., Woensdregt, C.F. (1988) Hydrothermally grown buddingtonite, an anhydrous ammonium feldspar ($NH_4AlSi_3O_8$). Physics and Chemistry of Minerals, 15, 323-328.

Vriend, S.P., Oosterom, M.G., Bussink, R.W., Jansen, J.B.H. (1985) Trace element behavior in the W-Sn-granite of Regoufe, Portugal. Journal of Geochemical Exploration, 23, 13 - 25.

Winchell, A.N. and Winchell, H.W (1964) The microscopical characteristics of artificial inorganic substances : optical properties of artificial minerals. Academic Press, New York, London.

Woensdregt, C.F. (1982) Crystal Morphology of monoclinic potassium feldspars. Zeitschrift für Kristallographie, 161, 15-33.

CHAPTER VII.

RUBIDIUM INCORPORATION IN MUSCOVITE BY ION EXCHANGE IN THE TEMPERATURE RANGE 400 - 600 °C AT 2 KBAR.

ABSTRACT

Ion exchange reactions between muscovite, Rb-muscovite, and 2M (K,Rb)Cl solutions are performed at 400, 500 and 600 °C at 2 kbar total pressure. Reaction rate experiments at 400 ° C indicate the ion exchange reaction probably takes place largely in the first week of the experiment. The data indicate the presence of a solvus in the binary system muscovite - Rb-muscovite. Experiments with two solids and a common fluid phase point to limiting compositions, expressed as K/(K + Rb), of 0.923 and 0.04 at 400 °C, 0.899 and 0.084 at 500 °C, and 0.856 and 0.153 at 600 °C. The solvus is very likely cut off by the stability field of feldspar + corundum + water before the consolute point is reached.

INTRODUCTION

Rb is found in many types of igneous, metamorphic and contact metamorphic rocks. It may be found in considerable amounts in hydrothermally altered granitic rocks and their contact aureoles (700 - 3600 ppm, Bussink, 1984; Vriend et al. ,1985) as well as in pegmatites (Cerny and Burt, 1984). Muscovite and biotite are the most important host minerals for Rb in these rocks. K/Rb variation in igneous rock suites is a tool for evaluation of magmatic differentiation (Shaw, 1968). Rb-incorporation in muscovite is of major importance for radio-active age determination (^{87}Rb-^{87}Sr) of muscovite-bearing rocks and of muscovite mineral separates (e.g. Majoor, 1988).

The study of the exchange of Rb and K between muscovite and (K,Rb)Cl solutions of varying K/Rb ratios may provide insight into the amount of Rb that can be incorporated into muscovite in equilibrium with these fluids. Alkali-chloride solutions may serve as models for water-rich fluids in the earth's crust as generally these fluids are considered to be chloride bearing.

Experimental studies on the incorporation of Rb in muscovite are described in several papers. Chelishev (1967) mentions experiments with natural muscovite. Volfinger (1969, 1976) describes exchange experiments between synthetic muscovites and alkali-chloride solutions with varying trace amounts of Rb. Voncken et al. (1987) report the synthesis of the

Rb-analogue of muscovite. The aim of this study is the investigation of the extent of solid solution between muscovite and its Rb-analogue at 2 kbar between 400 and 600 °C.

The following reactions are of interest in the muscovite-vapour exchange equilibria studied :

$$K^+_{aq} + Cl^- \rightleftharpoons KCl_{aq} \quad (1)$$

$$Rb^+_{aq} + Cl^- \rightleftharpoons RbCl_{aq} \quad (2)$$

$$\text{Muscovite} + Rb^+_{aq} \rightleftharpoons \text{Rb-muscovite} + K^+_{aq} \quad (3)$$

Data on reaction (1) provided by Helgeson and Kirkham (1976) predict mainly undissociated KCl at the run conditions. No data are available for reaction (2) for the experimental conditions. The standard molal dissociation constants for KCl and CsCl are comparable with that of the RbCl at the run conditions (Helgeson and Kirkham, 1976). RbCl may be expected to be mainly undissociated at the run conditions.

PREPARATION OF STARTING MATERIALS

All starting muscovites for exchange experiments were prepared synthetically at 600 °C and 5 kbar. Mixtures of K_2CO_3, γ-Al_2O_3, and cristobalite, prepared synthetically from purified quartz, and mixtures with a $K_2O.2SiO_2$ glass (prepared after Schairer and Bowen, 1955) were applied as starting materials for muscovite synthesis. Rb-muscovite was prepared with high purity Rb_2CO_3 (Table I) after the method of Voncken et al. (1987).

Table I. Used chemicals

Rb_2CO_3		Merck, no. 4928
Rb_2CO_3	extra pure	Merck, no. 7612
γ-Al_2O_3		Merck, no. 1095
SiO_2	quartz	Merck, no. 7536
KCl		Merck,no. 4936
RbCl		Merck, no. 7615
H_2O		double distilled

Alkali chloride endmember solutions were prepared with analytical grade KCl and RbCl, dissolved in double distilled H_2O and diluted to 2 Molar concentration. These solutions are probably rather concentrated in comparison to natural fluids. In similar studies (e.g. Beswick, 1973, Volfinger, 1976) much lower concentrations are used (e.g. Beswick : 0.7 M; Volfinger : 0.1 M or lower). The solutions are much more concentrated because then in the sample capsule smaller volumes of fluid can be used, which leaves room for larger amounts of solid material. Analytical procedures (see below) require relatively large amounts of solid material. The compositions of the fluids were checked by analysis of K and Rb by means of AAS and AES respectively, and the fluid compositions were $(K_{0.88}Rb_{0.12})Cl$, $K_{0.77}Rb_{0.23})Cl$, $(K_{0.70}Rb_{0.30})Cl$, $(K_{0.61}Rb_{0.39})Cl$, $(K_{0.49}Rb_{0.51})Cl$, $(K_{0.41},Rb_{0.59})Cl$, and $(K_{0.22}Rb_{0.78})Cl$.

EXPERIMENTAL METHODS

The runs at 400, 500 and 600 °C were carried out in conventional cold seal pressure vessels (Tuttle, 1949) and those at higher temperatures were carried out in an internally heated pressure vessel. Temperatures were measured to within ± 5 °C with chromel alumel thermocouples. The externally heated vessels were quenched to room temperature at the end of the run with compressed cold air in about 10 minutes. The internally heated vessel was water-cooled and quenched in about 2 minutes. Pressures were measured with Bourdon-type pressure gauges, which were regularly calibrated against a Heise precision gauge. Argon gas was the pressure medium in all cases and pressures are considered accurate to ± 10 bar. The moment at which the final experimental temperature was reached during the initial heating stage is chosen as the starting point of the run.

Aqueous solutions were put in gold capsules with a microsyringe. The amount was determined by weighing, and recalculated to volumes. Densities of the fluids were determined with a picnometer. The amounts of synthetic micas were weighed in the gold capsule. Finally the capsules were sealed by welding the upper side with a carbon arc under continuous cooling of the capsule by a water bath.

After the experiments, the capsules were weighed accurately to check for leakage. After thorough cleaning, the capsule was put upon a cleaned ceramic dish and held by a cleaned teflon sample holder. It was then pierced by a needle, and in the emerging bubble, subsequently the pH was measured with a micro-electrode (MicroElectrodes Inc.). The values are accurate to 0.05 pH units. Then the ceramic dish was slowly filled with distilled water and the capsule was cut open completely with a sharp knife. Solution and solid were washed out of the capsules. After being transferred into a cleaned plastic container, the solid was sedimented on the bottom of the container by means of a centrifuge. The fluids were

transferred into volumetric flasks and after appropriate dilution with double distilled water measured for K and Rb with a Perkin Elmer 460 AAS spectrometer. In some cases Rb was determined by flame emission, which has an accuracy for this element comparable to AAS.

Solids were washed carefully and dried. Finally they were checked with an optical

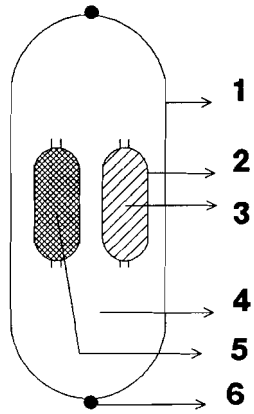

Figure 1. Sketch of the experimental setup for experiments with 2 solid phases and one vapor phase. 1 = welded outer gold capsule, 2 = crimped inner capsule 3 = muscovite, 4 = vapor phase, 5 = Rb-muscovite, 6 = weld.

microscope and XRD. In some cases, SEM was applied. In order to analyze the muscovites for K and Rb, accurately weighed amounts were decomposed with HF solutions. The HF-solution was evaporated on a sand bath and the residue dissolved in HNO_3. The resulting fluids were analyzed as described above. Mica crystals are generally about 3 micrometer in diameter and some tenths of a micrometer in thickness. The small size of the synthetic crystals generally made accurate analyses of the phases by electron microprobe impossible. It was also impossible to demonstrate that separate crystals were homogeneous.

In one series of experiments the fluid in the capsules coexisted with two muscovites. The experimental arrangement is schematically drawn in figure 1. Two capsules, of which the ends are only crimped tightly, are placed in one larger capsule. Each crimped capsule contained one of the mica compositions. The capsules are marked. The fluid is inserted in the larger capsule, which is shut by welding. During the run, both micas are accessible for the same equilibrium fluid, and can be separated simply after the run. Solids and fluid are subsequently treated and analyzed as above.

Table II. Reaction rate experiments.

Run	Run	X^{init} (1)		X^{fin} (2)	Rb^+/K^+ fin (3)	pH (4)	mg	µl
							mica	fluid
no.	time	sol.	vap.	vap.	vap.			
JV99a	1 hour	0.0	1.0	0.96	0.044	4.49	30.8	52.0
JV99b	1 hour	1.0	0.0	0.03	30.19	5.06	30.4	50.0
JV99c	4 hours	0.0	1.0	0.97	0.027	-	28.9	50.8
JV99d	4 hours	1.0	0.0	0.04	23.33	1.93	30.4	52.7
JV99e	1 day(*)	0.0	1.0	0.93	0.076	1.61	30.2	51.7
JV99f	1	1.0	0.0	0.06	15.68	1.40	28.6	50.4
JV99g	2	0.0	1.0	0.94	0.065	1.29	30.9	49.1
JV99h	2	1.0	0.0	0.04	22.06	1.16	28.6	54.9
JV99i	7	0.0	1.0	0.90	0.11	1.39	28.7	50.8
JV99j	7	1.0	0.0	0.09	10.78	1.36	30.2	49.8
JV99k	14	0.0	1.0	0.91	0.10	2.26	30.6	54.0
JV99l	14	1.0	0.0	0.14	6.05	2.18	30.6	50.7
JV99m	28	0.0	1.0	0.89	0.13	2.21	28.0	57.0
JV99n	28	1.0	0.0	0.18	4.43	3.14	29.3	35.5
JV99o	35	0.0	1.0	0.85	0.18	2.59	32.9	40.5

(*) : from run 99e-133 on the durations are counted in days (=24 hours).

(1) : $X^{init} = K^+/(K^+ + Rb^+)$ initial ratio in molar proportions

(2) : $X^{fin} = K^+/(K^+ + Rb^+)$ final ratio in molar proportions

(3) : Rb^+/K^+ fin = Rb^+/K^+ final ratio in molar proportions

(4) : Initial pH of KCl-solution : 5.30; initial pH of RbCl-solution : 4.00

RESULTS

The results of exchange experiments are graphically presented in tieline diagrams, which are used frequently for this kind of experiments (c.f. Orville, 1963; Beswick, 1973; Flux and Chatterjee, 1986; Bos et al., 1988). In these diagrams, the bulk composition of the experiment defines a point on the line connecting the initial muscovite and vapour compositions. This line is shown as a dashed line. Solid lines connect compositions measured after the

experiment. In a closed system and in case of comparable behavior of K^+ and Rb^+, the line connecting the muscovite and vapour composition will rotate around the point defined by the bulk composition to equilibrium position. If there is complete solid solution between the Rb- and K-endmembers, the tielines will rotate to parallel positions. If there is no complete solid solution, they will not. Figure 2 gives an illustration of the rotation of the tielines in the course of 42 days. These experiments were carried out to determine the time to reach equilibrium. They are discussed more in detail below.

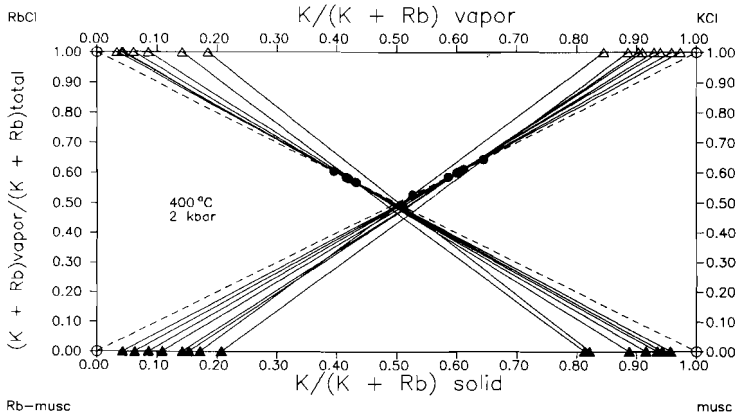

Figure 2. Tielines of the reaction rate experiments. Solid compositions are calculated. Fluid compositions are determined. Circles are rotation points.

It is important to note that if the amounts of the starting solid and fluid and their composition is known, only the composition of one phase has to be known in terms of both elements to construct the diagram or, alternatively, it is sufficient to know the amount of one of the elements in both muscovite and fluid phases after the experiment. If possible, the composition of both phases were determined, providing a check of the accuracy of the individual analyses. To determine the time necessary to approach equilibrium in the exchange reactions a series of runs with Rb-muscovite and KCl and one with muscovite and RbCl were performed at 400 °C and 2 kbar with durations varying from 1 hour to 35 days. The temperature of 400°C is the lowest investigated, and because reaction rates may be expected to increase with increasing temperature, any indication for the time in which equilibrium is approached at this temperature will be applicable for higher temperatures as well. In the examination of the run products of the JV99 series with XRD, only muscovite or Rb-muscovites were found in the run products. With respect to the starting micas, no line broadening was observed. SEM pictures of micas from experiments with very short durations show crystals with irregular edges (figure 3a) but experiments of several weeks yielded much better crystallized micas (figure 3b).

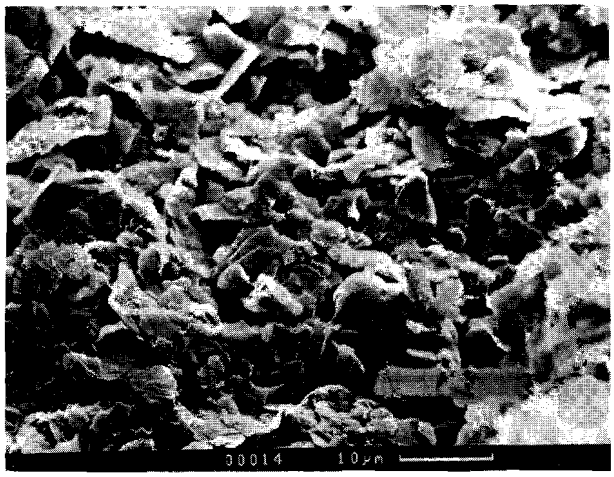

Figure 3a. SEM pictures of irregular micas from run JV99a (duration 1 hour).

In general, the dimensions of the micas remain about the same or are slightly enlarged in the course of the reaction. Recovered amounts of solid were very small and after subtraction of material necessary for XRD and SEM, not enough was left for chemical analyses. Therefore, for these particular experiments only the fluid analyses have been used to construct the tieline diagram. The determined compositions are presented in table II and in fig. 2 and 4.

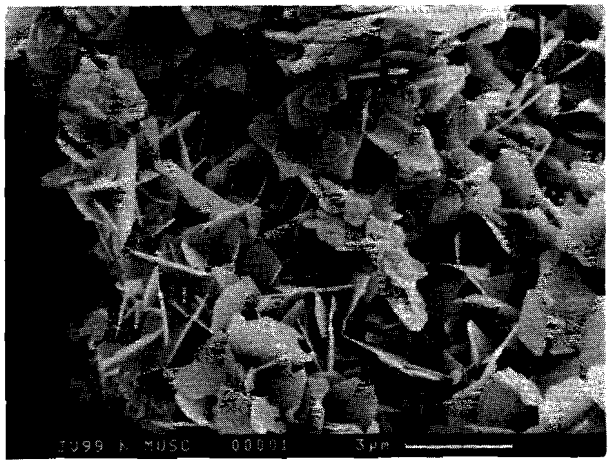

Figure 3b. SEM picture of well crystallized micas from run JV99n (duration 28 days).

Table III. Runs with endmember compositions solid and vapour at different temperatures.

Run	Run	T	P	X^{init} (1)		X^{fin} (2)		mg	µl
no.	time days	°C	kbar	sol.	vap.	sol.	vap.	mica	fluid
JV48	42	600	2	0.0	1.0	0.82	0.27	31.4	50.6
JV49	42	600	2	1.0	0.0	0.47	0.76	27.5	38.8
JV50	42	500	2	0.0	1.0	0.86	0.22	27.2	47.2
JV51	42	500	2	1.0	0.0	0.21	0.94	29.9	44.1
JV52	42	400	2	0.0	1.0	0.91	0.20	35.3	39.2
JV53	42	400	2	1.0	0.0	0.10	1.00	26.9	40.0

(1) : $X^{init} = K^+/(K^+ + Rb^+)$ initial ratio in molar proportions
(2) : $X^{fin} = K^+/(K^+ + Rb^+)$ final ratio in molar proportions
(3) : $Rb^+/K^{+\ fin} = Rb^+/K^+$ final ratio in molar proportions

Table IV. Exchange experiments with a fluid composition of $(K_{0.49},Rb_{0.51})Cl$ and muscovite and Rb-muscovite at 2 kbar

Run	Run	T	X^{init}		X^{final}		mg	µl
no.	time (days)	(°C)	sol	vap	sol	vap	mica	fluid
JV150	47	400	1.0	0.49	0.923	0.543	38.1	51.5
JV150	47	400	0.0	0.49	0.040	0.543	38.0	51.5
JV151	47	500	1.0	0.49	0.899	0.539	31.0	53.9
JV151	47	500	0.0	0.49	0.084	0.539	31.7	53.9
JV152	47	600	1.0	0.49	0.856	0.529	31.0	50.5
JV152	47	600	0.0	0.49	0.153	0.529	31.0	50.5

(1) : $X^{init} = K^+/(K^+ + Rb^+)$ initial ratio in molar proportions
(2) : $X^{fin} = K^+/(K^+ + Rb^+)$ final ratio in molar proportions

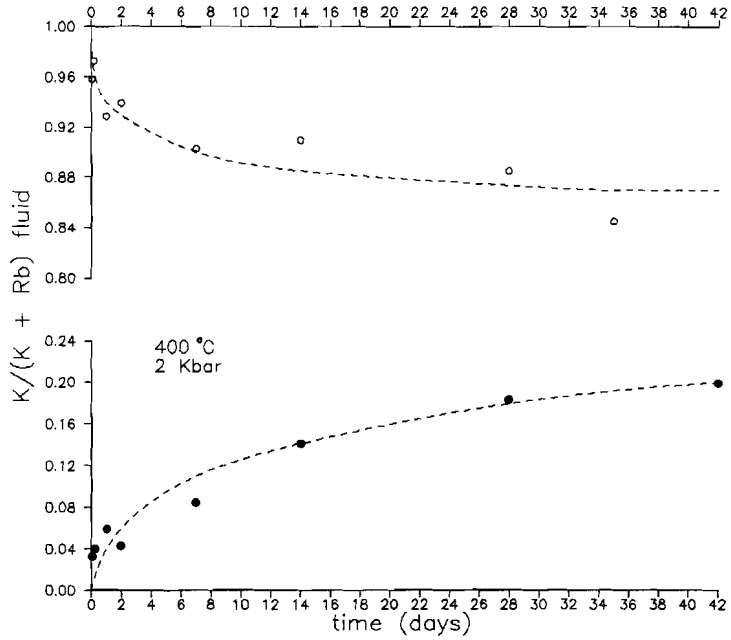

Figure 4. Fluid compositions from reaction rate experiments.Open circles represent compositions which were in contact with Rb-muscovite. Closed circles represent compositions which were in contact with muscovite.

There is a gradual change of the tielines in figure 2. The tielines do not shift to parallel or near parallel positions. In figure 4 the fluid compositions are plotted as a function of time. The fluid analyses of the exchange experiment JV52 (see Table III) with endmember compositions, which is described hereafter, is included, providing a 42 days data point. The data for both experimental series reasonably describe asymptotic curves, which are nearly symmetric for both series. pH-Values (Table II) of the quenched solutions are plotted versus time in figure 5. After falling steeply in the first two days of the reaction the pH rises again to reach a final pH of about 3. The values are rather similar for both series.

To investigate the extent of solid solution between muscovite and its Rb-analogue in equilibrium with pure RbCl or KCl, three pairs of experiments were conducted at 400, 500 and 600 °C. The results of these experiments are given in Table III and plotted in the tieline diagram of figure 6. Solid and fluid compositions were analyzed. Parallel tieline positions are not reached at any of the three temperatures. The tielines do not always exactly run through the rotation points, but pass nearby.

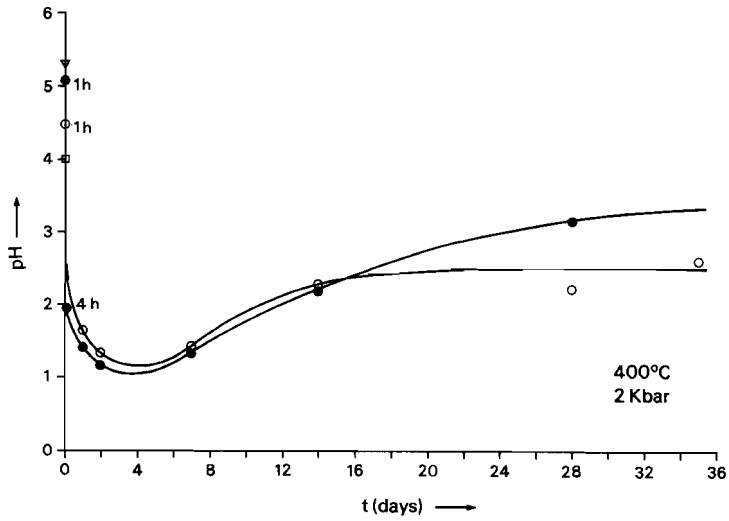

Figure 5. pH-curves for the reaction rate experiments. Symbols are as in figure 4. The open square is the starting pH for the series with open symbols, the open triangle is the symbol for the starting pH of the other series.

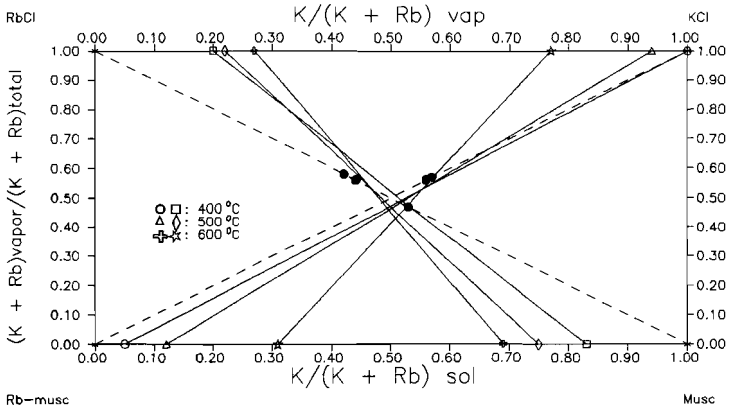

Figure 6. Tieline diagram for the exchange experiments with endmember micas and endmember fluids.

In the characterization of the solid phases of the runs, it was noted that generally XRD-peaks are broadened with respect to the starting micas. SEM investigations indicated slightly larger crystal sizes. There was no proof that two muscovites are present in one run. No other phases were established.

As the results of the experiments described above did argue for limited solid solution, between Rb-muscovite and muscovite, it was decided to test this by carrying out exchange experiments involving both muscovite and Rb-muscovite and one fluid composition. The experimental setup is explained in the section on experimental techniques (Figure 1). A fluid composition of $(K_{0.49},Rb_{0.51})Cl$ was chosen, to offer about as much K to the Rb-endmember as Rb to the K-endmember mica. The results are given in table IV and figure 7. It appears that at all temperatures, the fluid shifts to K-richer compositions. The K-enrichment slightly decreases with temperature, and the mica compositions increase in K and Rb to a lesser extent than found in earlier experiments (Table III, figure 6). Well defined XRD-patterns indicate the presence of 1 mica phase in each crimped capsule after the experiment. No formation of secondary mica either on the outer wall of the crimped capsules, nor at the wall of the larger, enclosing capsule was observed. To provide another test for limited miscibility, a synthesis experiment was carried out. A bulk composition of K/(K + Rb) = 0.5 was kept at 600 °C and 2 kbar (exp. no. JV102f). XRD investigation gave strong indications for the presence of <u>two</u> mica phases but their compositions could not be determined.

Next in the investigation of the solid solution, the (K/Rb)-ratio in the fluid is varied. Muscovite was for every run taken as starting solid. The muscovite side of the solid solution is the one occurring in nature, and thus the most interesting one. Experimental results at 500 °C are given in Table V and plotted in fig. 8 and 9. The micas in these experiments are out of equilibrium in a less extreme way than the previous experiments. The aim was to see the variation in the mica compositions as the fluid compositions increases in steps to the composition of the experiments with two micas and one fluid phase.

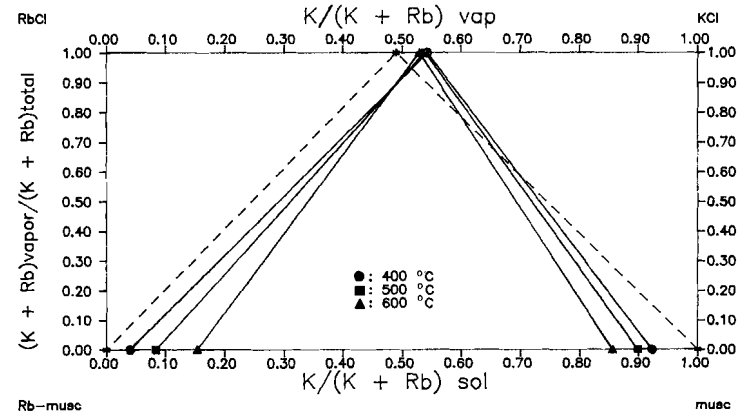

Figure 7. Tieline diagram for the experiments with one fluid phase which is in contact with two micas. Experiments for 400, 500 and 600 °C are plotted.

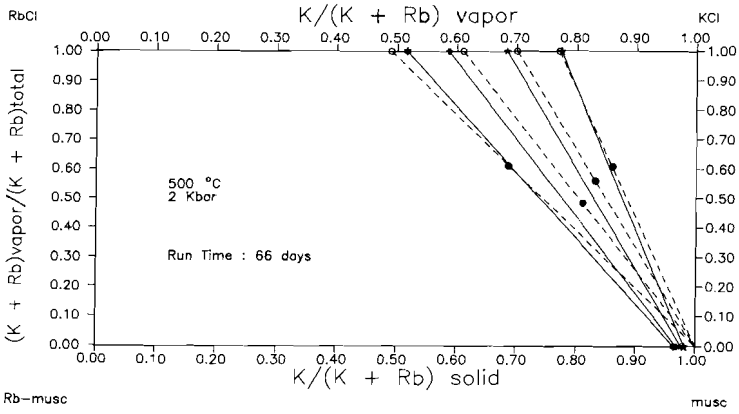

Figure 8. Exchange experiments at 500 °C.

Table V. Runs with intermediate solution compositions at 500°C at 2 kbar.

Run	T	Run	X^{init} (1)		X^{fin} (2)		Rb^+/K^+ fin (3)		K_D(4)	mg	µl
no.	(°C)	time (days)	sol.	vap.	sol.	vap.	sol.	vap.		mica	fluid
JV112b	500	66	1.0	0.77	0.98	0.77	0.019	0.293	0.065	25.4	49.6
JV112c	500	66	1.0	0.70	0.98	0.68	0.025	0.464	0.053	29.9	48.1
JV112d	500	66	1.0	0.61	0.97	0.59	0.033	0.706	0.047	32.0	37.8
JV112e	500	66	1.0	0.49	0.96	0.52	0.038	0.936	0.040	24.0	48.0
JV118b	500	56	1.0	0.70	0.98	0.68	0.016	0.465	0.035	29.8	64.1
JV118d	500	56	1.0	0.49	0.96	0.50	0.035	1.018	0.035	29.2	62.5
JV118e	500	56	1.0	0.41	0.95	0.44	0.053	1.287	0.041	14.0	60.4

(1) : $X^{init} = K^+/(K^+ + Rb^+)$ initial ratio in molar proportions

(2) : $X^{fin} = K^+/(K^+ + Rb^+)$ final ratio in molar proportions

(3) : $Rb^+/K^{+\,fin} = Rb^+/K^+$ final ratio in molar proportions

(4) : $K_D = (Rb^+/K^{+\,sol})/(Rb^+/K^{+\,vap})$ final ratio in molar proportions

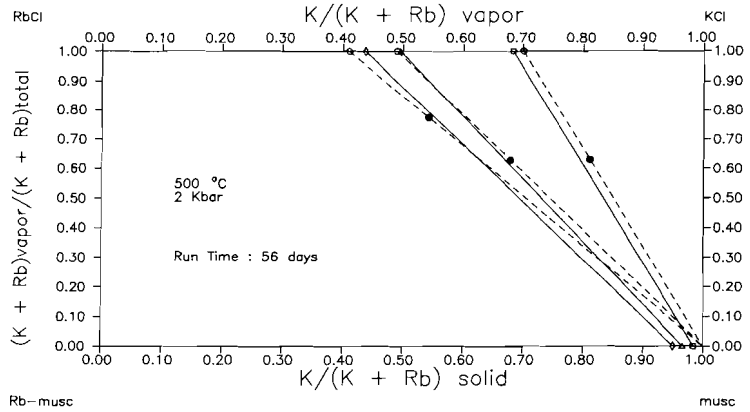

Figure 9. Exchange experiments at 500 °C. Run time 56 days.

DISCUSSION

In figure 6, 8 and 9, the lines connecting final compositions often do not pass exactly through the rotation point. This may be caused by analytical errors. The largest errors are to be expected for the analysis of the solid phase. The micas were decomposed using $HF-HNO_3$-decomposition. This method involves several analytical steps where errors may be introduced. Probably the most important source of error is the weighing of the amounts of solid phase for the decomposition, which are generally very small. Typically, 10 mg of mica is used for analysis and the rest has to be left for investigations with optical microscope, XRD, and SEM.

Equilibrium may be approached in the reaction rate experiments after about 42 days at 400 °C and 2 kbar. The asymptotic last part of the pH-curves also suggests that the fluid compositions are close to equilibrium after 42 days. Major variations take place in the first two days. The micas dissolve in the first days (figure 3a). After 42 days, they are apparently largely recrystallized (figure 3b).

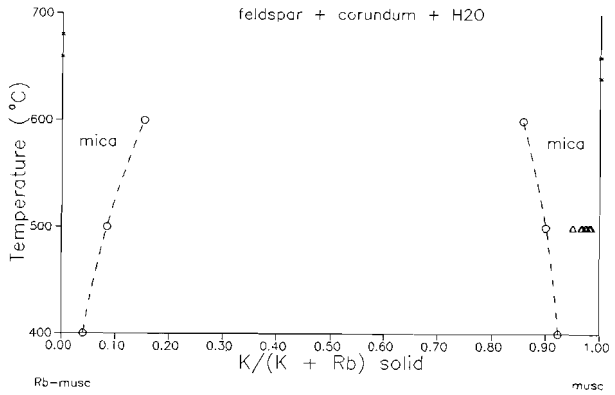

Figure 10. Plot of the solid compositions of the experiments JV151, JV152 and JV153 versus temperature. Dashed lines indicate the possible limbs of the solvus.

The experiments with two solid compositions which are equilibrated with one fluid of a composition $(K_{0.49},Rb_{0.51})Cl$ do not result in equal compositions of the solid phases. This is an argument for the presence of a solvus in the system muscovite - Rb-muscovite - H_2O at 2 kbar total pressure. This supposed miscibility gap occurs at 400 °C between the mole fractions of 0.923 and 0.040, at 500 °C between the mole fractions 0.899 and 0.084 and at 600 °C between the mole fractions 0.856 and 0.153 (Table IV). The compositions are plotted versus temperature in figure 10. The synthesis experiment JV102f, in which it was

attempted to synthesize a mica with composition K/(K + Rb) = 0.5, yielded very likely two micas. This is another argument for the existence of a solvus. Solvi in binary mica systems are well known (Eugster et al.; 1972, Beswick, 1973; Flux and Chatterjee, 1986, Juster et al, 1987). Exchange experiments with endmember compositions (JV48 to JV53), in which the micas were out of equilibium in an extreme way, yielded compositions that are within this miscibility gap. The muscovites produced in those experiments with XRD show line broadening with respect to the precursor micas, but have similar or slightly larger sizes. It it possible that they consist of intergrowths of micas with different compositions. Also, several muscovites from the reaction rate experiments fall within the immiscibility area indicated in figure 10. With XRD, no line broadening was observed for these micas. However, if the compositions reached with the experiments JV151, JV152, and JV153, establish the limiting compositions for the solid solution between muscovite and Rb-muscovite, several of the mica compositions of the reaction rate experiments (JV99e,g,i,j,k,l,m,n,o) must consist of 2 micas or intergrowths of 2 micas.

If during the exchange experiments the situation arises that a second mica composition at the other limb of the solvus will crystallize, it is possible that crystallization will take place on pre-existing nuclei which are similar in structure to the micas to be formed, i.e. the existing ones. Muscovite and Rb-muscovite are rather similar in structure (Voncken et al. 1987). These newly formed crystal layers might be incorporated in the existing mica when it grows or recrystallizes. In this way compositions may be formed which are too rich in K at the Rb-rich side of the system and vice versa. It was not possible to prove the existence of such intergrowths with TEM.

In chapter VI of this thesis, it is indicated that the equilibrium of the decomposition of Rb-muscovite to Rb-sanidine + chorundum + water takes place between 660 and 680 °C. The equilibrium for the similar reaction of the K-silicates is well known (Chatterjee and Johannes, 1974). If the position of the solvus, indicated in figure 10 is correct, it will likely not reach its consolute point before the feldspar stability field is reached. The resulting phase diagram will probably look like the one sketched in figure 11. Here the equilibrium temperatures for the mica decomposition reactions are for simplicity taken to be 650 °C (muscovite) and 670 °C (Rb-muscovite).

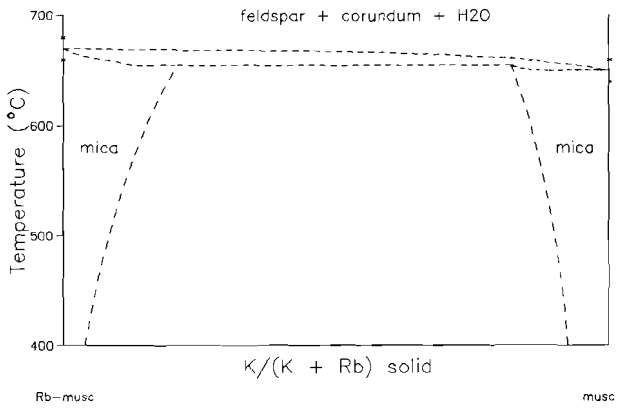

Figure 11. Sketch of the phase diagram, indicating the solvus and a compositional gap between feldspar and mica compositions.

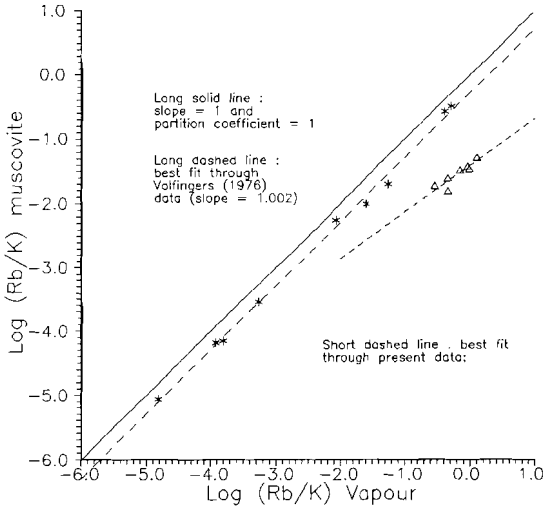

Figure 12. Log(Rb/K^{vapour}) versus Log(Rb/K^{solid}) for the experiments JV112 and JV118. Data from Volfinger (1976) are given for comparison.

The values of log Rb/K of muscovite and vapour from experiments at 500°C (table V) are plotted in figure 12. If ideal behavior in the fluid and solid phase is assumed, the points should plot on a line with a slope of one (c.f. Beswick, 1973; Volfinger, 1976). The partitioning coefficient K_D then becomes equal to the ratio

$(Rb/K)^{muscovite}$ $/(Rb/K)^{vapour}$ and it is constant in that case (McIntire, 1963). If the data points do not plot on such a line, the distribution coefficient is not constant, and consequently the system deviates from ideality (McIntire, 1963; Volfinger, 1976). The best fit through the present data is a line with a slope of 0.72. This suggests that the K_D is not constant in the concentration range. In comparison with Volfingers data, the amount and the span of the data points is rather small. A trend in the data is therefore not very well recognizable. If the data should be in accordance with a line with a slope of one, a partition coefficient of 0.045 is found. This value is about a factor of 10 lower than the value which can be deduced from the data of Volfinger (1976). Actually he gives a value of 2 ± 0.3 for a partition coefficient defined as $\underline{(Rb/K)^{vapour}}$ $/\underline{(Rb/K)^{muscovite}}$ (which is the reciprocal of our coefficient). Because of the smaller span of the compositions and the ambiguity about the demonstration of ideal behavior, it seems better not to use the data of the experiments JV112 and JV118 for determination of a unique distribution coefficient of K and Rb between muscovite and an aqueous phase for 500 °C and 2 kbar total pressure.

The mica compositions formed in the exchange experiments JV112 and JV118 do not reach the solvus. Volfinger (1976) carried out Rb - K exchange experiments on muscovite. His data do not indicate a solvus. Figure 12, in which the present data are compared with his data shows that Volfinger synthesized also micas that are even somewhat richer in Rb than the micas of the experiments JV112 and JV118. This is a confirmation that the compositions of the most Rb-rich micas formed in the experiments JV112 and JV118 do not reach the solvus. Rb-contents in Volfinger's micas vary between about 1 ppm and 2 % . The Rb-contents of micas from the runs JV112 and JV118 are also in that range. (up to 1.6 %). Natural Rb-contents in muscovite are seldom higher than a few hundred ppm and are occasionally a few weight percent (e.g. Heier and Billings, 1973; Cerny and Burt, 1984).

CONCLUSIONS

1) At 400°C and 2 kbar, equilibrium in the exchange reactions is reached in about 42 days. This is indicated by the variation of the composition with time, as well as by pH-values of the quenched hydrothermal fluids.

2) The exchange reaction likely takes largely place in the first week of the experiment, followed by recrystallization.

3) A solvus exists in the system muscovite - Rb-muscovite. Experiments with two solids and a common fluid phase point to limiting compositions, expressed as K/(K + Rb), of 0.923 and 0.04 at 400 °C, 0.899 and 0.084 at 500 °C, and 0.856 and 0.153 at 600 °C. Mica compositions produced in other experiments may suffer from intergrowths of individual crystals.

4) If the position of the solvus indicated above is correct, it is very likely cut off by the feldspar stability field before the consolute point is reached.

ACKNOWLEDGEMENTS

A.M.J. van der Eerden carried out some of the experiments and analyses and assisted with the other analytical work. Guinier photographs were taken by C. Laman or N. Slaats. G. Kastelein gave technical assistance with the high pressure apparatus.

REFERENCES

Beswick, A.E. (1973) An experimental study of alkali metal distributions in feldspars and micas. Geochimica et Cosmochimica Acta, 37, 183-208.

Bos A., Duit, W., Van der Eerden, A.M.J., Jansen, J.B.H. : Nitrogen storage in biotite : an experimental study of the ammonium and potassium partitioning between 1 M-phlogopite and vapour at 2kbar. Geochimica et Cosmochimica Acta, 52, 1275 - 1283.

Bussink, R.W. (1984) Geochemistry of the Panasqueira Tungsten-Tin deposit, Portugal. Thesis, University of Utrecht, the Netherlands, 170 pp.

Cerný, P. and Burt, D.M. (1984) Paragenesis, crystallochemical characteristics and geochemical evolution of micas in granite pegmatites. In: Micas, Reviews in mineralogy, vol. 13, (S.W. Bailey, editor), Mineralogical Society of America, 257-299.

Chatterjee, N.D. and Johannes, W. (1974) Thermal stability and standard thermodynamic properties of synthetic $2M_1$-muscovite, $KAL_2[Si_3ALO_{10}(OH)_2]$. Contributions to Mineralogy and Petrology, 48, 89-114.

Chelishev, N.F. (1967) Laboratory studies on the distributions of rare alkalies between potassium minerals and aqueous solutions at high temperatures and pressures. Doklady Academy of Sciences of the USSR., Earth Science Section, 175, 205-207.

Eugster, H.P. Albee, A.L., Bence, A.E., Thompson, J.B. Jr., & Waldbaum, D.R. (1972) The two- phase region and excess mixing properties of paragonite and muscovite solid solutions. Journal of Petrology, 13, 1, 147-179.

Flux S. and Chatterjee N.D (1986) Experimental reversal of the Na-K exchange reaction between muscovite-paragonite crystalline solutions and a 2 molal aqueous (Na,K)Cl fluid. Journal of Petrology 27, 3, 665-676.

Heier, K.S. and Billings. S.K. (1973) Rubidium. In : Handbook of Geochemistry, Vol. II-4, (K.H. Wedepohl. ed.), Springer Verlag, Berlin, Heidelberg, New York, D1-D4.

Helgeson, H.C. and Kirkham, D. H. (1976) Theoretical prediction of the thermodynamic properties of aqueous electrolytes at high pressures and temperatures III. Equation of state for aqeous species at infinite dilution. American Journal of Science 276, 97-240.

Juster T.C., Brown, P.E. & Bailey, S.W. (1987) NH_4-bearing illite in very low grade metamorphic rocks associated with coal, northeastern Pennsylvania. American Mineralogist 72, 555-565.

Orville, Ph. M. (1963) Alkali ion exchange between vapour and feldspar phases. American Journal of Science, 261, 201 - 237.

Majoor, F.J.M. (1988) A geochronological study of the axial zone of the central Pyrenees, with emphasis on Variscan events and Alpine resetting . Thesis, Free University of Amsterdam, 117 pp.

McIntire, W.L. (1963) Trace element partition coefficients - a review of theory and applications to geology. Geochimica Cosmochimica Acta, 27, 1209 - 1264.

Schairer, J.F., Bowen, N.L. (1955) The system K_2O-Al_2O_3-SiO_2. American Journal of Science, 253, 681 - 746.

Shaw, D.M. (1968) A review of K-Rb fractionation trends by covariance analysis. Geochimica Cosmochimica Acta, 32, 573 - 601.

Tuttle, O.F. (1949) Two, pressure vessels for silicate water studies. Bulletin of the Geological Society of America, 60, 1727 - 1729.

Volfinger, M. (1969) Partage de Rb et Cs entre sanidine, muscovite et solution à 600°C-1000 bars. Comptes Rendues, Academie des Sciences, Paris, 269, D1-D3.

Volfinger, M. (1976) Effet de la tempèrature sur les distributions de Na, Rb et Cs entre la sanidine, la muscovite, la phlogopite, et une solution hydrothermale sous une pression de 1 kbar. Geochimica et Cosmochimica Acta, 40, 267-282.

Voncken, J.H.L., Van der Eerden, A.M.J., Jansen, J.B.H. (1987) Synthesis of a Rb-analogue of $2M_1$ muscovite . Am. Mineral., 72, 551-554.

Vriend, S.P. , Oosterom, M.G., Bussink, R.W. ,Jansen, J.B.H. (1985) Trace element behavior in the W-Sn granite of Regoufe, Portugal. Journal of Geochemical Exploration, 23, 13-25.

CHAPTER VIII.

HYDROTHERMAL SYNTHESIS OF A MUSCOVITE-LIKE MICA WITH CESIUM

ABSTRACT

Hydrothermal experiments with the purpose to synthesize a Cs-analogue of muscovite were carried out with Cs_2CO_3-Al_2O_3-SiO_2 mixtures and excess H_2O in the temperature range 300 to 600 °C between 0.5 and 5 kbar total pressure. At the conditions 400 °C and 2 kbar, 400 °C and 5 Kbar and 500 °C and 5 kbar, a mica was formed. This mica is accompanied by quartz and pollucite, and, depending on the conditions, boehmite, diaspore, or corundum. XRD-results give evidence for mica formation. Additional evidence is gathered with SEM, IR-spectroscopy and TGA. The exact chemical composition of the mica could not be determined. Qualitative chemical analysis, however, do indicate that cesium is present in the mica. It is very well possible that the mica is not stoichiometric. The XRD-pattern of the mica is diffuse, allowing only approximate determination of the unitcell-parameters. It is a muscovite-like structure, which can be indexed according to an 1M-polytype. Unitcell-parameters (Å) are a : 5.23 $\pm$ 0.02; b : 9.01 $\pm$ 0.05; c : 10.77 $\pm$ 0.05; ß : 103.45 $\pm$ 0.03 °.

INTRODUCTION

In nature, Cs is often relatively enriched in pegmatites and hydrothermally altered granitic rocks with respect to the average cesium content in the Earth. Cs is often accompanied by Rb. These elements generally concentrate in the micas in these rocks, in amounts of hundreds to thousands of ppm (Heier and Adams, 1964).

Many studies have been carried out on the synthesis and crystal structure of pollucite and on the solid solutions between pollucite and related framework silicates (Kopp et al., 1963, Kumi and Koizumi, 1965; Martin and Lagache, 1975; Suito et al., 1974). The silicates pollucite ($CsAlSi_2O_6$), $CsAlSiO_4$ (Gallagher et al., 1977), and $CsAlSi_5O_{12}$ (Ito, 1976) were studied with the objective to find applications as refractory materials in nuclear waste locking the hazardous ^{137}Cs. (Gallagher and McCarthy, 1982; Komarneni and Roy, 1983; Ryerson et al., 1983).

In the field of mineralogy and geochemistry, the incorporation of Cs in micas, feldspatoids and feldspars by means of hydrothermal ion-exchange reactions is reported (Lagache, 1968; Roux, 1971; Volfinger, 1974, 1976; Carron and Lagache, 1980). Trioctahedral and dioctahedral micas are subject to a wide variety of cation substitutions. Considering interlayer substitutions only, phlogopite endmember compositions with Na^+ (Carman, 1974), NH_4^+ (Bos et al., 1987),

Rb^+ (Hazen and Wones, 1972; Beswick, 1973) and Cs^+ (Hazen and Wones, 1972) are described. For dioctahedral micas, the endmembers paragonite (Na^+, Chatterjee, 1970), muscovite (K^+, Yoder and Eugster, 1955; Chatterjee and Johannes, 1974), and margarite (Ca^{++}, Chatterjee, 1974), are well known. More rarely, endmember compositions with NH_4^+ (Eugster and Munoz, 1966;, Higashi, 1982; Voncken et al., 1987a) and Rb^+ (Voncken et al., 1987b) are reported. A Cs-analogue of muscovite or illite is as yet not described (c.f. Bailey, 1984).

The object of this paper is to study the possible hydrothermal synthesis of a Cs-analogue of muscovite ($CsAl_2Si_3AlO_{10}(OH)_2$).

EXPERIMENTAL AND ANALYTICAL TECHNIQUES

For synthesis of a Cs-analogue of muscovite, the method followed by Voncken et al. (1987b) for the synthesis of the Rb-analogue of muscovite was followed. A stoichiometric mixture of Cs_2CO_3, Merck, no. 2040), γ-Al_2O_3, (Merck, no 1095), and cristobalite on the composition of Cs-muscovite was prepared. Cristobalite was made synthetically from purified quartz (Merck, no. 7536) by heating it for 3 hours at 1500 °C and 1 atm. For the synthesis experiments, amounts of 200 mg of mixture and about 50 μl were sealed in gold capsules, and placed in conventional cold seal pressure vessels. The pressure medium was argon gas. The pressure was measured by a Bourdon-type pressure gauge, which was regularly calibrated against a Heise precision gauge. The pressure is accurate to 10 bars. Temperatures were measured with chromel-alumel thermocouples and are accurate to 5 °C.

Run products were studied with X-ray diffraction, applying CuKα1 radiation. Guinier photographs were made with an Enraf Nonius FR552 Powder Diffraction Camera. Diffractograms were made with a Philips PW1070 diffractometer (CuKα-radiation). For determination of unit cells, silicon was used as an internal standard.

Several charges were investigated with a Cambridge Stereoscan and a Cambridge M600 Scanning Microscope with analytical facilities (Link Systems, Ltd.). Spectrograms were taken from randomly oriented crystals.

The infrared spectra were taken with a Perkin Elmer 580 IR-spectrometer. KBr pellets, containing 2 mg of sample per 300 mg of KBr, were dried for one night at 110 °C. During recording a KBr-blank was positioned in the reference beam.

Thermogravimetric analysis were made in air with a Dupont 1090 Thermal Analyser, using about 20 mg of sample and a heating rate of 10 °C/min.

Table I. Synthesis results.

Run No.	T °C	P Kbar	Run Time Days	Phases produced* b	c	d	m	p	q	s
JV116	300	0.5	52	x				x	x	
JV115	300	2	52	x				x	x	
JV117	300	5	52	x				x	x	
JV114	400	0.5	52	x				x	x	x
JV131A	400	2	2.5	x				x	x	
JV120	400	2	5	x			x	x	x	
JV126	400	2	31	x			x	x	x	
JV131B	400	2	66		x	x	x	x	x	
JV121	400	5	36			x	x	x	x	
JV155	400	5	36			x	x	x	x	
E248	500	0.5	12	x				x	x	x
JV111	500	2	42		x			x	x	
JV122	500	5	36		x		x	x	x	
JV154A	500	5	5		x		x	x	x	
JV154B	500	5	16		x		x	x	x	
JV154C	500	5	36		x		x	x	x	
JV124	600	0.5	12		x			x	x	x
JV123	600	2	36		x			x	x	
JV93	600	5	20		x			x	x	

*: b = boehmite; c = corundum; d = diaspore; q = quartz, m = Cs-mica; p = pollucite, s = $CsAlSiO_4$

RESULTS

The experimental results are presented in table I. Pollucite is ubiquitous in the run products. At low pressure, besides pollucite, $CsAlSiO_4$ (Gallagher et al. 1977) occurs. Besides these silicates, quartz, and boehmite or diaspore or corundum occur (Table I). At 400°C, at a

pressure of 2 kbar and of 5 kbar, a phase resembling a mica is formed. At 500 °C, this material is only detected at 5 kbars. At 300 and 600 °C, it is not formed at any pressure.

The material is probably muscovite-like, and is recognized by XRD-lines which are characteristic for dioctahedral micas. In experiments with increasing run time at 400°C and 2 kbar (JV131A, JV120, JV126, JV131B) and at 500 °C at 5 kbar (JV154A,B,C), its amounts were observed to increase with time. The assumed mica could not be made pure even in experiments of 66 days.

Platy material, that was supposed to be a mica phase is shown in figure 1. Pollucite occurs generally as small dice, sometimes slightly rounded. Crystals of $CsAlSiO_4$ are similar to the one shown by Gallagher et al., (1977). In the runs in which corundum is formed, it is grown in a platy habit (c.f. Hartman, 1980).

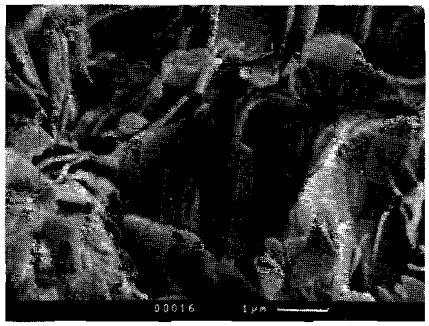

Figure 1. Irregular crystals of Cs-mica

Typical X-ray spectrograms of this silicate and pollucite are shown in figure 2a and 2b. The spectrogram of the supposed mica suggests a composition with Si about equal to Al, which would agree with a muscovite stoichiometry. The spectrogram of pollucite displays a similar picture, but apparently Si is about twice as high as Al. This agrees with the stoichiometry of pollucite ($CsAlSi_2O_6$). No quantitative analyses could be made. The size of the crystals proved to small for analysis by means of electronmicroprobe. As it is difficult to separate the phases in the run products, wet chemical analyses cannot be used to determine its composition. It was not possible to establish if the mica is an ideal stoichiometric Cs-analogue of muscovite ($CsAl_2Si_3AlO_{10}(OH)_2$).

The X-ray powder diffraction pattern of the supposed mica phase is diffuse. The XRD-pattern could, however be indexed on basis of an 1M polytype. The computation of accurate unit cell parameters could not be achieved. Unitcell parameters are given in table II. In contrast to the mica, pollucite reflections could be indexed very well according to the cubic space group Ia3d. Determined pollucite unitcell parameters (a = 13.686 $\pm$ 0.003) agree with literature values (Lagache and Martin, 1975; Richerson and Hummel, 1972, Kopp et all., 1963).

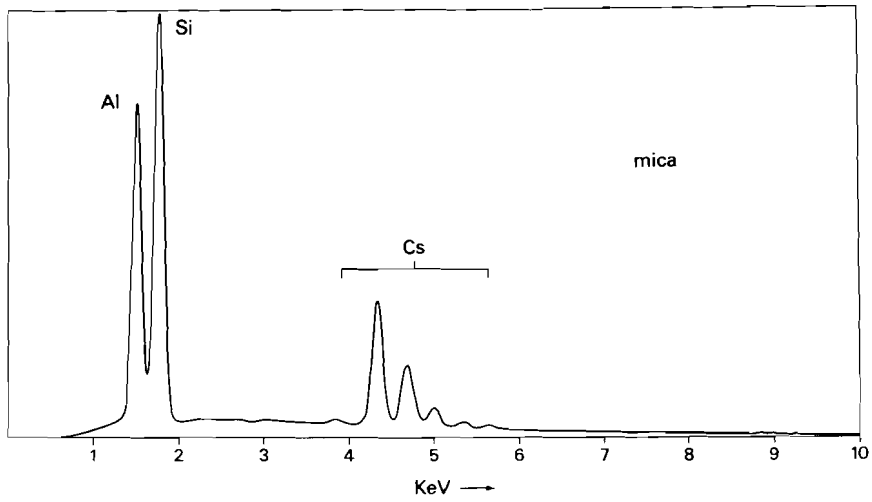

Figure 2a. E.D.S. spectrum of the assumed Cs-mica

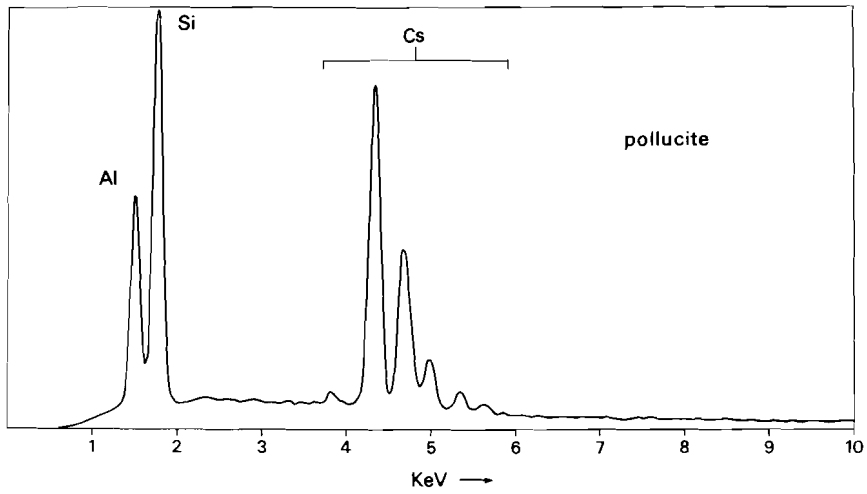

Figure 2b. E.D.S. spectrum of pollucite.

Table II. Unitcell parameters

	Cs-mica[1] 1M	Tobelite[2] 1M	Muscovite[3] 1M	Paragonite[4] 1M	Rb-muscovite[5] $2M_1$
a(Å)	5.23 ± 0.02	5.230 ± 0.007	5.208 ± 0.01	5.139 ± 0.003	5.215 ± 0.003
b(Å)	9.01 ± 0.05	9.02 ± 0.01	8.995 ± 0.002	8.885 ± 0.002	9.059 ± 0.005
c(Å)	10.77 ± 0.05	10.55 ± 0.01	10.275 ± 0.005	9.750 ± 0.003	20.59 ± 0.01
ß(°)	103.45 ± 0.03	101.56 ± 0.01	101.58 ± 0.08	89.87 ± 0.03	95.540 ± 0.003

[1] : This work; [2] : Voncken et al. (1987a); [3] : Yoder and Eugster, 1955;
[4] : Chatterjee, 1970; [5] : Voncken et al. (1987b);

Thermogravimetric analysis of the products of the runs JV93 (pollucite + corundum + quartz), JV121 (Cs-mica + pollucite + diaspore + quartz) and JV122 (Cs-mica + pollucite + corundum + quartz) are plotted in figure 3. The patterns of a corundum blank and of the Rb- analogue of muscovite are displayed for comparison. The curve of run JV93 displays a weight loss of about 0.5 wt% . Taking into account the weight loss of the corundum blank, the run products of JV93 may be considered to be anhydrous. The patterns of the runs JV121 and JV122 show a loss of about 0.5 wt % below 100 °C, and about 3.0 wt% over the rest of the temperature range. The loss occurs generally between 450 and 600 °C. The dehydroxylation of the Rb-analogue of muscovite takes place in the interval 500 - 600 °C.

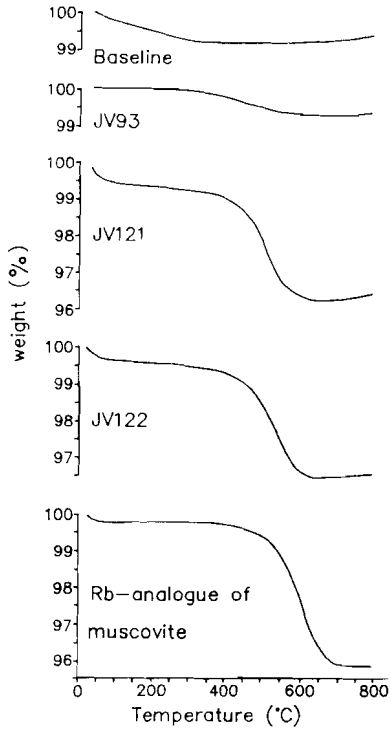

Figure 3. Thermogravimetric analyses

Infrared spectra of the products of the runs JV121, JV122 and a spectrum of the Rb-analogue of muscovite are shown in figure 4. Although the spectra of JV121 and 122 are somewhat complicated by vibrations of pollucite (P), diaspore (D), and corundum (C) and because of overlap (notably of Si-O and Al-O vibrational bands) of pollucite and mica, the general similarity with the pattern of the Rb-mica is obvious. The OH-vibrational band of the Rb-mica at 3630 cm^{-1} is found similarly in the spectra of the products of JV122 and JV122. In the products of run JV121, diaspore (α-AlOOH) is formed, but in the products of JV122, no other hydroxyl-bearing phase other than the supposed mica was detected with XRD.

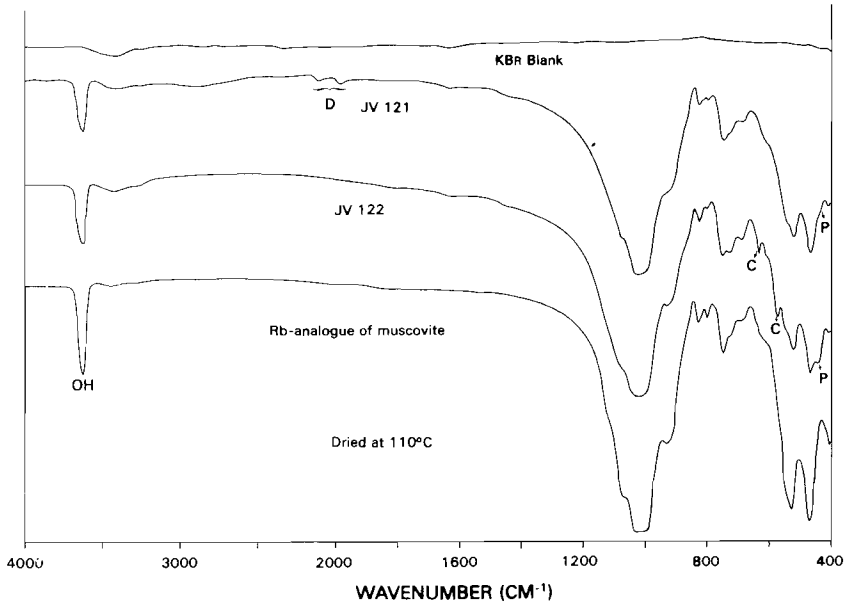

Figure 4. IR-spectra of the run products of JV121 and JV122. A spectrum of the Rb-analogue of muscovite is shown for comparison.

DISCUSSION

In the preceding section, data are presented which argue for the formation of a Cs-mica with a muscovite-like structure at the conditions 400 °C, at 2 and 5 kbar, and at 500 °C, at 5 kbar. As one of the starting materials was Cs_2CO_3, during the reaction a P_{CO2} will develop. Therefore, P_{H2O} is not equal to P_{Total}. At 400°C, the calculated P_{CO2} is about 100 - 120 bars and at 500°C it is 180 - 200 bars, for respectively 2 and 5 kbars. P_{H2O} will be nearly P_{total} for the mica containing runs.

The main argument for the presence of a mica-phase is the presence of diffuse XRD-reflections which are similar to reflections of muscovite or the Rb-analogue of muscovite. It is possible to index the XRD-pattern, based on an 1M-polytype. Hazen and Wones (1972) report the synthesis of a Cs-analogue of phlogopite. They mention also a diffuse XRD-pattern for this Cs-mica.

Additional arguments for the presence of a mica in the run products of experiments at the above mentioned conditions are based on SEM, TGA, and IR-spectroscopy. SEM illustrates the supposed micas to be irregular plates, and X-ray spectra indicate that they contain Cs. Crystals of diaspore or boehmite, which are observed in several of the mica-containing runs, also have a platy habit and might be mistaken for a mica, but the X-ray spectra leave no doubt.

Thermogravimetric analyses of the runs JV121 and 122 indicate important weight loss in the temperature range 450 - 600 °C. Guggenheim et al. (1987) describe dehydroxylation of muscovite in the temperature range 475 - 900 °C. Like in this study, they applied a heating rate of 10 °C/min. With this heating rate, the dehydroxylation of the Rb-analogue of muscovite takes place in the interval 500 - 650 °C. The ammonium-analogue of muscovite starts to decompose firstly by ammonium loss above 500 °C. The recorded interval of 450 - 600 °C for this mica is thus acceptable as interval in which the dehydroxylation may take place. The weight loss is about 3 % for both runs. The ideal stoichiometric Cs-analogue of muscovite, $CsAl_2Si_3AlO_{10}(OH)_2$, would lose 3.66 percent of weight. The run products do not consist of pure mica, so the value of 3.66 percent cannot be reached. Although in JV121 diaspore is present, which will contribute to the weight loss, the TGA-results of JV121 and especially JV122 are consistent with the presence of an important amount of a muscovite-like silicate in the run products. On basis of the amount of weight loss in TGA, the amount of mica in run JV122 will be about 80 percent.

Although from the foregoing the conclusion may be drawn that a Cs-containing muscovite-like mica is formed, there is some ambiguity about its composition and the relation to other

phases present. In all runs, a stoichiometric mixture on the composition of the Cs-analogue of muscovite and excess H_2O was the starting material. As in the mica containing runs pollucite was formed, not all the available Cs is incorporated in the mica.

There may be a reaction between the mica and other phases present (pollucite, quartz, diaspore, boehmite, or corundum). For runs with boehmite, this relation may be written as follows

$$CsAl_2Si_3AlO_{10}(OH)_2 \rightleftharpoons CsAlSi_2O_6 + SiO_2 + 2\ AlOOH \qquad (1)$$

For the runs with corundum one could write

$$CsAl_2Si_3AlO_{10}(OH)_2 \rightleftharpoons CsAlSi_2O_6 + SiO_2 + Al_2O_3 + H_2O \qquad (2)$$

In these reactions the mica is assumed to be stoichiometric. There are no chemical data to prove this assumption, nor are the mole ratios of the compounds in the run products known.

It may be that the mica did not crystallize in a stoichiometric composition, and that remaining Cs, Al and Si were used to form pollucite, quartz and AlOOH or Al_2O_3. If the interlayer of the mica is not completely filled, charge balance may be affected by substitution of Si for Al in the tetrahedral layer around vacant interlayer sites. Another possibility is incorporation of H_3O^+ in the vacant sites of the silicate, which for the rest stays stoichiometric. For incorporation of H_3O^+ there is no evidence. In IR-spectra, vibrations of H_3O^+ coincide with those of H_2O. TGA of the mica containing runs shows some weight loss at low temperature but this can just as well be explained by loss of adsorbed water. The diffuse XRD-pattern of the mica suggests an ill defined structure, which may be an argument for non-stoichiometry. Hazen and Wones (1972) did not succeed in making a pure Cs-endmember phlogopite, and produced also pollucite and forsterite besides mica. They do not discuss the composition of the mica and apparently assume a stoichiometric composition for it.

The dimension of the c-axis of the Cs-mica (10.77 $\pm$ 0.05 Å) approaches, taking into account the error in the measurement, the dimension of the c-axis of the Cs-analogue of phlogopite (10.85 $\pm$ 0.5 Å) (Hazen and Wones, 1972). Direct comparison with the Rb-analogue of muscovite is not possible, because the Cs-mica is likely of the 1M-polytype, whereas the Rb-analogue of muscovite is of the $2M_1$ polytype (Voncken et al., 1987b). However the dimension of the c-axis of the Cs-mica is in comparison with the value for half the c-axis of the Rb-analogue of muscovite clearly larger (table II). Differences for the a- and b-axes are not large.

In comparison with the c-axis of the NH_4-analogue of muscovite (tobelite) the c-axis is clearly much larger, whereas the other axes are not much enlarged. Hazen and Wones (1972) report only minor differences in the a- and b-axes of Rb-, NH_4- and Cs-phlogopites, whereas especially the increase of the c-axes on Cs-incorporation is substantial. This may be an indication that already in the case of incorporation of ammonium or Rb in dioctahedral as well trioctahedral micas the maximum enlargement of the a- and b-axes is reached. Hazen and Wones (1972) plot unit cell parameters of their micas versus effective ionic radii, and examine the relationships that evolve. It would be interesting to do this too for dioctahedral micas, but unfortunately, unitcell data for 1M $RbAl_2Si_3AlO_{10}(OH)_2$ are not known. The value of half the c-axis of the $2M_1$ Rb-analogue of muscovite is only an approximation of the c-axis of a 1M mica, and cannot be used for accurate analysis. Values for the effective ionic radius of NH_4^+ are ambiguous (Shannon, 1976), so the somewhat inaccurate data for the Cs-mica will heavily influence the results.

In the run products, several combinations of phases are found which suggest metastability. In the system Al_2O_3 - H_2O, boehmite (γ-AlOOH) is instable with respect to diaspore (α-AlOOH) at all conditions investigated in this study (Day, 1976). However, in most runs in which AlOOH is present, it appears to be in the boehmite form. The occurrence of diaspore instead of boehmite at the 5 kbar and 400 °C may perhaps be related to the lower molar volume of diaspore (17.44 cm^3) with respect to that of boehmite (19.8 cm^3). According to Haas and Holdaway (1973), diaspore + quartz and boehmite + quartz should react to form pyrophyllite. Pyrophyllite was not detected in any run. In some other runs, corundum + quartz is found together, whereas Al_2SiO_5 would be expected. Corundum is however known to react sluggishly, which may be an explanation for the absence of Al_2SiO_5.

Another reaction which could be expected is that of pollucite with quartz, yielding feldspar : $CsAlSi_2O_6 + SiO_2 = CsAlSi_3O_8$. The runs JV123 and JV93 yield pollucite and quartz, and no feldspar was formed. Bruno and Pentinghaus (1974) predicted that a Cs-endmember feldspar would not exist because the Cs^+ ion is too large to fit in the A-site of a feldspar structure. Experimentally determined distribution coefficients for the partitioning of Cs between hydrothermal solutions and feldspar are very small (Lagache, 1968, 1969; Roux, 1971), which supports this view. Although a Cs-endmember feldspar may perhaps synthesized, the fact that in this system quartz and pollucite coexist is suspicious.

CONCLUSIONS

1) A cesium containing dioctahedral mica, with a structure resembling that of muscovite was synthesized at 400 °C at 2 kbar and at 5 kbar at 400 and 500 °C. Evidence is presented in the form of XRD-data, SEM, X-Ray analyses, IR-spectra and thermal analyses (TGA). The exact composition of the mica could not be determined. The mica is accompanied by boehmite or diaspore or corundum and quartz and pollucite.

2) Unit cell determinations, based on an 1M polytype are a : 5.23 $\pm$ 0.02 Å, B; 9.01 $\pm$ 0.05 Å; C: 10.77 $\pm$ 0.05 Å. Because the XRD-pattern is diffuse, no accurate unit cell parameters could be calculated.

3) Under the conditions studied, no $CsAlSi_3O_8$ is formed. $CsAlSi_2O_6$ and SiO_2 do not react to feldspar. This may be support for the theory (Bruno and Pentinghaus, 1974) that a Cs-analogue of alkali-feldspar does not exist.

ACKNOWLEDGEMENTS

Thanks are due to A.M.J. van der Eerden for assistance in the laboratory and for carrying out some of the long term experiments. M. Broekmans assisted with one of the low pressure experiments. P. van Krieken and T. Zalm performed the TGA. N. Slaats and V. Govers made the XRD-recordings. Ing. J. Pieters (E.M.S.A., University of Utrecht) assisted with analytical electron microscopy.

REFERENCES

Bailey, S.W. (1984) Reviews in Mineralogy, Vol. 13 : Micas. Mineralogical Society of America, 584 p.

Beswick, A.E. (1973) An experimental study of alkali metal distributions in feldspars and micas. Geochim. Cosmochim. Acta, 37, 183-208.

Bos, A., de Haas, G.J., Voncken, J.H.L., Van der Eerden, A.M.J., and Jansen, J.B.H. (1987) Hydrothermal synthesis of ammonium phlogopite. Geol. en Mijnb., 66, 251-258.

Bruno, E. and Pentinghaus, H. (1974) Substitutions of cations in synthetic and natural feldspars. In : The Feldspars. Proceedings of NATO-ASI, Manchester, 1972. W.S. Mackenzie and J. Zussmann, eds., Manchester University Press, 1974, 574- 610.

Carman, J.H. (1974) Synthetic sodium phlogopite and its two hydrates : stabilities, properties and mineralogical implications. Am. Miner. 59, 261-273.

Carron, J-P and Lagache, M. (1980) Etude experimentale du fractionnement des èlèments Rb, Cs, Sr, et Ba entre feldspaths alcalins, solutions hydrothermales, et liquides silicatès dans le systéme Q.Ab.Or.H_2O á 2 kbar entre 700 et 800 °C. Bull. Mineral., 103, 571-578.

Chatterjee N.D. (1970) Synthesis and upper stability of paragonite. Contrib. Mineral. Petrol. 27, 244 - 257.

Chatterjee, N.D. (1974) Synthesis and upper thermal stability limit of margarite, $CaAl_2[Al_2Si_2O_{10}(OH)_2]$. Schweiz. Min. Petr. Mitt., 54, 753 - 767.

Chatterjee, N.D. and Johannes, W. (1974) Thermal stability and standard thermodynamic properties of synthetic $2M_1$ muscovite, $KAl_2[Si_3AlO_{10}(OH)_2]$. Contrib. Min. Petrol., 48, 89 -114.

Day, H.W. (1976) A working model of some equilibria in the system alumina-silica water. Am. Journ. Sci, 276, 1254-1284.

Eugster, H.P. and Munoz. J. (1966) Ammonium micas: possible sources of atmospheric ammonia and nitrogen. Science, 151, 683-686.

Gallagher, S.A., McCarthy, G.J., Smith D.K. (1977) Preparation and X-ray characterization of $CsAlSiO_4$. Mat. Res. Bull., 12, 1183-1190

Gallagher, S.A and McCarthy, G.J. (1982) : High temeprature stability of $CsAlSiO_4$ and $CsAlSi_2O_6$. Mat. Res. Bull, 17, 89-94.

Guggenheim, S., Chang, Y.H., Koster van Groos, A.F. (1987) Muscovite dehydroxylation : High-temperature studies. Am. Mineral., 72, 537 - 550.

Haas, H. and Holdaway, (1973) Equilibria in the system Al_2O_3-SiO_2-H_2O involving the stability limits of pyrophyllite, and thermodynamic data of pyrophyllite. Am . Journ. Sci., 273, 449-464.

Hartman P. The attachment energy as a habit controlling factor. III. Application to corundum. Journ. Cryst. Growth, 49, 166-170.

Hazen, R.M. and Wones, D.R. (1972) The effect of cation substitutions on the physical properties of trioctaedral micas. Am. Miner., 57, 103-129.

Heier, K.S., and Adams, J.A.S. (1964) The geochemistry of the alkali metals. In : Physics and Chemistry of the Earth, Volume 5, L.H. Ahrens, ed., Pergamon Press, Oxford, London, New York, 253 - 381.

Higashi, S. (1982) Tobelite, a new ammonium dioctahedral mica. Miner. Journ, 11, nr 3, 138-146.

Ito, J. (1976) Crystal synthesis of a new Cs aluminosilicate, $CsAlSi_5O_{12}$. Am. Miner., 61, 170-171.

Komarneni, S. and Roy, R. (1983) : Hydrothermal reaction and dissolution studies of $CsAlSi_5O_{12}$ in water and brines. Journ. Am. Ceram. Soc., 66, 471-474.

Kopp, O.C., Harris, L.A., Clark, G.W. and Yakel, H.L. (1963) A hydrothermally synthesized iron analog of pollucite- its structure and significance. Am. Miner., 48, 100 - 109.

Kumi, S. and Koizumi, M. (1965) : Synthetic pollucites in the system $Cs_2O.Al_2O_3.4SiO_2$-$Cs_2O.Fe_2O_3.4SiO_2$-H_2O- their phase relationship and physical properties. Am. Mineral. 50, 587- 592.

Lagache, M. (1968) Etude experimentale de la rèpartition des èlèments- traces sodium et cesium entre la leucite, l' orthose et des solutions hydrothermales a' 600°C. C.R. Acad. Sci. Paris, 267, D141-D144.

Lagache, M. (1969) Etude expèrimentale de la rèpartition du cesium entre les feldspaths sodipotassiques et des solutions hydrothermales a' 700 °C and 1000 bars. C.R. Acad. Sci. Paris, 272, D1328-1330.

Martin R.F. and Lagache, M. (1975) Cell edges and infrared spectra of synthetic leucites and pollucites in the system $KAlSi_2O_6$ - $RbAlSi_2O_6$ - $CsAlSi_2O_6$. Can. Miner., 13, 275- 281.

Richerson, D.W. and Hummel, F.A. (1972) Synthesis and Thermal expansion of polycristalline cesium minerals. J. Am. Ceram. Soc., 55, 269-273

Roux, J. (1971) Fixation du rubidium et du cesium dans la nèphèline et dans l'albite a' 600°C dans les conditions hydrothermales. C. R. Acad. Sci. Paris, D1469-D1472.

Ryerson, F.J., Bazan, F., and Campbell, J.H. (1983) Dissolution of nuclear waste ceramic : an experimental and modeling study. J. Am. Ceram. Soc. , 66, 462-470.

Shannon, R.D. (1976) Revised ionic radii and systematic studies of interatomic distances in halides and chalcogenides. Acta Cryst., A32, 751-767.

Suito, K., Lacam, A. and Iiyama, J.T. (1974): Stabilite' des solutions solides de la serie leucite-pollucite sous une pression d'eau de 30 kbar. C.R. Acad. Sc. Paris, 278, D2397-D2400.

Volfinger, M. (1974) Effet de la composition des micas trioctaedriques sur les distributions de Rb et Cs a l'etat de traces. Earth Plan. Sci. Lett. 24, 299-304.

Volfinger, M. (1976) Effet de la tempèrature sur les distributions de Na, Rb et Cs entre la sanidine, la muscovite, la phlogopite, et une solution hydrothermale sous une pression de 1 kbar. Geochim. Cosmochim. Acta, 40, 267-282.

Voncken, J.H.L., Wevers, J.M.A.R., Van der Eerden, A.M.J., Bos, A. and Jansen, J.B.H. (1987a) Hydrothermal synthesis of tobelite, $NH_4Al_2Si_3AlO_{10}(OH)_2$, from various starting materials and implications for its occurrence in nature. Geol. en Mijnb. 66, 259-269.

Voncken, J.H.L., Van der Eerden, A.M.J., Jansen, J.B.H. (1987b) Synthesis of a Rb-analogue of $2M_1$ muscovite. Am. Miner., 72, 551-554.

Yoder, H.S. and Eugster, H.P. (1955) Synthetic and natural muscovites. Geochim. Cosmochim. Acta, 8, 225 - 280.

CURRICULUM VITAE

Jakobus Hubertus Lambertus Voncken werd geboren op 17 april 1959 te Heerlen. In juni 1977 werd het diploma Atheneum-B behaald aan het Romboutscollege te Brunssum. In september van dat jaar werd begonnen met de studie Geologie aan de Rijksuniversiteit te Utrecht. In december 1980 werd het kandidaatsexamen G3 afgelegd en in mei 1984 het doctoraalexamen (met genoegen) met als hoofdvak Petrologie en als bijvakken Economische Geologie en Exploratie Geochemie. In de jaren 1980 tot 1984 werden diverse student-assistentschappen vervuld bij de afdelingen Petrologie en Mineralogie. Vanaf 1 oktober 1984 tot 1 oktober 1988 was de schrijver als wetenschappelijk assistent in dienst van het Instituut voor Aardwetenschappen, bij de Vakgroep Petrologie, Mineralogie, Kristallografie, Geochemie en Bodemkunde (PMKGB). Het onderzoek, dat is beschreven in dit proefschrift werd uitgevoerd in het laboratorium voor High Pressure and Temperature research (HPT-laboratorium). Van mei tot augustus 1988 werd een stage vervuld op het gebied van de hydrothermale kristalgroei bij Prof. A. Baronnet aan het Centre de Recherche sur les Mêcanismes de la Croissance Cristalline ($CRMC^2$-CNRS) te Marseille, Frankrijk. Sinds 1 november 1988 is de schrijver als medewerker onderzoek in dienst van de Faculteit der Chemische Technologie van de Universiteit Twente te Enschede, waar hij bij de Vakgroep Anorganische Chemie, Materiaalkunde en Katalysator Materialen onderzoek verricht in het kader van het IOP-projekt "Drager-Scheidingslaag Interactie en het Vormingsmechamisme van Keramische Membranen".

Exit to System
C:\>